Diagnostic Value and Regulation of Selected *Candida albicans* Cell Surface Proteins

Von der Fakultät für Lebenswissenschaften

der Technischen Universität Carolo-Wilhelmina

zu Braunschweig

zur Erlangung des Grades eines

Doktors der Naturwissenschaften

(Dr. rer. nat.)

genehmigte

D i s s e r t a t i o n

von Hani Kaba
aus Münster (Westfalen)

1. Referentin: Professor Dr. Ursula M. Bilitewski
2. Referent: Professor Dr. Dieter Jahn
eingereicht am: 13.05.2013
mündliche Prüfung (Disputation) am: 13.08.2013
Druckjahr 2013

Vorveröffentlichungen der Dissertation

Teilergebnisse aus dieser Arbeit wurden mit Genehmigung der Fakultät für Lebenswissenschaften, vertreten durch die Mentorin der Arbeit, in folgenden Beiträgen vorab veröffentlicht:

Publikationen

Kaba, H., Nimtz, M., Müller, P., & Bilitewski, U. Involvement of the mitogen activated protein kinase Hog1p in the response of *Candida albicans* to iron availability. BMC Microbiology 13:16 (2013).

Tagungsbeiträge

Kaba, H. & Bilitewski, U.: Studies on the regulation of the *Candida albicans* cell wall protein Bgl2p and its value as potential diagnostic marker. (Poster) 4th International HZI Grad School Symposium, Braunschweig (2010).

Kaba, H. & Bilitewski, U.: Studies on the multicopper ferroxidases of *Candida albicans*. (Vortrag) 2nd JSMC Micom, Jena (2011).

Kaba, H., Hust, M., van den Heuvel, J., Müller, P., Mayer, Y. & Bilitewski, U.: Studies on *Candida albicans* cell wall proteins and their antigenic properties. (Poster) Potsdam Days on Bioanalysis 2011, Potsdam (2011).

Kaba, H. & Bilitewski, U.: Signaling pathways involved in Response to environmental iron in the human fungal pathogen *Candida albicans*. (Poster) 11th European Conference on Fungal Genetics, Marburg (2012).

Kaba, H., Nimtz, M., Müller, P., & Bilitewski, U.: Involvement of the mitogen activated protein kinase Hog1p in the response of *Candida albicans* to iron availability. (Poster) Potsdam Days on Bioanalysis, Potsdam (2012).

Acknowledgements

I would like to express my thanks to many people who supported me, both in and outside the lab.

First of all I would like to thank my supervisor Prof. Dr. Ursula Bilitewski, who gave me the opportunity to investigate these interesting and challenging topics of my PhD thesis, as well as for the excellent supervision and continuous motivation during PhD time. The intense discussions of results, experimental problems, presentations, posters or publications with Prof. Bilitewski have been of great importance during the PhD time. The way she transfers knowledge to her students is unique. Danke Ursula!

I would like to thank Prof. Dr. Dieter Jahn for kindly agreeing to participate in my PhD defense committee and Prof. Dr. Dietmar Schomburg for kindly accepting to chair the PhD defense committee.

Special thanks belong to Prof. Dr. Peter Müller, not only for being member of my PhD thesis committee, but also for the huge support during the course of PhD, including his contribution to the different projects as well as his permanent readiness to answer questions, discuss results and review texts.

My best thanks to Prof. Dr. Andre Fleißner for his valuable suggestions and ideas shared during the meetings of the PhD thesis committee meetings.

Special thanks belong also to Dr. Edie Kaba, Nawaf Kaba and Dr. Said Kaba for proof reading parts of this thesis.

I would like to acknowledge the effort of many colleagues and friends from the Helmholtz Centre for Infection Research (HZI) in Braunschweig, as well as from other research institutions, who contributed to or supported the different projects of this thesis:
Yvonne Mayer (Microdiscovery GmbH, Berlin) for the search for suitable *Candida albicans* Bgl2p peptides, Dr. Birgit Hofmann (HZI) for her support during *In silico* analysis of protein sequences, Dr. Werner Tegge and co-workers (HZI) for the synthesis of *C. albicans* Bgl2p peptides, Prof. Dr. Katja Heilmann and co-workers (University of Potsdam) for the generation of anti-*C. albicans* Bgl2p antibodies, Dr. Manfred Nimtz, Anja Meier, Beate Jashok-Kentner and Dr. Josef Wissing (HZI) for their help in mass spectrometric and protein sequence analysis, Dr. Joop van den Heuvel and co-workers (HZI) for kindly providing knowledge, lab

space and equipment for cloning and recombinant protein expression, Dr. Matthias Stehr (HZI) for numerous attempts of protein purification, Dr. Michael Hust, Saskia Helmsing and Dr. Thomas Schirrmann (TU-Braunschweig) for attempts of identifying Bgl2p binding partners by phage display, Dr. Lothar Gröbe (HZI) for introducing flow cytometric analysis and Dr. Rebeca Alonso-Monge (Universidad Complutense de Madrid, Spain) for generously providing hAHGI strain. I would also like to thank all project partners from the *Taschentuchlabor* project for several important discussions during project meetings as well as the BMBF for financial support during PhD time. Special thanks belong also to the HZI Graduate School for providing an excellent PhD program as well as for financial support during conference participations.

I would also like to thank all present and past members of our BiSA group, especially Dr. Anna Buschart, Dr. Shuna Cui, Mohammed El-Mowafy and Dr. Rabeay Hassan, for the nice working atmosphere in lab and office. Also special thanks to Carolin Kanzler for being responsible for autoclaving service as well as for our microorganism strain collection.

My great and deep gratitude to my Mother, who supported me during the three years of my PhD in an inimitable way. Her endless attitude and devotion have always been a source of inspiration to me **شكراً أمي الحبيبة**.

Finally, I would like to thank all family members and friends in Syria and the Diaspora for their continuous support and encouragement, especially during the difficult times our country has witnessed in the past two years.

Hani Kaba, Northeim, 28.04.2013

Table of contents

List of Figures

List of Tables

List of abbreviations

aa	Amino acid(s)
BPS	Bathophenanthroline disulfonate
CHX	Cycloheximide
CM-H_2DCFDA	5-(and-6)-chloromethyl-2',7'-dichlorodihydrofluorescein diacetate, acetyl ester
CWP	Cell wall protein
ELISA	Enzyme Linked Immunosorbent Assay
FACS	Fluorescence activated cell sorting
Fdx	Fludioxonil
Fe^{3+}	Ferric iron
Fe^{2+}	Ferrous iron
Flc	Fluconazole
GH17	Glycosyl hydrolase domain 17
GPI	Glycosylphosphatidylinositol
HAIU	High affinity iron uptake
HRP	Horse radish peroxidase
Ipro	Iprodione
kDa	Kilo Daltons
LB	Luria-Bertani
MAP	Mitogen activated protein
MALDI-TOF	Matrix assisted laser desorption-ionisation-time of flight
MCFO	Multicopper ferroxidase
MeOH	Methanol
MSA	Multiple sequence alignment
NAC	N-acetyl cysteine
NACS	Non-albicans *Candida* species

OD	Optical density
PAGE	Polyacrylamide gel electrophoresis
PBS	Phosphate buffered saline
rBgl2p	Recombinant Bgl2p
rBgl2p-SP	Recombinant Bgl2p lacking signal peptide coding sequence
RFU	Relative fluorescence unit
RIM	Restricted iron medium
RIUP	Reductive iron uptake pathway
ROS	Reactive oxygen species
RT	Room temperature
SAV	Streptavidin
SC	Systemic candidiasis
SDS	Sodium dodecyl sulphate
SP	Signal peptide
TB	Terrific broth
Tf	Transferrin
TFs	Transcription factors
YNB	Yeast Nitrogen Base
YPD	Yeast Peptone Dextrose (Sufficient iron medium)

Summary

The aim of the thesis was to identify cell surface proteins of the pathogenic fungus *Candida albicans* which could be used for diagnostic purposes. Additionally, regulatory pathways, which govern the expression of such cell surface proteins, in particular those involved in iron uptake, were studied.

We applied different methods of cell surface proteins extraction and selected the ß-(1,3)-glucosyltransferase Bgl2p as first target protein for diagnosis of *C. albicans* infections. Based on sequence homologies as well as on a modeled structure of Bgl2p, we identified a unique 14 aa peptide from Bgl2p, against which monoclonal antibodies were produced by project partners. Different supernatants of hybridoma cell cultures, containing monoclonal antibodies directed against this peptide, could bind a recombinant version of purified Bgl2p. Furthermore, two of these monoclonal antibodies could bind to whole *C. albicans* cells in a manner that was most likely dependent on Bgl2p. Thus, these antibodies are promising tools for diagnosis of *C. albicans* infections.

Multicopper ferroxidase (MCFO) proteins are cell surface components of the reductive iron uptake pathway (RIUP) and were isolated from whole cells by heat extraction. As MCFOs expression was regulated by iron availability as well as by the high osmolarity glycerol (HOG) pathway, we studied phenotypic and molecular responses of *C. albicans* to different iron concentrations with respect to the activity of the Hog1p mitogen activated protein (MAP) kinase module of the HOG pathway in particular. This thesis shows, for the first time in fungi, that Hog1p of *C. albicans* is involved in the response to changes in extracellular iron concentrations. Hog1p was found to have a dual role in *C. albicans* iron homeostasis: basal Hog1p activity repressed high affinity iron uptake components independently of iron availability, and hyper-activity of Hog1p led to the activation of a specific response to high iron concentrations.

The effect of the HOG activating antifungal fludioxonil on the expression or activity of cell surface high affinity iron uptake proteins of the RIUP was investigated. Fludioxonil repressed RIUP components under conditions of iron restriction, during which these components are normally induced. Furthermore, fludioxonil decreased the growth of *C. albicans* during iron restriction. Interestingly, the fludioxonil mediated repression of RIUP components appeared to be independent of the HOG pathway, as well as of the iron responsive negative regulator of iron uptake proteins, Sfu1p. This indicates the existence of a complex regulatory network for iron uptake proteins involving Hog1p dependent as well as Hog1p independent components.

Zusammenfassung

Ziel dieser Doktorarbeit war die Identifikation von Zelloberflächenproteinen aus dem pathogenen Pilz *Candida albicans*, welche in der Diagnostik dieses Pilzes verwendet werden könnten. Weiterhin wurden regulatorische Mechanismen untersucht, welche die Expression von solchen Zelloberflächenproteinen, insbesondere Eisenaufnahmeproteinen, kontrollieren.

Wir haben verschiedene Methoden für die Isolierung von Zelloberflächenproteinen angewendet und wählten die ß-(1,3)- Glucosyltransferase Bgl2p als erstes Zielprotein zur Diagnose von *C. albicans* Infektionen. Auf der Basis von Sequenzhomologien sowie eines Modells für die Proteinstruktur von Bgl2p, konnten wir ein für *C. albicans* Bgl2p spezifisches 14 Aminosäuren langes Peptid identifizieren. Es wurden monoklonale Antikörper gegen dieses Peptid von Projektpartnern hergestellt. Mehrere solcher Antikörper, die aus Überständen von Hybridomazelllinien-Kulturen stammten, konnten eine rekombinante, aufgereinigte Version des Bgl2p binden. Zwei von diesen Antikörpern konnten auch an ganze *C. albicans* Zellen binden, höchstwahrscheinlich in Abhängigkeit von Bgl2p. Diese Antikörper sind somit vielversprechend für die diagnostische Erkennung von *C. albicans* Zellen.

Es wurden Eisenaufnahmeproteine aus der Gruppe der Multi – Copper – Ferroxidasen durch Hitzeextraktion isoliert. Da die Expression dieser Proteine sowohl durch Eisenverfügbarkeit als auch durch die Mitogen Aktivierte Protein Kinase Hog1p reguliert war, wurde die Rolle von Hog1p in der Antwort von *C. albicans* auf verschiedenen Eisenkonzentrationen untersucht. Es konnte zum ersten Mal bei Pilzen gezeigt werden, dass *C. albicans* Hog1p an der Antwort des Pilzes auf veränderte Eisenkonzentrationen im extrazellulären Milieu beteiligt ist. Die basale Hog1p Aktivität reprimiert die Expression von hoch affinen Eisen-Aufnahme Proteinen unabhängig von der Verfügbarkeit von Eisen, während die Hyper-Aktivität von Hog1p eine spezifische Antwort auf erhöhte Eisenkonzentrationen aktiviert. Das Hog1p-aktivierende Antimykotikum Fludioxonil reprimierte die Expression von hochaffinen Eisenaufnahmeproteinen des reduktiven Wegs selbst unter Eisenmangelbedingungen, unter denen diese normalerweise induziert werden. Weiterhin verursachte Fludioxonil leichte Wachstumsdefekte von *C. albicans* unter Eisenmangelbedingungen. Die Fludioxonil abhängige Repression von Eisenaufnahmeproteinen war jedoch weder von Hog1p, noch vom negativen Regulator von Eisenaufnahmeproteinen, Sfu1p, abhängig. Dies deutet auf einen komplexen Regulationsmechanismus von Eisenaufnahmeproteinen hin, der sowohl Hog1p-abhängige als auch -unabhängige Komponenten enthält.

Chapter 1 Introduction

1.1The fungal kingdom

Fungi constitute a large and diverse group of eukaryotic microorganisms, distinguished by successful adaptation to different environmental niches. The total number of fungal species is estimated to be 1.5 million of which merely 70000 have been described (Hawksworth & Rossman, 1997). Several fungi are of high value for humans. Yeasts of the genus *Saccharomyces* facilitate production of bred, beer and wine since thousands of years, while several filamentous fungi are important sources for production of antibiotics (*Penicillium spp.*) or antioxidants (*Aspergillus niger*). Others are used to protect crops from other microorganisms (*Trichoderma spp.*) and are thus of high importance for the global ecosystem. However, in addition to the high nutritional, medical or ecological value of several fungal species, other species belonging to this kingdom of eukaryotes have adapted to a parasitic lifestyle in plant (*Ustilago maydis*, *Magnaporthe grisea*), animal or human hosts (*Candida spp* and others, see below). Therefore, fungal pathogens could threaten human life in addition to causing devastating effects to the economy.

Fungal pathogens of humans evolved diverse lifestyles allowing them to infest different niches inside the host. Different host organs and tissues could be affected by fungal infections, such as mucocutaneous surfaces (*Candida spp.*), the respiratory system (*A. fumigatus*, *Cryptococcus neoformans*, *Histoplasma capsulatum*), or the skin (*Trichophyton spp.*, *Blastomyces dermatidiis*). Several factors are under consideration to elicit fungal infections. The use of immunosuppressive, chemotherapeutic as well as broad spectrum antibiotic agents has been proposed to boost the development of fungal infections in addition to HIV infection or other causes for immune disorders (Enoch et al, 2006). Indwelling

medical devices and implants such as catheters also provide a source for fungal infections, especially by *Candida spp*. (Kojic & Darouiche, 2004).

The diversity of fungal pathogens and their ability to adapt to different stress conditions, e.g., the acquirement of drug resistance, led to increased frequency of invasive fungal infections during the recent years (Pfaller, 2012). Thus, not only new active antifungal agents are urgently required, but in addition, a better understanding of fungal adaptation to hostile environments is needed.

The focus of this work is on the human pathogenic fungus *Candida albicans*, a commensal which can cause severe systemic infections, especially in patients with a compromised immune system.

1.2 *Candida albicans*

1.2.1 Classification, morphology, genetics and medical relevance

The genus *Candida* was first described by Christine Marie Berkhout at the University of Utrecht, the Netherlands, in 1923. However, the species *C. albicans* was isolated earlier by C.P. Robin in the 19th century as *Odium albicans* (Barnett, 2004).

Candida spp. belong to the phylum of the *Ascomycota*, or sac fungi, and are classified within the family of *Saccharomycetaceae* along with the baker's yeast *Saccharomyces cerevisiae*. About 150 *Candida spp.* are known, but only few of them have medical relevance. The *Candida* clade (Alby & Bennett, 2010; Butler et al, 2009) includes diploid (e.g. *C. albicans*, *C. dubliniensis*, *C. tropicalis*, *C. parapsilosis* and *Lodderomyces elongisporus*) as well as haploid (e.g. *C. guilliermondii*, *C. lusitaniae* and *Debaromyces hansenii*) yeasts (Figure 1.1). Not included in this clade is the pathogenic yeast *C. glabrata*, originally known as *Torulopsis glabrata*, which is haploid and is phylogenetically more related to *S. cerevisiae* (Dujon et al, 2004).

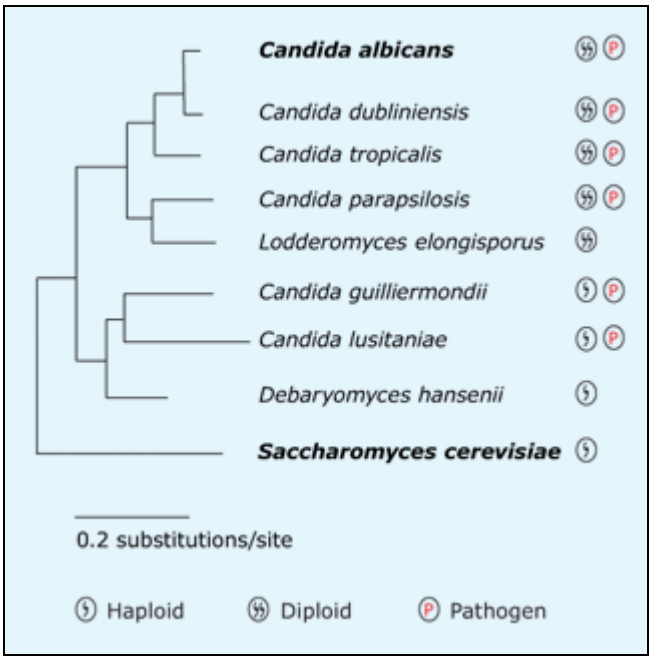

Figure 1.1 – Phylogeny of the *Candida* clade and *S. cerevisiae*.

Dendrogram acquired from http://www.broadinstitute.org/annotation/genome/candida_group/MultiHome.html.

C. albicans is characterized by polymorphism. It can grow as a unicellular yeast, as well as filamentous pseudo-hyphae or true hyphae (Figure 1.2). Pseudo-hyphae of *C. albicans* appear as elongated cells with constrictions at the septa, while true hyphae lack such structures and can be distinguished by their parallel-sided walls (Sudbery et al, 2004). Figure 1.2 shows these three morphologies of *C. albicans* within one culture. In addition to the three morphologies mentioned above, *C. albicans* can form chlamydospores, i.e. spores with thick cell walls seen under distinct growth conditions, such as carbon source starvation (Jansons & Nickerson, 1970).

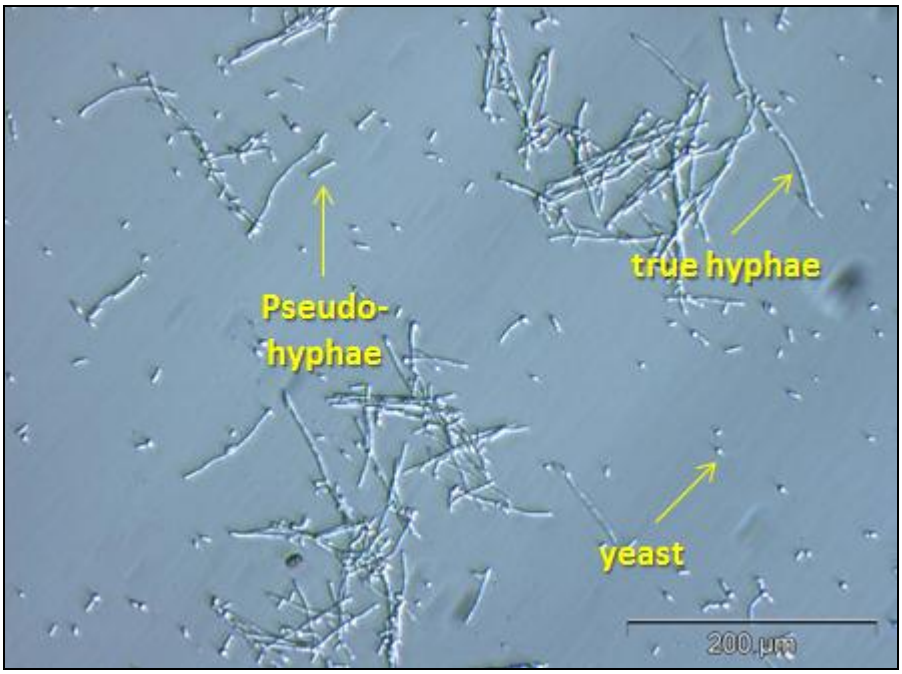

Figure 1.2 – The three morphological forms of *C. albicans*.

Microscopic analysis of SC5314 cells incubated in RPMI medium (+10% FBS) at 37 °C for 5 h. Arrows indicate the different morphologies (yeast, pseudo-hyphae and hyphae).

Eight chromosomes (1 – 7 and R) represent a haploid genome size of ca. 14.9 MBp containing up to 6400 open reading frames (ORFs) (Braun et al, 2005; Odds et al, 2004). The clinical isolate SC5314 was the first *C. albicans* strain to be sequenced.

For a long time, *C. albicans* was considered to be an imperfect fungus, lacking a complete sexual cycle. However, this yeast has been found to possess a DNA region, called the Mating Type Like (*MTL*) locus, orthologous to the mating type locus (*MAT*) of *S. cerevisiae* (Hull & Johnson, 1999). Engineered *C. albicans* cells were able to undergo mating both *in vitro* and in a murine infection model (Hull et al, 2000; Magee & Magee, 2000).

Additionally, mating competent haploid cells were recently discovered suggesting that *C. albicans* could be no more considered as an obligate diploid (Hickman et al, 2013).

Mating competent diploids have to be homozygous at the *MTL* (*MTL***a/a** or *MTL*α/α locus). Such cells have been termed "opaque" because of the appearance of colonies formed by those cells on agar plates (Slutsky et al, 1987). Opaque cells are elongated, thus differing

morphologically from the “white” colonies, formed by the round to oval yeasts. Mating competence could result either from mitotic recombination or from loss of one copy of chromosome 5 and duplication of the homologous chromosome (Sasse et al, 2013). White-to-opaque switch in *C. albicans* is regulated by the Wor1p transcription factor. In strains which are heterozygous at the *MTL* locus, the a1-α2 factor represses Wor1p expression to basal levels, thus locking the cells in the white phase. The repression of Wor1p is relieved in *MTL* homozygous cells, which allows switching to the opaque phase when Wor1p levels are above a critical threshold. This phenomenon points to the stochastic nature of the white-to-opaque switch regulation (Morschhauser, 2010b).

Another important genetic feature of *C. albicans* is the non-standard codon usage, whereby CTG encodes serine instead of leucine (Santos & Tuite, 1995). This may complicate heterologous expression of *C. albicans* proteins in other organisms like *Escherichia coli*.

C. albicans is an opportunistic pathogen. It colonizes as commensal up to 30 – 70% of healthy individuals (Gow et al, 2012). Patients with a compromised immune system are at high risk to acquire systemic infections by *Candida spp.*, which constitute the fourth highest cause for nosocomial bloodstream infections with a lethality rate of up to 40% (Pfaller & Diekema, 2007). One of the reasons for the success of *C. albicans* as a pathogen is its high adaptability to various environmental niches, which are characterized by the availability of nutrients and essential elements.

Cell surface proteins are of high importance for pathogens, and have a wide range of functions, as enzymes, receptors or transporters. They play a role in adhesion to host tissues, cell-cell aggregation, nutrient uptake, efflux of deleterious compounds or remodeling of the cell wall (Chaffin, 2008; Hiller et al, 2011; Morschhauser, 2010a; Verstrepen & Klis, 2006). By this, cell surface proteins support the adaptation of *C. albicans* to environmental changes.

1.2.2 The *C. albicans* cell wall

The cell wall is the outermost boundary of fungal cells. It confers rigidity and protection from alterations of chemical and physical parameters in the surrounding milieu. Additionally, cell walls of fungal pathogens play a major role in virulence, as adhesion and first interaction of pathogenic fungi with host cells are mediated by cell wall components (Ruiz-Herrera et al, 2006). Basically, the cell wall of *C. albicans* shows similar molecular organization to that of the baker's yeast *Saccharomyces cerevisiae* (Gozalbo et al, 2004). Previous studies have shown that the *C. albicans* cell wall is composed of a network of three major polysaccharides. Mannans, ß-glucans and chitin, make up 80 to 90 % of the cell wall composition, whereas proteins and lipids (e. g. phospholipomannan) present about 5 – 20 % and 1 – 7 % respectively (Gozalbo et al, 2004). A schematic structure of the *C. albicans* cell wall is shown in Figure 1.3.

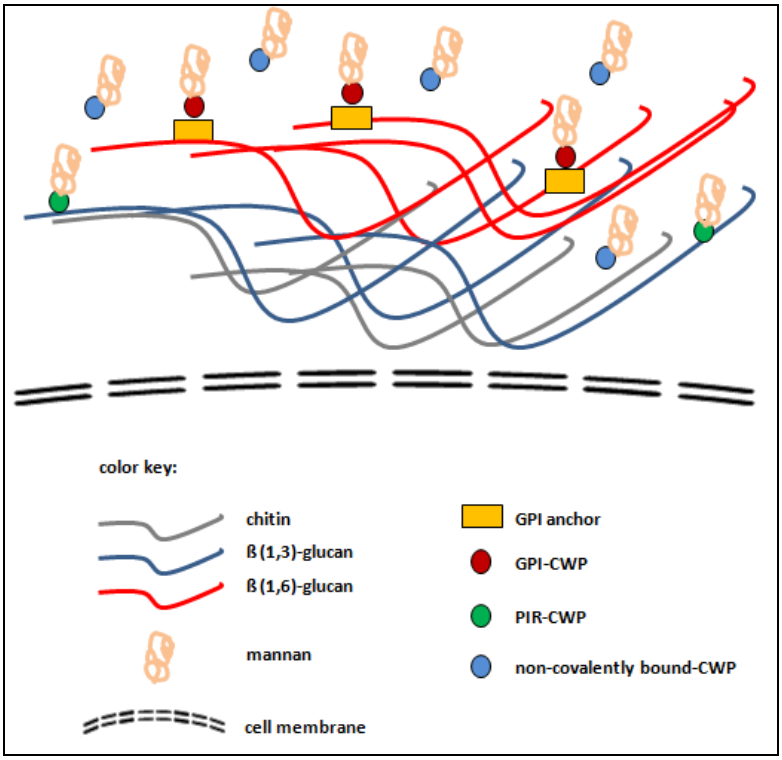

Figure 1.3 – Schematic organization of the *C. albicans* cell wall.

1.2.2.1 Cell wall carbohydrates

ß-glucans are glucose polymers containing ß-(1,3)- and ß-(1,6) -linkages, while chitin is the polymer of N-acetyl-D-glucosamine (GlcNAc) and mannan the polymer of mannose, an isomer of glucose. ß-glucans and chitin are prevalently located in the inner layer of the cell wall and are responsible for cell wall rigidity. Mannose polymers (linked to mannoproteins) cover the cell wall's outermost layer forming the so called "mannan coat".

The human immune system is able to bind *C. albicans* yeast ß-glucans by means of the dectin-1 receptor. Thus, *C. albicans* shields its cell wall glucan network underneath outer cell wall components (e.g. the mannan coat), rendering it hidden and thus inaccessible by phagocytes (Gantner et al, 2005).

Synthesis of ß-(1,3)-glucans is inhibited by echinocandine antifungals such as caspofungin, micafungin or anidulafungin (Kofla & Ruhnke, 2011). *C. albicans* responds to such cell wall perturbing agents by inducing the cell wall integrity and cell wall remodeling pathways leading to increased cell wall chitin content as well as to induction of the expression of proteins involved in glucan branching (Angiolella et al, 2009; Costa-de-Oliveira et al, 2013; Roman et al, 2009; Walker et al, 2008). The role of mitogen activated protein (MAP) kinases in response to cell wall stresses will be discussed in later parts of this chapter.

1.2.2.2 Cell wall proteins

Cell wall proteins (CWPs) are generally divided in two major classes according to the nature of their attachment to the *C. albicans* cell wall: covalently and non-covalently bound CWPs. The most abundant covalently bound CWPs are linked to ß-(1,6)-glucan through a glycophosphatidylinositol (GPI) anchor remnant (GPI-CWPs). GPI-CWPs are linked to the ß-(1,6)-glucan polymer by phosphodiester bonds that can be specifically cleaved by HF-pyridine, thus releasing GPI-CWPs from the cell wall (de Groot et al, 2004). It was suggested,

that the GPI anchors might play a role in targeting those proteins to the cell surface (Chaffin, 2008).

PIR proteins (Proteins with internal repeats) constitute another class of CWPs which are covalently attached to the polysaccharide network. These proteins are linked directly to ß-(1,3)-glucan by alkali sensitive linkages and are thus extractable by NaOH treatment (de Groot et al, 2004).

On the other hand, non-covalently bound CWPs lack any covalent attachment to cell wall polysaccharides. Such proteins can be removed from cell wall preparations by heat (Klebl & Tanner, 1989) or with denaturing agents such as urea or combination of SDS and heat (de Groot et al, 2004; Rico et al, 1997). Some of these proteins may be secreted to the external milieu or have substrates within the cell wall (Goldman et al, 1995; Hartland et al, 1991; Hiller et al, 2007; Sorgo et al, 2010).

Several proteins with cytosolic functions were reported to be localized on the cell surface of *C. albicans* (Eroles et al, 1997; Gil-Navarro et al, 1997; Urban et al, 2003). Some of these proteins have been implicated with binding to host extracellular matrix proteins thus indicating a moonlighting activity (Crowe et al, 2003).

In general, CWPs could be involved in a variety of function such as cell wall assembly and remodulation, adhesion to host cells and tissues or potentially acting as modulators of the host immune system (Nather & Munro, 2008). Additionally, others are involved in the cell response to stress situations, e.g. heat shock (Chaffin et al, 1998; Lopez-Ribot et al, 1996) or exposure to antifungal drugs (Angiolella et al, 2002; Angiolella et al, 2009).

The cell wall proteome of *C. albicans* is dependent on the morphology. It has been reported that hyphal cell walls have a characteristic protein composition (Heilmann et al, 2011). Furthermore, it has been suggested that some CWPs could carry a “morphogenetic code”, resulting in active modulation of the molecular organization of the cell wall constituents

(Valentin et al, 2000). Other works reported that some cell wall proteins, which are usually located in the outer surface of the cell wall in one morphology, are found cryptic following dimorphic transition (Ollert & Calderone, 1990).

Alterations in the cell wall proteome generate cell surface variation, boosting the immune evasion strategies of the fungus. Such generation of cell surface variation could possibly be accomplished at least through three processes:

(i) By transcriptional or post-transcriptional regulation of CWP expression leading thus to changes in cell wall proteome composition.

(ii) By alteration of characteristic properties of individual proteins.

(iii) By differential glycosylation of proteins targeted to the cell wall (Nather & Munro, 2008).

Thus, expression, regulation, localization and functional analysis of CWPs have been subjected to intensive studies for the past years.

1.2.2.3 Adhesion, aggregation and biofilm formation

Adhesion of fungal cells is mediated by specialized cell surface proteins, which can bind amino acids or sugar residues present on surfaces of other cells (Verstrepen and Klis, 2006).

Adhesion of *C. albicans* to host cells and tissues as well as to implants is mediated by several cell wall proteins. The Agglutinin Like Sequence (ALS) family of *C. albicans* includes at least eight glycoprotein encoding genes (*ALS1* to *ALS7* and *ALS9*) (Hoyer et al, 2008). Recently, a new gene was described in the *C. albicans* WO-1 strain resulting from a recombination event between the adjacent *ALS1* and *ALS5* genes (Zhao et al, 2011). Members of the ALS protein family have been implicated in adhesion and biofilm formation (Hiller et al, 2011; Hoyer et al, 2008; Murciano et al, 2012), as in iron uptake or cellular aggregation (Almeida et al, 2008; Fu et al, 2002; Gregori et al, 2011). Expression of the ALS members Als1p and Als5p in *S. cerevisiae* allowed this non-pathogenic yeast to adhere to human cells

and extracellular matrix components as well as to synthetic peptides (Fu et al, 1998; Gaur & Klotz, 1997; Klotz et al, 2004).

Some *C. albicans* adhesins are restricted to the yeast form, such as Yw1p, while others are hyphae specific, such as Als3p or Hwp1p. Transcripts of *HWP1* are only found in hyphae but never in blastospores, so that this specificity could be used as reporter (Almeida et al, 2008; Granger et al, 2005; Heintz-Buschart et al, 2012; Staab et al, 1996; Staab & Sundstrom, 1998; Uhl & Johnson, 2001).

Adhesion of *C. albicans* cells to each other mediates the formation of large aggregates or 'flocs'. Flocculation in yeasts is defined as a non-sexual, homotypic, reversible and multivalent aggregation of thousands to millions of yeast cells leading to the formation of flocs (Soares, 2011). Due to its importance in brewing industry, flocculation of yeasts has been under extensive study during the past century. As flocculation in yeasts is known to be induced on response to stress situations (Verstrepen & Klis, 2006), the interest in studying this phenomenon in pathogenic yeasts increased. *C. albicans* is known to flocculate in response to various changes in the surrounding milieu, such as nutrient availability or exposure to different chemicals (Bianchi, 1964; Cleary et al, 2012; Gregori et al, 2011; Kaba et al, 2013; Kamaya, 1969). One of the mechanisms resulting in this form of cellular aggregation is the interaction of carbohydrate binding proteins (lectins) of one cell with mannans attached to proteins on the other cell. However, knowledge on the molecular level is still sparse.

Biofilms are surface associated populations of microorganisms embedded in a matrix of extracellular polymeric substances (Nobile et al, 2009). *C. albicans* has the ability to form biofilms on both biotic (mucosa) as well as abiotic (medical devices such as catheters or dental prosthetics) substrates (Mayer et al, 2013). *C. albicans* biofilms have increased resistance to several antifungals including fluconazole, amphotericin B, nystatin and

voriconazole (Fanning & Mitchell, 2012). The architecture of *Candida* mucosal biofilms is complex. They include yeast and hyphal morphologies, as well as commensal bacterial species and host components (Dongari-Bagtzoglou et al, 2009).

1.2.3 Iron uptake

1.2.3.1 Iron availability in the host

Iron is essential for almost all organisms as it is a co-factor of a variety of proteins involved in important cellular processes. Its biological importance is attributed to its ability to undergo single electron redox reactions, thus oscillating between the oxidized ferric (Fe^{3+}) and the reduced ferrous (Fe^{2+}) states. However, this redox reactivity itself is a potent source of toxicity as ferrous iron leads to the generation of the highly reactive hydroxyl radical ($OH^{\cdot}$) by Fenton chemistry (Hentze et al, 2004).

Iron acquisition by pathogens is a limiting factor for fungal, bacterial and protozoan infections (Nairz et al, 2010; Schaible & Kaufmann, 2004; Sutak et al, 2008; Weinberg, 2009). Thus, iron accessibility for pathogens is restricted in mammalian hosts by proteins which bind iron with high affinity, such as hemoglobin, transferrin and ferritin (Weinberg & Miklossy, 2008). This strategy of iron withholding restricts iron accessibility to pathogens in addition to the reduction of iron mediated toxicity. However, most pathogens on their turn have developed different strategies for iron acquisition to counteract this restricted iron environment inside the host.

The major iron binding protein in human serum is transferrin. This glycoprotein has a high Fe^{3+} chelation affinity at physiological pH. Transferrin's affinity for iron ions decreases with increased acidity (Jurado, 1997). Each transferrin molecule has two ferric iron ion binding sites (Harris, 2012). Accordingly, serum transferrin can be present as di-ferric transferrin (loaded with two Fe^{3+} ions; saturated transferrin), mono-ferric transferrin (loaded with one Fe^{3+} ion) or apo-transferrin (iron free). In healthy individuals, ca. 30% of total transferrin

molecules are saturated. However, iron overload, due to hereditary hemochromatosis or due to repeated blood transfusions in thalassemia and leukemia patients (Hunter et al, 1984; Musallam et al, 2012; Siddique & Kowdley, 2012), results in high iron saturation of transferrins thus increasing the risk of elevated free iron concentrations.

Human serum has been known for a long time to inhibit *C. albicans* growth, mainly through the iron chelating activity of apo-transferrin (Caroline et al, 1969; Minn et al, 1997). Such effect could be abolished by addition of iron to the growth medium or in sera with high saturation of transferrin as found in leukemia patients. Indeed, *C. albicans* infections are known associated with leukemia or other diseases with iron overload (Bullen et al, 2006; Khan et al, 2007).

In general, iron uptake during infection by *C. albicans* is considered as virulence factor (Almeida et al, 2009). Pretreatment with iron chelators protected endothelial and epithelial cells from *C. albicans* mediated injury, while loading cells with iron reversed this effect (Almeida et al, 2008; Fratti et al, 1998). Furthermore, genes of iron acquisition proteins were upregulated during *C. albicans* liver tissue infection (Thewes et al, 2007). On the other hand, iron availability was linked to drug resistance as well as to morphology of this fungus (Hameed et al, 2008; Prasad et al, 2006).

1.2.3.2 *C. albicans* iron uptake systems

Three systems for iron uptake by *C. albicans* are known:

(i) Recently, a heme uptake system allowing the utilization of iron bound to hemoglobin was identified, including hemoglobin receptors, e.g. Rbt5p (Weissman & Kornitzer, 2004; Weissman et al, 2008).

(ii) *C. albicans* acquires iron from ferrichrome type siderophores via the receptor Sit1p (Heymann et al, 2002; Lesuisse et al, 2002). Considering the lack of genes required for siderophore biosynthesis in *C. albicans*, it is believed that

this pathway allows the uptake of iron bound to siderophores produced by other pathogens or commensals (Almeida et al, 2009).

(iii) The third pathway is called the reductive pathway, as first ferric iron is reduced to ferrous iron by membrane associated ferric reductases (Morrissey et al, 1996), before being reoxidized by members of the multicopper ferroxidase (MCFO) family (Knight et al, 2002).

MCFOs form together with the iron permease Ftr1p a high affinity iron uptake (HAIU) complex in the plasma membrane (Ramanan & Wang, 2000; Ziegler et al, 2011). This pathway was shown to be responsible for iron uptake not only from iron salts but also from iron loaded host proteins such as transferrin and ferritin (Almeida et al, 2008; Knight et al, 2005). Loss of *FTR1* rendered *C. albicans* completely avirulent in a mouse model of systemic infection and abolished damage of oral epithelial cells (Almeida et al, 2008; Ramanan & Wang, 2000). This underlines the importance of this pathway for virulence of *C. albicans*. Figure 1.4 shows a schematic illustration of the *C. albicans* reductive iron uptake pathway (RIUP).

Whereas reduction of ferric iron to ferrous iron by reductases increases solubility and availability of iron, the function of MCFOs leading to the re-oxidation of Fe^{2+} is not as well understood. Complex formation with the permease and channeling of Fe^{3+} could maintain the availability of iron and deliver iron in the oxidized, i.e. the less reactive and toxic form, to the cytosol.

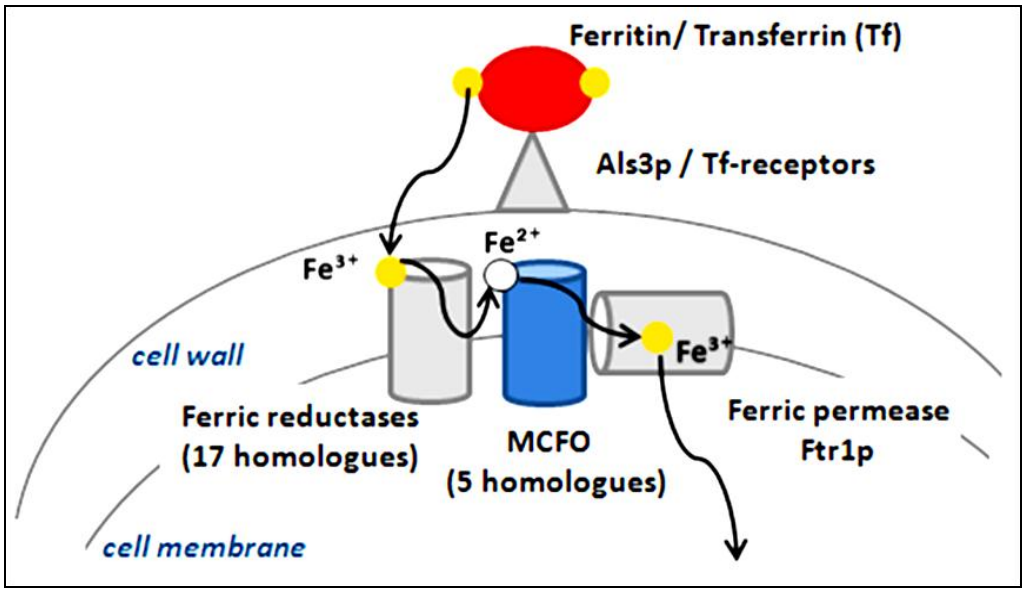

Figure 1.4 – Schematic illustration of the *C. albicans* reductive iron uptake pathway (RIUP).

C. albicans is able to acquire both free as well as host-protein bound iron (e.g. by ferritin or transferrin; red ellipse) by means of this pathway. Iron binding host proteins are bound by their respective receptors (grey rectangles). Ferric iron (oxidized, yellow circles) is first reduced (Fe^{2+}; white circle) by means of membrane associated ferric reductases (vertical grey cylinder), and becomes subsequently re-oxidized by one or more multicopper ferroxidase (MCFO) member (blue cylinder). The resulting oxidized iron is channeled by means of a ferric permease Ftr1p (horizontal grey cylinder) to intracellular compartments.

1.2.3.3 Regulation of iron uptake components in *C. albicans*

Due to the toxic potential of iron by generating reactive oxygen species (ROS) (Galaris & Pantopoulos, 2008), cellular iron homeostasis is subjected to tight regulation. Several microorganisms possess transcriptional repressors which are responsible for downregulation of iron uptake genes under sufficient iron conditions, such as the bacterial *Fur* repressor (Cornelis et al, 2011; Smaldone et al, 2012). In several fungi, iron uptake genes are mainly repressed by GATA family transcription factors which are believed to act as iron sensors (Haas, 2012; Haas et al, 1999; Jung et al, 2006; Pelletier et al, 2002; Zhou et al, 1998).

In *C. albicans*, the transcriptional regulators Sfu1p, Hap43p and Sef1p constitute what is known as the iron responsive regulatory network (IRRN) (Chen et al, 2011) (Figure 1.5). Sfu1p is a GATA-type repressor, which is active under high iron conditions and negatively

regulates genes encoding for ferric reductases, MCFOs, iron permeases, as well as Hap43p, the regulatory element of the CCAAT-binding complex (CBC) (Chen et al, 2011; Lan et al, 2004). Hap43p is a transcription factor that is activated under low iron conditions and represses the expression of Sfu1p and of iron utilization genes so that repression of genes involved in iron uptake is relieved and the limited amount of iron is efficiently used for vital proteins (Hsu et al, 2011). Sef1p was identified recently as a transcriptional activator of iron uptake genes (Homann et al, 2009), and is repressed by Sfu1p, but activated under low iron conditions. It induces Hap43p and iron uptake genes, such as *FET3* (encoding an MCFO), as well as a copper-transporting ATPase encoding gene (*CCC2*) required for MCFO activity (Chen *et al.* 2011). Very recently, Sfu1p was found to regulate iron uptake by post-transcriptionally inhibiting Sef1p in addition to its inhibition on transcriptional level (Chen & Noble, 2012).

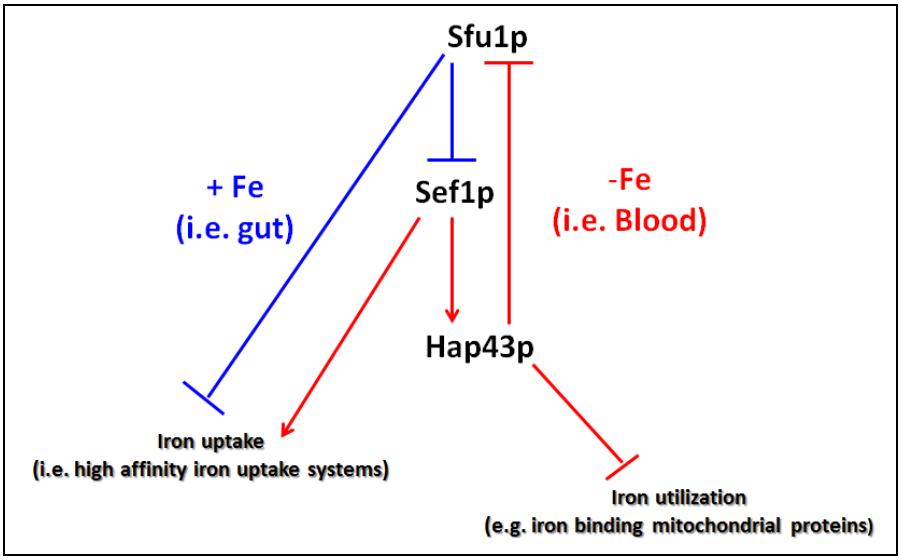

Figure 1.5 – The iron responsive regulatory network of *C. albicans*.

C. albicans possesses a network of three transcription factors (Sfu1p, Sef1p and Hap43p), which is responsible for adaptation of this fungus to host niches with different iron availability. Under iron repleted conditions, Sfu1p negatively regulates Sef1p on both transcriptional and post-transcriptional levels. Under iron depleted conditions, Sef1p activates Hap43p expression which negatively regulates Sfu1p as well as iron utilizing proteins. Sef1p induces expression of high affinity iron uptake proteins.

In addition to the IRRN, other transcription factors, such as Tup1p and Rim101p, are involved in regulation of iron uptake genes, but their roles are not as obvious. Tup1p is a global repressor which may be recruited to iron responsive genes via interaction with Sfu1p (Lan et al, 2004), while regulation by Rim101p is influenced by pH (Bensen et al, 2004). This complex regulation of iron uptake probably helps *C. albicans* to successfully adapt to niches with different iron levels (Chen et al, 2011).

1.2.4. Morphologic switching

Morphologic switching is a central factor in virulence of *C. albicans*. While the hyphal morphology accounts for invasive growth in host tissues (Sudbery et al, 2004), the yeast form is important for dissemination and colonization of the host especially in the early stage of infection (Saville et al, 2003; Thompson et al, 2011). Thus, both morphologies contribute to the infection process.

In filamentous fungi, hyphae grow as filaments in a polarized manner with accumulation of secretory vesicles at the apical tip, forming an organelle known as the *Spitzenkörper* (Steinberg, 2007). *C. albicans* possess such an organelle which is only found in hyphal cells (Crampin et al, 2005).

Several parameters are known to induce formation of hyphae. Neutral to basic pH, growth at 37 °C as well as the presence of serum shift *C. albicans* morphology towards the hyphal form. Remarkably, all of these factors are present in the bloodstream. Furthermore, quorum sensing compounds such as homoserinelactone or farnesol repress hyphae formation while N-acetyl glucosamine and nitrogen limitation induce it (Sudbery, 2011).

1.2.5. Stress activated signaling pathways and stress adaptation in *C. albicans*

C. albicans is confronted with different stress situations inside the host. Phagocytes such as macrophages induce reactive oxygen (ROS) and nitrogen (RNS) species (Brown et al, 2009). Nutrient scantiness inside the host is a further stress factor. Additionally, antifungal drug

treatment demands further flexibility in order to survive. In order to adapt successfully to such hostile environments, *C. albicans* possesses a complex network of signaling pathways which regulate cellular responses to different stress situations.

Hog1p encodes the mitogen activated protein kinase (MAPK) orthologous to human p38 (Cheetham et al, 2011) and to stress – activated protein kinases (SAPK) in other yeasts (Enjalbert et al, 2006). In *C. albicans*, Hog1p responds to at least three environmental stresses; namely osmotic, oxidative and cell wall stress (Monge et al, 2006). In response to those stresses, Hog1p becomes phosphorylated and translocates to the nucleus (Smith et al, 2004). *hog1* null mutants were found to be hypersensitive to those stress conditions, which lead to Hog1p activation, in particular to extracellular oxidizing agents (Alonso-Monge et al, 2003; Smith et al, 2004). At least the response to oxidative and osmotic stress depends on the mitogen activated protein kinase kinase Pbs2p (Arana et al, 2005). Among the substrates of Hog1p is the transcription factor Sko1p (Alonso-Monge et al, 2010) so that the activation of Hog1p modulates gene expression profiles (Enjalbert et al, 2006).

The fungal cell wall is considered as an attractive target for antifungal drug development, as this organelle is missing in humans (Gozalbo et al, 2004). As mentioned in 1.2.2.1, echinocandine antifungals represent a major class of cell wall targeting drugs. *C. albicans* responds to cell wall stress by means of the cell integrity pathway, with Mkc1p as its final MAPK (Ernst & Pla, 2011). The MAPK Cek1p is involved in cell wall biosynthesis and responds to caspofungin mediated cell wall damage as does Mkc1p. In this case, the activation of Cek1p is dependent on the cell surface sensor mucin Msb2p (Roman et al, 2009).

1.2.6 Diagnostic approaches for *C. albicans* and other *Candida spp.* in infected patients

Due to the high mortality rate of *Candida spp.* infections, early identification of *Candida spp.* is very important for successful treatment.

The microorganisms can be detected in whole blood, serum, saliva or other body fluids or on mucosal surfaces. Approaches based on blood cultivations are time consuming and in many cases insensitive as fungemia is thought to occur with only < 10 CFU/ mL of whole blood (Pryce et al, 2003). Thus, rapid identification is required especially the case in the early phase of infection.

Several other techniques have been used for diagnosis of *C. albicans* based on nucleic acid (Pryce et al, 2003), protein (Lain et al, 2007) or carbohydrate (Lew et al, 1982; Ostrosky-Zeichner et al, 2005) detection. Approaches which are based on the detection of anti- *C. albicans* antibodies in serum are not appropriate for immunocompromised patients, since the immune response of those individuals is severely restricted.

Specificity of the applied tests is also critical for correct treatment, since some *Candida spp.* are resistant to antifungals, such as *C. glabrata* (Fidel et al, 1999). Thus, correct identification of the *Candida spp.* is critical for convenient selection of antimycotic therapy (Kragelund et al, 2013). Furthermore, distinguishing infection from colonization would also be of great importance for diagnostic approaches. This could be achieved by targeting antigens involved in virulence.

Detection of *Candida spp.* is thus currently one of the most important fields of microbial diagnosis with new tools being permanently described for this purpose (El-Kirat-Chatel et al, 2013; Neely et al, 2013)

1.3 Aim of this study

Within the "*Lab in a Hankie*[1]" project, we aimed to identify cell wall proteins which could serve as diagnostic markers for *C. albicans* infections. The main target of this project is to specifically recognize viable pathogens, such as *C. albicans*, by sensor molecules (e.g.

[1] http://www.taschentuchlabor.de/index1a6a.html?id=75

antibodies), which recognize the pathogen through proteins present on the pathogen cell's surface. This would help early identification of the pathogen and thus shortens diagnosis time and accelerates suitable medical treatment of the infected patient. Suitable target proteins should be identified for this aim and antibodies recognizing these proteins should be generated and evaluated on recognizing whole *C. albicans* cells. The desired antibodies should be specific for *C. albicans* and allow differentiation between *C. albicans* and non-albicans *Candida* species.

The ability of *C. albicans* to adapt to various stress situations enabled this pathogen to persist in hostile environments inside the host. Although iron accessibility by pathogens is restricted by healthy hosts, several hematological or genetic diseases have been connected with iron disorders; including iron overload. The increase of free iron means this nutrient would be more accessible for pathogens; however, iron toxicity constitutes a major stress factor for those pathogens. *C. albicans* infection has been known to be associated with iron overload diseases (Caroline et al, 1969) and this fungus has been suggested to grow well during iron overload conditions (Minn et al, 1997). However, the mechanisms allowing this fungus to adapt to high iron concentrations are still unknown. Even though transcriptional regulators of the iron responsive network were identified, signaling pathways, which govern the activity of these regulators, are less well known. Four iron uptake genes, namely the ferric reductase *FRE10*, the hemoglobin receptor *RBT5*, the high affinity iron permease *FTR1* and the MCFO *FET34*, were found to be de-repressed in cells lacking *HOG1* under sufficient iron conditions, which are usually repressive for these genes (Enjalbert et al, 2006). As mentioned above, Hog1p becomes activated by phosphorylation in a Pbs2p (MAPKK) dependent manner. Thus, an aim of this thesis was to determine whether the Hog1p MAPK plays a role in the response to iron availability.

Synergistic use of iron chelators and drugs which repress the expression of *C. albicans* high affinity iron uptake (HAIU) proteins could help fighting *C. albicans* infections of iron overload patients. Repression of HAIU components during iron restricted conditions (created by the iron chelators) should prevent *C. albicans* from full utilization of its HAIU machinery and may thus affect its growth. As the antifungal compound fludioxonil is known to activate the HOG pathway of *C. albicans* by targeting the histidine kinase Cos1p upstream of Hog1p (Buschart et al, 2012b; Ochiai et al, 2002), we studied whether fludioxonil had any effect on the expression or enzymatic activity of iron uptake proteins of the reductive pathway. Fludioxonil was further tested on its effect on *C. albicans* growth under conditions of different iron availability.

Chapter 2 Materials and Methods

2.1 Strains, media and culture conditions

C. albicans strains used in this study are listed in Table 1. DAY286, JJH37, JMR114 JJH31, FB63-1 and FB63-3, TF117, TF147 and TF156 were purchased from the Fungal Genetics Stock Centre (Kansas, USA) (McCluskey et al, 2010). Strains CNC13, BRD3 and hAHGI were kind gifts from Jesús Plá and co-workers (Madrid, Spain) (Arana et al, 2005; San Jose et al, 1996). *Escherichia coli* strains are listed in Table 2.

Routinely, all *C. albicans* strains were cultivated overnight (16 - 24 h) from frozen glycerol stocks in 20 or 50 ml YPD medium (Sigma-Aldrich Y1375) at 30 °C. Preparation of all cultures was performed under sterile conditions (MaxiSafe 2020 or Herasafe clean benches, Thermo Scientific). Inoculation loops were sterilized by sufficient glowing by means of Fireboy and Fireboy eco (Integra Biosciences) Bunsen burners. Unless otherwise indicated, incubation of *C. albicans* liquid cultures in growth media was performed in Multitron Shakers (Infors-HT) at 30 °C or 37 °C and 160 rpm. Growth was followed by measurements of optical densities (OD) of cultures at λ = 600 nm (OD_{600}) in transparent 96 well plates by the µQuant microtiter plate reader (Biotek, Bad Friedrichshall, Germany) in triplicates (each 180 µl). Liquid media used in this study are summarized in Table 3.

Table 1 - *C. albicans* strains used in this work.

Strain	**Genotype**	**Reference**
SC5314 (MYA-2876)	Wild type (WT)	(Gillum et al, 1984)
CAF2-1	*URA3/ura3::imm434 IRO1/iro1::imm434*	(Fonzi & Irwin, 1993)
DAY286	*ura3*Δ*::imm434/ura3*Δ*::imm434, iro1/iro1, ARG4::URA3::arg4::hisG/arg4::hisG, his1::hisG /his1::hisG*	(Davis et al, 2002)
JMR114 (Δ*hog1*)	*ura3*Δ*::imm434/ura3*Δ*::imm434, iro1/iro1, arg4::hisG/arg4::hisG,his1::hisG/his1::hisG, hog1::ARG4/ hog1::URA3*	(Nobile & Mitchell, 2009)
CNC13 (Δ*hog1*)	*ura3*Δ::*imm434/ura3*Δ::*imm434, iro1/iro1, his1*Δ::*hisG/his1*Δ::*hisG hog1*::*hisGURA3-hisG/hog1*::*hisG*	(San Jose et al, 1996)
JJH31 (Δ*pbs2*)	*ura3*Δ*::λimm434/ura3*Δ*::λimm434, iro1/iro1, arg4::hisG/arg4::hisG,his1::hisG/his1::hisG, pbs2::ARG4/ pbs2::URA3*	(Nobile & Mitchell, 2009)
BRD3 (Δ*pbs2*)	*ura3*Δ*::imm434/ura3*Δ*::imm434, iro1/iro1, his1*Δ*::hisG/his1*Δ*::hisG pbs2*Δ : : cat/*pbs2*Δ :: cat-*URA3*-cat	(Arana et al, 2005)
hAHGI (Δ*hog1 + HOG1)*	*CNC13, ACT1p-HOG1-GFP : : leu2/LEU2*	(Arana et al, 2005)
JJH37(Δ*cos1*)	*ura3*Δ*::λimm434/ura3*Δ*::λimm434, iro1/iro1, arg4::hisG/arg4::hisG,his1::hisG/his1::hisG, cos1::ARG4/ cos1::URA3*	(Nobile & Mitchell, 2009)
FB63-1 and FB63-3 (Δ*bgl2*)	*ura3*Δ*::imm434/ura3*Δ*::imm434, iro1/iro1, arg4::hisG/arg4::hisG,his1::hisG/his1::hisG, bgl2::ARG4/ bgl2::URA3*	(Nobile & Mitchell, 2009)
WT-arg	*arg4*Δ*/arg4*Δ *LEU2/leu2*Δ *HIS1/his1*Δ *URA3/ura3*Δ::*imm434 IRO1/iro1*Δ::*imm434*	(Homann et al, 2009)
TF156 (Δ*efg1*)	*arg4*Δ*/arg4*Δ *LEU2/leu2*Δ *HIS1/his1*Δ *efg1*Δ*/efg1*Δ *URA3/ura3*Δ::*imm434 IRO1/iro1*Δ::*imm434*	(Homann et al, 2009)
TF117 (Δ*tup1*)	*arg4*Δ*/arg4*Δ *LEU2/leu2*Δ *HIS1/his1*Δ *tup1*Δ*/tup1*Δ *URA3/ura3*Δ::*imm434 IRO1/iro1*Δ::*imm434*	(Homann et al, 2009)
TF147 (Δ*sfu1*)	*arg4*Δ*/arg4*Δ *LEU2/leu2*Δ *HIS1/his1*Δ *sfu1*Δ*/sfu1*Δ *URA3/ura3*Δ::*imm434 IRO1/iro1*Δ::*imm434*	(Homann et al, 2009)

Table 2 - *E. coli* strains used in this work.

Strain	Genotype	Reference
XL-1 BLUE	*rec*A1 *end*A1 *gyr*A96 *thi*-1 *hsd*R17 *sup*E44 *rel*A1 *lac*	(Arias et al, 2000)
Rosetta™ 2 (DE3)	*F⁻ompT hsdS*$_B$ (r_B^- m_B^-) *gal dcm* pRARE2 (cam^R)	(Machner & Isberg, 2006)
*Ca_BGL2*_FLAG3x_His8x_-SP3	Rosetta™ 2 (DE3) + *Ca_BGL2*_FLAG3x_His8x_-SP	This study
*Ca_BGL2*_FLAG3x_His8x_+SP6	Rosetta™ 2 (DE3) + *Ca_BGL2*_FLAG3x_His8x	This study

Table 3 – Liquid growth media used in this work.

Medium	Composition
RPMI	8.4 g l^{-1} RPMI 1640 (Sigma-Aldrich R1383), 2 g l^{-1} glucose, 0.165 M 3-(N-morpholino) propanesulfonic acid (MOPS), adjusted to pH 7.3 with 10 N NaOH
YNB	6.7 g l^{-1} Yeast Nitrogen Base (Sigma Y1250), 2 g l^{-1} glucose, 0.165 M 3-(N-morpholino) propanesulfonic acid (MOPS), adjusted to pH 7.3 with 10 N NaOH
YPD	Sufficient iron medium; 10 g l^{-1} yeast extract, 20 g l^{-1} peptone, 20 g l^{-1} dextrose (Sigma-Aldrich Y1375)
RIM	Restricted iron medium; YPD + 200 µM bathophenanthroline disulfonate (BPS) (Sigma 146617)
TB	Terrific Broth; 12 g l^{-1} tryptone, 24 g l^{-1} yeast extract, 0.4 % (v/v) glycerol, 2.31 g l^{-1} KH_2PO_4, 12.54 g l^{-1} K_2HPO_4
LB	Luria-Bertani low salt medium; 10 g l^{-1} tryptone, 5 g l^{-1} yeast extract, 5 g l^{-1} NaCl

The pH of respective media and buffers was adjusted by a Hanna Instruments pH 211 microprocessor pH meter (Kehl, Germany). Unless otherwise indicated, cells from overnight cultures were diluted to an OD_{600} ~ 0.2 in YPD medium or restricted iron medium (RIM) which was produced by adding 200 µM of the potent iron chelator bathophenanthroline disulfonate (BPS) to YPD, and grown until early exponential phase (3 h) at 30 °C (pre-culture). When overnight cultures growth did not exceed OD_{600} ~ 0.5, no pre-culture was prepared. Cells were harvested from this pre-culture by centrifugation at 4500 x g and room

temperature (RT) for 5 min, followed by resuspending in the respective growth medium. RPMI1640 is a medium comprising no iron salts; YNB is a defined medium with a basal concentration of 1.2 µM Fe^{3+} (information from the suppliers). All liquid media used in this study were prepared in ultrapure Milli-Q (MQ) water (Milli-Q Academic A10, Millipore, Billerica, USA) and sterilized by filtration using 0.2 µm bottle top filters (Milian) placed on top of autoclaved 1 l or 500 ml glass flasks (Schrott) in combination with a KNF Neuberger 78 (Freiberg) vacuum pump. YPD was also occasionally sterilized by autoclaving at 121 °C for 20 min. For autoclaving, HST-4-5-6 (Zirbus, Bad Grund) or BelliMed Infection Control autoclaves were used.

During all experiments, ferric chloride ($FeCl_3$, Sigma-Aldrich) was chosen as ferric iron source, while ferrous sulfate ($FeSO_4$, Sigma-Aldrich) served as source for ferrous iron. All iron containing stock solutions were freshly prepared immediately before use. For cultivations exceeding a cultivation time of 10 min in iron supplemented media, iron stock solutions were sterile filtered by 0.2 µm Minisart sterile filters (Sartorius, Göttingen, Germany) before being added to the media. Fludioxonil and iprodione were both purchased from Sigma and 5 mg ml^{-1} stocks of each antifungal were prepared in MeOH. Fetal bovine serum (FBS) was purchased from Lonza (charge no. 0SB008) while human plasma was kindly provided by Stefanie Ehrentraut and Katja Gremmer (BISA, HZI, Braunschweig).

Solid media were prepared by adding 12 g l^{-1} of agar (BD Bacto™) to RPMI, YPD, YP-glycerol (10 g l^{-1} yeast extract (BD Bacto™), 20 g l^{-1} peptone (BD Bacto™), 2% glycerol (Merck)) and YP-galactose (10 g l^{-1} yeast extract, 20 g l^{-1} peptone, 20 g l^{-1} galactose (Serva)) or 14 g l^{-1} agar to LB and 15 g l^{-1} agar to TB media.

Glucose was purchased from Fluka, Sorbitol from Sigma and MOPS from J.T.Baker or Sigma.

Sartorius Excellence, Sartorius Research and Kern&Sohn balances were used for weighing chemicals and medium constituents.

2.2 Protein analysis

2.2.1 Extraction of cell surface proteins from whole cells

For the extraction of Bgl2p and MCFOs, an overnight culture was diluted in YPD to an OD_{600} ~ 0.1 - 0.2 and grown until the early exponential phase (pre-culture). Working cultures were prepared by resuspending *C. albicans* cells from the pre-culture in 20 ml of the respective medium at an OD_{600} ~ 0.3. Cultures were incubated at the respective temperature for 3 – 5 h. For overnight cells, overnight cultures were diluted in YPD at an OD_{600} ~ 0.1 and incubated at 30 °C for 16 -17 h in 20 or 50 ml YPD. For extraction of Bgl2p at different growth stages, an overnight culture was grown in YPD until an OD_{600} of ca. 0.4 was reached. Cells were diluted in 20 ml YPD at an OD_{600} of ca. 0.1 and grown at 30 °C until an OD_{600} of ca. 0.4, 1.5 or 3.2 was reached respectively. For all experiments, cells were harvested by centrifugation (4500 x g, 5 min and RT) and washed twice with PBS, pH 7.4 (8.0 g l^{-1} NaCl, 0.2 g l^{-1} KCl, 1.44 g l^{-1} $Na_2HPO_4 \cdot 2\ H_2O$, 0.24 g l^{-1} KH_2PO_4). Occasionally, the supernatant was removed and the pelleted cells were washed with 1 ml PBS and subjected to a further centrifugation step (4500 x g, 1 - 5 min, and RT). The supernatant was removed and 30 – 100 µl PBS were added to the wet cell pellet. Proteins from resuspended cells were extracted by boiling at 90 °C (Memmert incubator) for 10 min. The suspension was centrifuged at 10000 x g and 4 °C for 10 min and the supernatant was transferred to a new 1.5 ml Eppendorf tube. This centrifugation step was repeated once to remove residual cells. The protein extract (supernatant) was subjected to protein determination using bicinchoninic acid (Smith et al, 1985). Briefly, BCA solution A (10 g l^{-1} BCA (Sigma), 17.1 g l^{-1} Na_2CO_3, 1.9 g l^{-1} Na_2Tartrat 2 H_2O) was mixed with BCA solution B (40 g l^{-1} $CuSO_4$ 5 H_2O) in a ratio of 50:1 (BCA mix). 195 µl BCA mix was added

to 5 µl protein extract (1:1 and 1:2) in 96 well plates in duplicates. Alternatively, undiluted protein extract was measured in triplicates. As standard, 5 µl of a 5, 2.5, 1.25, 0.625 or 0.3125 mg ml^{-1} lysozyme solution (in PBS) was added to 195 µl BCA mix each. Samples were incubated at 37 °C and 450 rpm (comfort 5355R Thermomixer, Eppendorf) for 30 min followed by absorption measurement at $\lambda = 570$ nm.

Equal protein amounts were applied on gels when comparison was necessary. In distinct cases, bovine serum albumin (BSA) was added to each sample at a final concentration of 5 µg ml^{-1} as a loading control.

2.2.2 Extraction of cell wall proteins from disrupted cells

Cells were disrupted either by grinding in liquid nitrogen with clean mortars and pestles (Haldenwanger, Berlin, Germany) or by means of a microdismembrator (Mikro-Dismembrator U, B. Braun Biotech International, Melsungen, Germany).

For cell disruption by grinding in liquid nitrogen, cells were inoculated from single colonies grown on YPD plates into 20 ml YPD and cultivated overnight at 30 °C. Cells were directly harvested for extraction by centrifugation (4500 x g, 5 min, 4 °C). Cells were grinded in liquid nitrogen and grinded cell powder equivalent to a volume of 2 ml was mixed with 600 – 1000 µl 5 mM Tris· HCl pH 7.5 supplemented with protease inhibitors (complete, mini, Roche) and 1 mM PMSF. The slurry was centrifuged (at least 10000 x g, 10 min, 4 °C), the supernatant was discarded and the washing step with the PMSF and protease inhibitor supplemented 5 mM Tris·HCl pH 7.5 was repeated 2 – 3 times.

For cell disruption by microdismembrator, overnight or exponential cells were diluted to an OD_{600} ~ 0.04 – 0.1 and subsequently cultivated overnight in 50 ml YPD at 30 °C. Cells were directly harvested for extraction by centrifugation (4500 x g, 5 min, RT). Cells were dropped in a liquid nitrogen pre-cooled plastic vial forming cell pearls and frozen in liquid nitrogen and eventually stored at -80 °C until further use. Frozen cells were transferred into a liquid

nitrogen pre-cooled Teflon vessel with a wolfram-graphite bead. Cells were disrupted by the microdismembrator at 2000 rpm for 1 min followed by a cooling step in liquid nitrogen for 1 min and a subsequent 1 min second disruption step. After disruption, cell powder was resuspended in appropriate volumes of 5 mM or 10 mM Tris·HCl pH 7.5 supplemented with 1 mM PMSF and protease inhibitor (cOmplete, mini or complete protease inhibitor cocktail) from Roche (Mannheim, Germany). The slurry was centrifuged (10000 x g, 10 min, 4 °C) and subsequently washed 3 - 5 times with 5 mM or 10 mM Tris·HCl pH 7.5 supplemented with 1 mM PMSF and protease inhibitor.

All disrupted cells were washed three times with Butanol·H_2O mix (0.7:1) for 15 min on ice followed by a washing step with ice cold MQ- H_2O. Pellets (cell walls) were occasionally saved at -80 °C after disruption or after the different washing steps.

From this point on, cell walls were differently treated according to each extraction method. For heat extraction, cell walls were either resuspended in 5 mM Tris·HCl pH 7.5 with or without 2% SDS or alternatively resuspended in 12 M Urea (prepared in water) and boiled at 90 °C for 10 min. Cell walls were pelleted (at least 10000 x g, 10 min, 4 °C) and the supernatant was transferred to a new pre-cooled tube. Occasionally, the last centrifugation step was repeated to remove residual cellular remains. The extraction step with 12 M Urea at 90 °C was repeated one further time and the resulting supernatant pooled with the supernatant from the previous step.

For extraction of cell wall proteins by enzymatic digestion of cell wall carbohydrates, cell walls were resuspended in 50 mM Tris·HCl pH 6.8 containing 20 U ml^{-1} Zymolyase (Seikagaku BC, Tokyo, Japan), 1 mM PMSF and 1x protease inhibitor (Roche). Incubation followed at 37 °C and 160 rpm (Multitron Shaker, Infors-HT) for 2 h. Suspension was centrifuged (10000 x g, 10 min, 4 °C) and the supernatants were collected in pre-cooled Falcon- or Eppendorf tubes.

Extracts deriving from 5 mM Tris·HCl pH 7.5 (without SDS), 12 M Urea and Zymolyase were concentrated with appropriate Vivaspin columns of 3 - 10 kDa MWCo. Protein determination was performed as mentioned above.

Proteins were extracted from CAF2-1 or DAY286. Equally treated extracts from Δ*bgl2* (FB63-1 or FB63-3) served as negative controls for rapid Bgl2p identification from DAY286. Presence of Bgl2p from DAY286 or CAF2-1 derived extracts was confirmed by MS or MS/MS analysis.

2.2.3 SDS-PAGE

All protein samples were mixed with 5x protein sample buffer (1.5 g sodium dodecyl sulphate (SDS), 1.116 g dithiothreitol, 0.015 g bromphenol blue, 7.5 ml 0.5 M Tris·HCl pH 6.8, 7.5 ml glycerol) in a ratio of 4:1, boiled at 95 °C for 10 min, shortly centrifuged (up to 10 sec) and stored at -20 °C until use. Before loading on SDS-gels, frozen samples were shortly boiled again (5 min) at 95 °C and shortly centrifuged (up to 10 sec). Proteins were separated on 11%T, 2.6%C 1 D SDS-running gels. SDS-gels were prepared as the following:

Stacking gel (5%):
1.45 ml MQ-H_2O
625 µl 0.5M Tris, pH 6.8
12.5 µl 20% SDS
12.5 µl 10% ammonium persulphate (APS)
3.5 µl N,N,N',N'-Tetramethylethylendiamin (TEMED)
425 µl polyacrylamide (Rotiphorese® Gel 30 (37.5:1), Roth, Karlsruhe)

Running gel:
1.95 ml MQ-H_2O
2.50 ml 1.5M Tris, pH 8.8
30.5 µl 20% SDS
30.5 µl 10% APS
4.9 µl TEMED
2.50 ml polyacrylamide (Rotiphorese® Gel 30 (37.5:1))

In some cases, the stacking gel total polyacrylamide concentration was 4 %. Running gels (5 ml) were poured in fixed glass cassettes (Biometra, Jena, Germany) and the stacking gel was directly poured on the running gel until the top of the glass cassettes. Alternatively, a small

layer of isopropanol was added on top of the running gel. After polymerization of the running gel, the isopropanol layer was removed and the stacking gel was poured on top of the running gel. Occasionally, polymerized gels were stored at 4 °C.

Polymerized gels were fixed in gel electrophoresis apparatus (Minigel-Twin, Biometra) which was filled with running buffer (25 mM Tris, 0.192 mM glycine, 0.1 (v/v) SDS, pH 8.3). Gels were as indicated for each experiment using Power Pac 200, Power Pac 300 or Power Pac 1000 (Bio-Rad, München, Germany). Gels were subsequently stained with coomassie staining solution (0.25% Coomassie-G25, 50% H_2O, 42% Ethanol, 8% acetic acid) at RT for 0.5 - 2 h followed by destaining with distilled water (dH_2O) overnight with an occasional interval in destaining solution (50% H_2O, 42% Ethanol, 8% acetic acid) for 15 - 30 minutes. Coomassie staining was extended overnight if required. Occasionally, gels were incubated in destaining solution before coomassie staining. Documentation of all gels was performed with the GS-800 gel scanner (Bio-Rad) using the Quantity One 1-D analysis software (Biorad), except for the gel shown in Supplemental data 2D which was covered with a transparent envelope and scanned with Konica Minolta bizhub C353.

2.2.4 Mass spectrometric and N-terminal sequencing analysis

For matrix assisted laser desorption ionization-time of flight (MALDI-TOF) peptide mass fingerprinting, protein bands were cut out from 1D SDS-gels, washed 3 – 5 times with MQ-H_2O and sent to the proteomic facility for further analysis. Mass spectrometric analysis was performed by Dr. Manfred Nimtz and Anja Meier (CPRO, HZI, Braunschweig). Briefly, proteins were reduced and carboxamidomethylated, and then subjected to in-gel tryptic digestion. The resulting peptides were extracted, desalted using ZipTip devices (Millipore, Bedford, USA) and analyzed by MALDI-TOF-MS using a Bruker Ultraflex time-of-flight mass spectrometer (Bruker Daltonics, Bremen, Germany). Laser induced dissociation of selected peptides for sequence confirmation was performed on the same instrument.

Identification of proteins was performed with the mascot search engine at http://www.matrixscience.com/. Manual comparison with peptide mass fingerprints of known proteins was performed via http://web.expasy.org/peptide_mass/.

For N-terminal sequencing, proteins were blotted on polyvinylidene fluoride (PVDF) membranes (Immunoblot PVDF Membran, Bio-Rad) and stained with Coomassie G-25 at room temperature for 5 min. Background color was removed by incubation in destaining solution for 30 min. Bands of interest were cut off from the membrane and were subjected to N-terminal sequencing using a 494A HT Protein Sequencer (Applied Biosystems) (Edman & Begg, 1967). Protein sequencing was performed by Beate Jaschok-Kentner (MOSB, HZI, Braunschweig).

2.2.5 Western blots

To investigate Hog1p phosphorylation, an overnight culture grown was diluted to an OD_{600} ~ 0.2 in YPD and grown at 30 °C for another 3 h. Then cells were resuspended in 20 ml of the respective medium at an OD_{600} ~ 0.3 or 0.1 and were incubated with or without addition of $FeCl_3$ at 30 °C for the given time points. Occasionally, cells were washed with the same medium before adding iron. As positive control for Hog1p phosphorylation, cells were incubated with 1 M of the osmotic stress inducer sorbitol in RPMI at 30 °C for 15 min. Protein preparation and western blotting were performed as previously described (Buschart et al, 2012b) with some modifications. Briefly, cells were frozen in liquid nitrogen and disrupted with the Microdismembrator (see 2.2.2) and the resulting cell powder was resuspended in extraction buffer (10 mM sodium phosphate buffer, pH 8.5 containing 5 mM NaCl, 5 mM KCl, 11 g l^{-1} glucose, supplemented with 1x protease inhibitor (cOmplete, mini or cOmplete, mini EDTA free) and 1 - 2x phosphatase inhibitor (PhosSTOP, Roche)). Protein content of each sample was determined as described above. Protein samples were separated by SDS-PAGE as indicated above (11%T, 2.5%C). Gels were run at 80 V for 30 min and subsequently

at 120 V for 90 min. After SDS-PAGE, gels were soaked in blotting buffer (25 mM Tris, 192 mM glycine, 0,0375% (v/v) SDS) for 30 min at RT. PVDF membranes were shortly soaked in MeOH and then in blotting buffer. Proteins were transferred to the PVDF membranes (30 min, 15 V) using Trans-Blot SD Semi-Dry Electrophoretic Transfer Cell (Biorad) and Power Pac 1000 (Bio-Rad). After blotting, membranes were washed for 5 min with TBS-T (20 mM Tris HCl, 140 mM NaCl, 0.1% (v/v) Tween-20, pH 7.4) at RT. The membrane was incubated with 5% (w/v) nonfat dried milkpowder (Euroclone, Italy) to block unspecific binding of the used antibodies to the membrane. Blots were probed at 4 °C overnight with anti-phospho p38 MAPK (Thr180/Tyr 182) 3D7 rabbit mAB (Cell Signaling Technology) (1:1000) and with horse-radish-peroxidase (HRP)-linked anti-rabbit IgG antibody #S7074 (Cell Signaling Technology) (1:3000) (1 h at RT) to detect phosphorylated Hog1p. After each incubation step, membranes were washed for 4 x 10 min with TBS-T at RT. For detection of total Hog1p, membranes were stripped with Re-Blot stripping buffer (Millipore) for 15 min at RT, washed for 2 x 10 min with TBS-T and re-blocked with 5% (w/v) nonfat dried milkpowder as indicated above. Membranes were probed at RT for 1 h with anti-Hog1p (y-215) sc 9079 rabbit polyclonal IgG (Santa Cruz Biotechnology) (1:2000) and the HRP-linked anti-rabbit antibody mentioned above to detect total Hog1p content. Visualization of protein bands was performed as indicated below.

For detection of recombinant Bgl2p (rBgl2p-SP) by western blot, blotting, blocking and washing were performed as mentioned above. Membranes were probed at RT for 1 h with HRP-linked Monoclonal ANTI-FLAG® M2 antibody (Sigma) (1:50000). This antibody will be referred to as anti-FLAG for simplification.

All incubation and washing steps were performed with gentle swaying on Heidolph Doumax 1030, Rockomat (TECNO MARA) or WS5 (Edmund Bühler). All protein bands were visualized by chemiluminescence using the ECL Advance Western Blotting Detection Kit

(GE Healthcare) or the ECL Prime Western Blotting Detection Kit (GE Healthcare) in a LAS-3000 (CCD camera, Fujifilm). All antibody working solutions contained 5% (w/v) BSA.

2.2.6 Dot blots

For Dot blot analysis, purified rBgl2p was dropped on pre-wetted PVDF membranes and the membranes were allowed to dry. Blocking, washing, stripping and protein visualization were performed as mentioned in 2.2.5 except for that the Tween-20 concentration of TBS-T was reduced to 0.05% (v/v). Membranes were treated at 4 °C overnight with different anti-Bgl2-a7/8 or anti-Bgl2-a10 containing supernatants and with HRP-linked anti-mouse IgG antibody #S7076 (Cell Signaling Technology) (1:3000) containing 5% (w/v) BSA. Some membranes were stripped and re-blocked before being subsequently probed with anti-FLAG at RT for 1 h.

2.3 Expression and purification of recombinant Bgl2p

2.3.1 Design and synthesis of *Ca_BGL2_FLAG3x_His8x*

Design of this gene (*Ca_BGL2_FLAG3x_His8x*) sequence was performed by Prof. Dr. Peter Müller (RDIF, HZI, Braunschweig). The resulting *Ca_BGL2_FLAG3x_His8x* sequence was synthesized by GENEART AG (Regensburg, Germany). See Supplemental data 1 for the full sequence of *Ca_BGL2_ FLAG3x_His8x*.

2.3.2 Cloning of *Ca_BGL2_FLAG3x_His8x*

Upon delivery, *Ca_BGL2_FLAG3x_His8x* was cloned in the pMK-RQ vector. For amplification the delivered vector was transformed in *E. coli* XL-1 BLUE by electroporation (for procedure, see 2.3.3). Transformants were selected on kanamycin (Kan, 30 µg mL^{-1}) supplemented solid media. Plasmids (minipreps) were isolated with the NucleoSpin® Plasmid (Machery-Nagel, Düren, Germany) from 2 mL cultures according to the manufacturer's instructions (2 x 25 µl TE buffer were used in the elution step). Correct *Ca_BGL2_FLAG3x_His8x* size was confirmed by double digestion with *NdeI* (20000 U ml^{-1},

New England Biolabs, Ipswich, USA) and *EcoRI* (20000 U ml^{-1}, New England Biolabs), or *NcoI* (10000 U ml^{-1}, New England Biolabs) and *EcoRI*. Digestions were performed as following (digestion protocol 1):

x µl DNA (1 µg)
2 µl 10x NEB4 (New England Biolabs)
0.25 µl Enzyme 1
0.25 µl Enzyme 2
(17.5 – x) µl nuclease free water (Promega)

Incubation was performed at 37 °C for 2 h, followed by inactivation at 65 °C for 17 min and subsequent running on ethidium bromide (EtBr) containing 0.8% agarose gels.

Positive clones were cultivated in 100 mL LB + Kan and plasmids were isolated in large scale (midipreps) with PureYield™ Plasmid Midiprep (Promega, Fichtburg, USA) according the manufacturer's instructions. Plasmids were digested either with *NdeI/ EcoRI* for rBgl2p or *NcoI/ EcoRI* for the rBgl2p version lacking the signal peptide (rBgl2p-SP). pET28c (Merck Milipore, Darmstadt, Germany), kindly provided by Dr. Joop van den Heuvel, RPEX, HZI, Braunschweig) was digested with the same enzyme combination respectively. Digestions were performed as the following (digestion protocol 2):

x µl DNA (5 µg)
4 µl 10x NEB4 (New England Biolabs)
2 µl Enzyme 1
2 µl Enzyme 2
(37.5 – x) µl with nuclease free water (Promega)

Incubation was performed at 37 °C for 4 h. Insert and linearized vector were run on EtBr containing 0.8% agarose gels. DNA bands were visualized in a (Kodak Gel logic 212 Imaging System), excised and extracted with NucleoSpin® Extract II (Machery-Nagel) according the manufacturer's instructions (final elution step prolonged to 2 min). Ligase reaction of insert and vector was performed as the following for each version:

Ligation mix for rBgl2p-SP:

4 µl Insert DNA encoding rBgl2p-SP (133 ng)
4 µl pET28c (ca. 60 ng)
2 µl 10x T4 DNA Ligase buffer (Roche)
1 µl T4 DNA Ligase (Roche, 1 U μl^{-1})
9 µl nuclease free water (Promega)

Incubation was performed overnight at 16 °C (Biometra TPersonal).

Ligation mix for rBgl2p:

9 µl Insert DNA encoding rBgl2p (189 ng)
4 µl pET28c (ca. 60 ng)
2 µl 10x T4 DNA Ligase buffer (Roche)
1 µl T4 DNA Ligase (Roche, 1 U μl^{-1})
4 µl nuclease free water (Promega)

Incubation was performed 1 h 40 min at 23 °C (Eppendorf Thermomixer Compact) and subsequently overnight at 16 °C (Biometra TPersonal).

Each ligation mix was transformed into *E. coli* XL-1 BLUE (see below). Positive clones were selected on LB + Kan plates and several transformants were inoculated into 2 ml LB + Kan medium. Plasmids were purified (minipreps) as indicated above. Purified plasmids were digested with the respective restriction enzyme combination (*NdeI/ EcoRI* for rBgl2p or *NcoI/ EcoRI* for the rBgl2p-SP) according to digestion protocol 1. Clones showing correct size of digested DNA fragments were cultivated in large scale (200 ml LB + Kan) and plasmids were purified by midipreps. Correct sequence was confirmed by sequencing (performed by Stephanie Thies and Tschong-Hun Im, GMAK, HZI) using T7 rev (5' CTAGTTATTGCTCAGCGGT 3') and T7 fw (5' TAATACGACTCACTATAGGG 3') sequencing primers [10 pM] (both provided by Dr. Joop van den Heuvel). DNA sequence analysis was performed with FinchTV program. Plasmids were then transformed into the expression strain, *E. coli* Rosetta™ 2 (DE3) (see below).

2.3.3 *E. coli* transformation

All *E. coli* transformations were performed by electroporation. Recipient strains were either *E. coli* Rosetta™ 2 (DE3) or *E. coli* XL-1 BLUE. Electrocompetent cells were generously provided by Dr. Joop van den Heuvel. Briefly, 60 µl electrocompetent cells were thawed up on ice and added to the ligation mix from 2.3.2 or plasmid DNA (1 – 2 ng). The mixture was pipetted into a cold cuvette (0.2 cm) and incubated for 1 min on ice. Cells were pulsed at 25 µF and 2.5 kV (Bio-Rad Gene Pulser). 1 ml of LB medium was added to the cells followed by incubation at 37 °C for 30 min and 225 rpm (Eppendorf Thermomixer Compact). Cells were plated on solid medium (LB or TB) supplemented with Kan and chloramphenicol (Cam, 34 µg ml^{-1}) for pET28c variants transformation in *E. coli* Rosetta™ 2 (DE3) or only Kan for pET28c variants or pMK-RQ transformation in *E. coli* XL-BLUE1. As controls *E. coli* Rosetta™ 2 (DE3) was transformed with pET42a (selected on Kan supplemented plates) or *E. coli* XL-BLUE1 was transformed with pUC19 (selected on 100 µg ml^{-1} ampicillin supplemented plates). Transformants were grown overnight in a 37 °C incubator (Heraeus Function line). Several transformants were cultivated in the respective medium followed by plasmid preparation. The resulting *E. coli* Rosetta™ 2 (DE3) strains carrying either genetic version were subsequently dubbed as *Ca_BGL2*_FLAG3x_His8x_+SP6 (for rBgl2p) and *Ca_BGL2*_FLAG3x_His8x_-SP3 (for rBgl2p-SP), where the numbers at the end represent the selected clone respectively.

2.3.4 Expression of rBgl2p-SP under non-denaturing conditions

*Ca_BGL2*_FLAG3x_His8x_-SP3 was inoculated from frozen glycerol stock in 20 ml of TB + Kan + Cam and cultivated at 37 °C overnight (up to 19 h). Cells were diluted 1:20 in the same medium (20 – 200 ml) and cultivated for 5 h at 37 °C and subsequently for up to 19 h at 30 °C.

Cultures were divided in 15 or 50 mL falcon tubes and cells were harvested by centrifugation for 1 min at 15000 x g. Pellet was resuspended in 300 µl Lysis buffer (4 mL BugBuster® Protein Extraction Reagent (Merck Millipore), 0.2 mg ml^{-1} lysozyme and 4 µL Benzonase® 2.5 kU (Merck Millipore)) for each 10 ml culture. Slurry was transferred to clean 2 ml Eppendorf tubes and shaken at RT and 350 rpm (comfort 5355R Thermomixer, Eppendorf) for 20 min. Samples were centrifuged (13000 x g, 20 min and 4 °C). Supernatants were pooled (lysate) and expression of rBgl2p-SP was confirmed by SDS-PAGE and subsequent western blotting using an anti-FLAG antibody (see 2.2.5). For rBgl2p-SP purification, the lysate was concentrated in a Vivaspin6 column, 3 kDa MWCo (Sartorius, Göttingen, Germany) to ca. 1 - 2 ml.

2.3.5 Purification of rBgl2p-SP under non-denaturing conditions

For rBgl2p-SP purification, 2.5 ml 50% Protino® Ni-NTA Agarose beads (beads) from Machery-Nagel were pipetted on top of a PD-10 column (GE Healthcare, Braunschweig, Germany) and washed with a total of 25 ml NP-10 buffer (50 mM $NaH2PO_4$, 300 mM NaCl, 10 mM imidazole, pH 8.0). *E. coli* lysate containing rBgl2-SP was concentrated to ca. 1 – 2 ml (see above) and mixed with the beads for 2 min followed by 20 x 1 ml washing steps with NP-60 buffer (50 mM $NaH2PO_4$, 300 mM NaCl, 60 mM imidazole, pH 8.0). rBgl2p-SP was eluted with a total of 7.8 ml NP-500 buffer (50 mM $NaH2PO_4$, 300 mM NaCl, 500 mM imidazole, pH 8.0) and collected in a Vivaspin6 column, 3 kDa MWCo on ice. Eluate was concentrated up to 1.5 ml, before being aliquoted, frozen in liquid nitrogen and stored at -20 °C. Purification of rBgl2p was controlled by SDS-PAGE and subsequent coomassie staining as well as by western blotting (see 2.2.5).

2.4 Flocculation and sedimentation assays

Unless otherwise indicated, *C. albicans* cells from an overnight culture were diluted in YPD to an OD_{600} of 0.2 and grown to the early logarithmic phase. Cells were pelleted (4500 x g, 5 min and RT) and resuspended in 2 ml of the respective medium containing different iron concentrations in 14 ml polypropylene (PP) round bottom falcon tubes (BD sciences, USA) at an OD_{600} of 0.1. Flocculation was observed microscopically after incubation of cells at 30 °C for up to 2 h. Alternatively, 20 ml cultures were prepared in 100 ml shaking flasks. Flocculation was quantified by determining sedimentation rates of cells based on the protocol given in previous reports (Gregori et al, 2011). Briefly, 1 ml of the cell suspension was transferred to a plastic cuvette (Plastibrand®, Brand, Wertheim, Germany) after incubation at 30 °C for 2 h. OD_{600} (UV1, Spectronic Unicam) was determined directly after vortexing the cell suspension (OD1) and after additional 15 min without vortexing (OD2). The R-value was calculated as percentage of OD2 relatively to OD1 (OD2/OD1 * 100) and reflects a decrease in OD with increased sedimentation rate. Each experiment contained three independent replicates, and the mean of the three obtained R-values was taken as a final result.

2.5 Intracellular ROS determination

C. albicans cells from an overnight culture were diluted in YPD to an OD_{600} of 0.2 and grown to the early logarithmic phase. Cells were pelleted (4500 x g, 5min and RT), washed once with RPMI and resuspended in 2 ml RPMI with or without iron in round bottom falcon tubes at an OD_{600} of 0.1. Cells were incubated at 30 °C for 10 min and immediately pelleted and washed twice with MQ-H_2O. Cells from all samples were resuspended each in 1.2 ml water and each sample was split in two 600 µl samples containing either 70 µM CM-H_2DCFDA (Invitrogen) or the same volume of DMSO. From those stocks, 3 x 180 µl were pipetted into the wells of a 96 well plate (CytoOne, Starlab), leaving empty columns between different

samples and incubated in the dark at 30 °C for 30 min (Alonso-Monge et al, 2009). Fluorescence intensity was quantified by measuring relative fluorescence intensities (RFUs) using the Synergy 4 fluorescence microtiter plate reader (BioTek Instruments GmbH) at an excitation wavelength of 485 nm and an emission wavelength of 528 nm. ROS accumulation was calculated with respect to background fluorescence of the sample: ROS accumulation = (RFU-H_2DCFDA / RFU-DMSO). To reverse ROS accumulation, the radical scavenger N-acetyl cysteine (Sigma-Aldrich) was used at 10 mM final concentration together with iron.

2.6 Determination of iron levels in growth media and culture supernatants

Determination of ferric iron concentration in media and culture supernatants was performed indirectly by reducing total ferric iron to ferrous iron by ascorbic acid at low pH and measuring ferrous iron content through the chromogenic iron chelator bathophenanthroline disulfonate (BPS). Briefly, *C. albicans* cells were prepared as described in the flocculation part. Cells were incubated in 2 ml RPMI (OD_{600} ~ 0.1) containing 30 µM $FeCl_3$ at 30 °C for 15 min. After incubation, cells were removed by centrifugation (4500 x g, 5 min and RT), and 880 µl from the supernatants were mixed with 100 µl of 10 mM ascorbic acid and 20 µl of 50 mM BPS. A medium sample lacking iron was used as negative control, while medium supplemented with 30 µM $FeCl_3$ without cells represented the starting conditions and was equally treated. All samples were acidified by addition of 10 µl 32% HCl and 180 µl of this mixture were pipetted in a transparent 96 well plate and the absorption of the BPS·Fe^{2+} complex was measured in triplicates at λ = 535 nm (Nilsson et al, 2002; Tamarit et al, 2006) immediately after acidification. Absorption of the iron free sample was used to correct absorption of all other samples. For each strain, three samples were measured simultaneously, each obtained from an independent culture. The whole experiment was repeated three times.

2.7 Determination of cell surface ferric reductase activity

Unless otherwise indicated, *C. albicans* overnight cultures were diluted in 20 ml of the respective medium to an OD_{600} of 0.2. Antifungal compound, iron or solvent controls were added at the respective concentration to the medium. All cultures were incubated at 30 °C for 3 h. After this growth period, the ferric reductase assay was performed according to (Jeeves et al, 2011) with minor modifications. Briefly, early exponential cells were washed once with MQ-H_2O (4500 x g, 5 min, RT), resuspended in assay buffer (50 mM sodium citrate, 5% glucose, pH 6.5) and shaken in round bottom falcon tubes at 30 °C for 15 min. $FeCl_3$ and BPS were then added at a final concentration of 1 mM each, to give a final volume of 2 ml at an OD_{600} of 0.1. Cells were incubated at 30 °C for additional 5 min, pelleted (8000 x g, 3 min, RT) and the OD_{520} (λ = 520 nm) of the supernatant was determined (3 x 180 µl). For SC5314 and DAY286 strains incubated with 30 µM $FeCl_3$ in RPMI medium, no OD_{600} could be determined since those strains formed flocs. In this case, same volumes were taken as for the H_2O control culture.

2.8 Viability test

Viability of cells was measured using the alamarBlue® assay (Invitrogen), which indicates particularly the metabolic activity of a culture. *C. albicans* cells were prepared as described in the flocculation part and resuspended in 2 ml RPMI with addition of 30 µM $FeCl_3$ or MQ-water at an OD_{600} of 0.1. Cells were incubated at 30 °C for 60 min and immediately pelleted and washed once with MQ-H_2O. They were resuspended in 2 ml MQ-H_2O and 3 x 162 µl from each sample was added to 3 x 18 µl alamarBlue® which were previously pipetted in three wells of a 96 well plate (CytoOne, Starlab) leaving empty columns between different samples. The fluorescence intensity was quantified (t = 0) with the Synergy 4 fluorescence microtiter plate reader (BioTek Instruments GmbH) at an excitation wavelength of 540 nm

and an emission wavelength of 590 nm. The reagent was incubated at 30 °C for 30 min and the fluorescence intensity was quantified again (t = 30 min). The difference to the values obtained at t = 0 was taken as indicator of the viability of the cells and the relative metabolic activity was calculated according to: Relative metabolic activity (%) = 100 x (RFU_{iron} / $RFU_{MQ\text{-}water}$). The experiment was performed three times (n = 3) in total and means of the three experiments were taken as final result.

2.9 Flow cytometric analysis

Flow cytometric analysis by fluorescence activated cell sorting (FACS) of viable *C. albicans* was based on binding of mouse hybridoma cell culture supernatants containing monoclonal anti-a10 antibody (primary antibody) to *C. albicans* cells, followed by binding of Alexa fluor 488 anti-mouse IgG antibody (Invitrogen) (secondary antibody) to the primary antibody and subsequent analysis in a BD FACSCanto (BD, Franklin Lakes, USA) using the FACSDiva 6.0 software. C25HD4H4 and C25HD4H8 were concentrated in a Vivaspin500 column (MWCo 50 kDa) and resuspended in PSB to give a final concentration of 2.3 fold of the original unknown concentration. Briefly, *C. albicans* stationary phase cells (SC5314 OD_{600} ~ 4.0; DAY286 OD_{600} ~ 4.6; Δ*bgl2* OD_{600} ~ 5.4) were resuspended in 500 µl PBS at an OD_{600} of 0.01 and pelleted (8000 x g, 3 min, RT). Cells were incubated with 200 µl (OD_{600} = 0.025) of each concentrated hybridoma cell culture supernatant at RT (Thermomixer 5437, shaking level 8, Eppendorf) for 30 min followed by three times washing with 500 µl PBS (8000 x g, 3 min, RT). Cells were incubated with 200 µl of 10 µg ml^{-1} Alexa fluor 488 anti-mouse IgG (Invitrogen) on ice for 15 min with swaying (30 rpm, Heidolph Doumax 1030) followed by three times washing with 500 µl PBS (8000 x g, 3 min, RT). For negative controls, primary antibody was substituted by the same volume of PBS or only PBS (unstained cells) was used during all incubation steps respectively.

For biotinylation of cell surface proteins, overnight SC5314 cells were resuspended in 500 µl PBS at an OD_{600} of 0.01 and pelleted (8000 x g, 3 min, RT). Cells were incubated with 200 µl (OD_{600} = 0.025) of a 1 mg ml^{-1} EZ-Link Sulfo-NHS-LC-LC-Biotin (Pierce) in PBS pH 8.0 at RT (Thermomixer 5437, shaking level 8, Eppendorf) for 30 min followed by three times washing with 200 µl PBS pH 8.0 + 100 mM Glycine (8000 x g, 3 min, RT). Cells which were not biotinylated were incubated instead with 200 µl PBS pH 8.0. Biotinylated as well as not-biotinylated cells were incubated with 200 µl of 0.025 mg ml^{-1} FITC labeled Streptavidin (BD Pharmingen™) at RT (Thermomixer 5437, shaking level 8, Eppendorf) for 15 min followed by three times washing with 500 µl PBS.

Finally, all cell samples were resuspended in 500 µl PBS in FACS tubes (Sarstedt) before being analyzed by flow cytometry. Results are shown for 10^4 events.

2.10 Growth tests on agar plates

For growth tests on solid medium containing fludioxonil or MeOH, *C. albicans* SC5314 cells were pre-cultivated either in YPD or in YPD + 400 µM BPS at 30 °C for 7 h. Cell were resuspended in PBS (OD_{600} = 0.01) and dilutions ranging from 1:1 to $1:10^5$ were dropped (3 µl each) on agar plates (30 ml) containing the respective combination of medium and supplements. Plates were incubated at 30 °C for 16 h. Each growth test was performed on two separate plates of the same medium combination.

For growth tests on RPMI plates, cells of different strains were grown overnight at 30 °C for ca. 19.5 h (for SC5314, cells were diluted to an OD_{600} of 0.1 after 15.5 h and incubated for further 4 h). Cells were diluted to ca. 0.5 $*10^6$ cells ml^{-1} and 5 µl of each strain were dropped on RPMI (30 ml) with or without the given Fe^{3+} concentration. Serial dilutions were prepared (up to $1:10^5$) and 5 µl were dropped on the plates. Incubation followed at 30 °C for 2 days. Each growth test was performed on three separate plates of the same medium combination.

Agar plates were prepared by mixing 500 ml filter sterilized 2x concentrated respective medium with 500 ml of pre-autoclaved liquid 2x Bacto^{TM}-agar (24 g l^{-1}).

A Brother Hi-Speed microwave machine was used for liquidation of sterile solid agar when necessary. Supplements such as iron, BPS or fludioxonil, as well as solvent controls, were added to the agar containing medium prior pouring plates. RPMI plates were stored at 4 °C until use. Fludioxonil/ MeOH containing plates were used immediately for growth tests. *C. albicans* was incubated on agar plates in either Titramax/ Inkubator 1000 (Heidolph) or Multitron Shaker (Infors-HT) without shaking. After incubation, pictures of agar plates were taken with the GS-800 gel scanner and colors were occasionally inversed with Adobe Photoshop CS3 Extended for proper display if required.

2.11 Microscopic analysis

Microscopic analysis of culture was performed with CKX41/U-RFLT50 (Olympus). 10 µl of cell suspension were dropped on Superfrost glass slides (Menzel). Pictures of cultures were taken with ColorView SIS FireWire Camera 3.0 and analyzed with CellA^ 3.0 software (Olympus). For cell counting, 10 µl of diluted or not diluted cell suspensions were dropped on an Neubauer Improved counting chamber (Brand, 0.1 mm depth) and cells were counted under an Axioplan microscope (Zeiss, Jena). The total cell number ml^{-1} was determined by counting cells in all 25 small squares of 1 mm^2 total surface area. The cell concentration was calculated as following:

$$\text{Cells ml}^{-1} = \Sigma \text{ cells (25 small squares)} \cdot 10^4 \cdot \text{dilution factor}$$

2.12 *In silico* protein sequence analysis

The amino acid sequence of *C. albicans* Bgl2p (orf19.4565) was obtained from the *Candida* Genome Database (CGD, http://www.candidagenome.org). BLAST of the *C. albicans*

SC5314 Bgl2p aa sequence was performed at UniprotKB (http://www.uniprot.org) and Bgl2p orthologs from *C. dubliniensis* (accession number B9WFS5), *C. glabrata* (Q6FTS0), *C. tropicalis* (C5M280), *C. guilliermondii* (A5DGI5) and *C. lusitaniae* (C4YA41) were identified respectively. The *C. parapsilosis* (CPAG 04005) Bgl2p ortholog was identified after performing BLAST in the *Candida* Database of the Broad Institute (http://www.broadinstitue.org). A putative Bgl2p ortholog from *C. krusei* could not be identified as the genome of this species was not yet sequenced and annotated at the time during which this work was performed. The presence of a GH17 domain in each of the 6 non-albicans *Candida* species (NACS) orthologs was confirmed using Pfam (http://pfam.sanger.ac.uk/search). Bgl2p sequence from *C. albicans* ATCC102161 was similarly obtained from UniprotKB (P43070). While Bgl2p sequence from *C. albicans* WO-1 was obtained from the CGD (CAWG_03569). The Bgl2p sequences of the *C. albicans* strains SC5314, WO-1, ATCC10261 and their orthologs from 6 NACS were subjected to multiple sequence alignment using ClustalW2 (http://www.ebi.ac.uk/Tools/clustalw2/index.html).

2.13 Other equipment and materials

Discovery Comfort pipettes (0.1 – 2 µl, 2–20 µl, 20–200 µl and 100-1000 µl) as well as Eppendorf Research pipettes (0.5 – 10 µl and 100 – 1000 µ) were used. Multichannel pipettes used were Brand Transferpette (20 – 200 µl) and Eppendorf Research (30 – 300 µl). Pipette tips (10 µl, 200 µl and 1000 µl) were purchased from Starlab. Glass pipettes from Hirschmann (20 ml, 10 ml, 5 ml and 2 ml) or plastic pipettes from Corning (25 ml, 10 ml and 5 ml) were used in combination with Easypet® (Eppendorf) and CellMate Matrix (Thermo Scientific) pipetting helpers. For OD measurements by the µQuant microtiter plate reader, unsterile flat bottom 96 well plates (Ratiolab) or CytoOne (Starlab) 96 well plates were used. 24 well plates as well as Petri dishes were purchased from Greiner. transparent 0.5 ml,

transparent 1.5 ml, light protected 1.5 ml and transparent 2 ml tubes were purchased from Eppendorf while Falcon tubes (50 ml centrifugation, 50 ml safe standing, 15 ml were obtained from Corning. For washing of *C. albicans* cells and preparation of protein extracts from *C. albicans* or *E. coli*, Eppendorf 5804R (Rotors A4-44, F34-6-38, F-45-30-11) or Eppendorf 5415R centrifuges were mainly used. Biofuge fresco (Heraeus) was only occasionally used. 5415 centrifuge (Eppendorf) was used for short spinning of protein extracts mixed with protein sample buffer after heating at 95 °C. Beckman Avanti® J-20XP was used for plasmid midipreps, while Heraeus Fresco17 (Thermo Scientific) was used for plasmid minipreps or DNA extraction from agarose gels. VF2 (Janke & Kunkel IKA Labortechnik) and VortexGenie 2 (Scientific Industries) were used as vortex apparatuses, while IKAMAG RCT, Heidolph MR2002 and Heidolph MR-82 served as magnet mixers. Microbial strains stocks were stored in a GFL – 80 °C freezer. Other freezers (- 20 °C or – 30 °C) and fridges used were AEG Electrolux, Liebherr Premium, Liebherr Profiline. Liebherr Glassline and Liebherr Ökosuper Premium. Ice machines used were manufactured by Ziegra.

2.14 Preparation of texts and figures

Preparation of texts and figures was performed with Microsoft® Office products, Paint and Adobe Photoshop CS3 Extended. Analysis of SDS- gels and western blot images was performed with Aida Image Analyzer v.4.15, when necessary.

Chapter 3 Results

3.1 The cell wall antigen Bgl2p allows detection of *C. albicans* cells by monoclonal antibodies

3.1.1 Background

We aimed to identify cell wall proteins (CWPs), which could serve as diagnostic markers for *C. albicans* infections. The candidate proteins (antigens) had to comply with several characteristics:

(i) Candidate proteins must be accessible for binding partners. This requires that the candidate protein must be permanently attached to the cell surface and exposed to be recognized by a binding partner. Thus, cell wall proteins (CWPs) are suitable targets.

(ii) The target protein should be abundant to allow sensitive detection.

(iii) It should have low homology to human proteins or to proteins from other pathogens or commensals.

(iv) It should allow distinction of *C. albicans* infection from colonization.

As the desired diagnostic monoclonal antibodies should be specific for *C. albicans*, the epitopes recognized by these antibodies should be unique for this fungus. However, many CWPs are not only conserved among *Candida spp.*, but also among different fungi. We concentrated on the identification of unique peptide sequences from *C. albicans* CWPs. Corresponding peptides could be generated *in vitro* and diagnostic, monoclonal antibodies directed against their sequences could be generated by immunization in mice. A major disadvantage of peptide mediated immunization is that generated antibodies may not bind to the target protein in its native fold.

Suitable cell surface candidates for recognition by antibodies are antigenic proteins. Humoral immune recognition of pathogens is mediated by antibodies targeting epitopes of such proteins.

A seven point strategy was followed for this project:

(i) Identification of suitable candidates. For the identification of candidates, comprehensive literature search for strongest antigenic proteins was performed. In parallel, several methods were applied for extraction of cell surface proteins from *C. albicans* in order to identify the most abundant proteins.

(ii) Studies on the suitable candidates. As mentioned above, any suitable candidate must be accessible for binding partners, and thus should be permanently attached to the cell surface. Taking in account the polymorphic nature of *C. albicans*, cell surface composition of this fungus is variable depending on morphology or environmental factors. Changing cell surface composition could help *C. albicans* to evade immune recognition (Brawner & Cutler, 1986; Nather & Munro, 2008), which suggests that *C. albicans* may change its cell surface composition during different growth and infection stages.

(iii) Identification of unique peptide sequences of the desired candidate antigen.

(iv) Production and synthesis of these peptides.

(v) Production of monoclonal antibodies against peptide antigens.

(vi) Selection of antibodies in terms of binding to the candidate antigen.

(vii) Selected antibodies are evaluated by their ability to specifically recognize whole *C. albicans* cells.

3.1.2 Identification of Bgl2p as a target protein

Several studies have been undertaken to identify antigenic proteins of *C. albicans* in both, the pre- and post-genomic era (Clancy et al, 2008; Gutierrez et al, 1993; Mochon et al, 2010; Pitarch et al, 2006; Pitarch et al, 1999; van Deventer et al, 1994). These studies have resulted in the identification of several proteins of cytosolic functions, such as glycolytic enzymes. As mentioned above (1.2.2.2), some of these proteins, such as Eno1p, Tdh3p, Adh1p or Tef1p were reported to have cell surface localization (Eroles et al, 1997; Gil-Navarro et al, 1997; Urban et al, 2003). However, as such proteins are highly conserved (Martinez et al, 1998), they were not considered as suitable candidates. On the other hand, more recent studies have used modern approaches to identify antigens of *C. albicans*. A 34 kDa protein, named Bgl2p, was found among a group of the most immunodominant proteins of *C. albicans* (Clancy et al, 2008; Mochon et al, 2010; Pitarch et al, 2006). Simultaneously, our experimental investigation of abundant *C. albicans* cell surface proteins resulted in the isolation of this protein by almost every method applied, from both whole and disrupted cells (Table 4, Figure 3.1.1 and Supplemental data 2).

Table 4 – Bgl2p is isolated from *C. albicans* cell wall by different methods.

Extraction method	**Zymolyase (disrupted cells)**	**Hot Urea (disrupted cells)**	**Hot SDS (disrupted cells)**	**Heat (disrupted cells)**	**Heat (whole cells)**
Bgl2p isolated	+	+	-	+	+

Several other proteins were identified by MS or MS/MS analysis. Among those proteins were proteins of cytosolic localization (See Supplemental data 2D), which were released by hot SDS treatment of cell walls. Heat extraction of whole cells, grown in RPMI + 10% FBS at 30 °C, isolated members of the multicopper ferroxidase (MCFO) protein family (see

Supplemental data 2F and section 3.2.6). One member of this family was included in a group of the forty most serodominant antigens in acute candidemia patients (Mochon et al, 2010).

Bgl2p is a cell wall ß-(1,3)-glucosyltransferase belonging to the glycosylhydrolase (GH)-17 protein family (Chaffin, 2008). Homozygote Δ*bgl2* mutants were found attenuated in virulence in a murine model compared to an isogenic parental strain suggesting a role for this cell wall protein in virulence of *C. albicans* (Sarthy et al, 1997).

Bgl2p is one of the most abundant proteins in the cell wall of *C. albicans* (Angiolella et al, 2009). Furthermore, Bgl2p was also shown to interact with basic proline rich proteins (bPRP) of the human saliva, suggesting that Bgl2p has adhesion like properties (Jeng et al, 2005).

However, the probably most important feature of *C. albicans* Bgl2p for this work is its antigenic property. It has been described as a highly antigenic protein, eliciting a strong antibody response in *C. albicans* infected patients (Clancy et. al, 2008; Mochon et al, 2010; Pitarch et al, 2006). This would mean that the immune system detects *C. albicans* by means of anti-Bgl2p antibodies (among others) and that Bgl2p is accessible for antibody binding in principle.

Taking all existent data dealing with *C. albicans* Bgl2p together, this protein was judged to be an excellent candidate antigen for the development of diagnostic tools for identification of *C. albicans* in infected patients.

3.1.3 Bgl2p is associated with the cell wall during different growth stages as well as during initial hyphal formation

As *C. albicans* Bgl2p was reported to be secreted to medium supernatants (Sorgo et al, 2010), further studies were required to investigate attachment of Bgl2p to the cell wall of *C. albicans*.

Bgl2p was isolated by short time boiling of whole overnight (17.5 h) *C. albicans* DAY286 cells resuspended in PBS, pH 7.4 at 90 °C (Figure 3.1.1). The appearance at ca. 35 kDa and

comparison with an isolate derived from an equally treated Δ*bgl2* mutant, allowed initial identification of the Bgl2p band. Furthermore, mass spectrometric analysis (peptides IFLVGSEALYR, 1267.7 m/z; and AWGINVAVYEAFDEAWKPDTSGTSSVEK, 3057.4 m/z) and N-terminal sequencing analysis (sequence MGDLAFNLGVKNDDG corresponds to Bgl2p starting position 19, i.e. after excision of an 18 aa signal peptide sequence (Angiolella et al, 2009)) confirmed the presence of Bgl2p. This protein was also released by the same method when PBS was exchanged by 25 mM Tris·HCl pH 8.0 (not shown).

The release of Bgl2p by heat is indicative for its non-covalent attachment to the *C. albicans* cell wall. This complies with previous knowledge on this protein (Chaffin, 2008). Supplementing PBS with reducing (DTT, ß-mercapthoethanol) or denaturing agents (SDS, urea) did not lead to significant increase in isolated Bgl2p amounts (not shown). To confirm that the Bgl2p found in isolates of boiled cells did not derive from medium supernatants due to inappropriate washing of cells, *C. albicans* DAY286 cells from the same culture were resuspended in PBS but left at room temperature (RT) for 10 min instead of being boiled at 90 °C. The obtained supernatants apparently contained no protein (Figure 3.1.1).

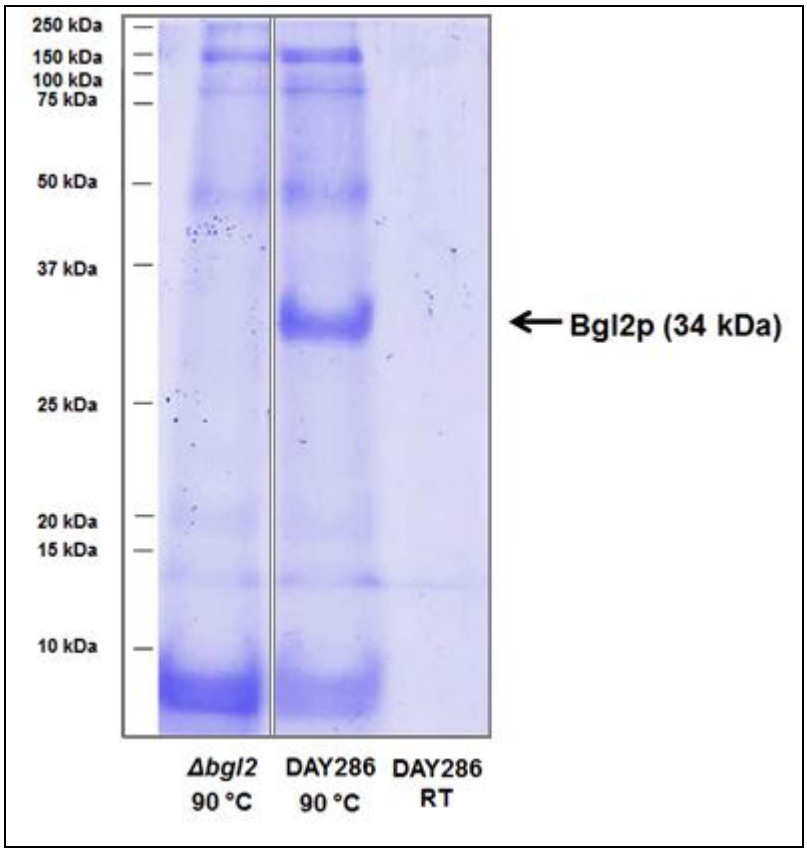

Figure 3.1.1 – Extraction of Bgl2p from whole cells.

SDS-PAGE analysis of proteins extracted by heating whole yeast cells of *C. albicans* DAY286 or Δ*bgl2* in PBS. Cells were cultivated overnight in YPD. As a control, DAY286 was resuspended in PBS and kept at RT. Gel was run for 30 min at 80V and 100 min at 120 V.

Next, Bgl2p was isolated from whole DAY286 cells from different growth phases. Thus, cells were grown in YPD at 30 °C for different periods until an OD_{600} of 0.4, 1.5 or 3.2 was reached respectively. Bgl2p was found to be present in all extracts, meaning that Bgl2p was attached to the cell wall during all growth phases (Figure 3.1.2A). Bgl2p was also found to be associated with the cell wall in the early stages of hyphal formation at 37 °C in RPMI medium supplemented with 10% fetal bovine serum (FBS) (Figure 3.1.2B). See Supplemental data 3 for cell morphology.

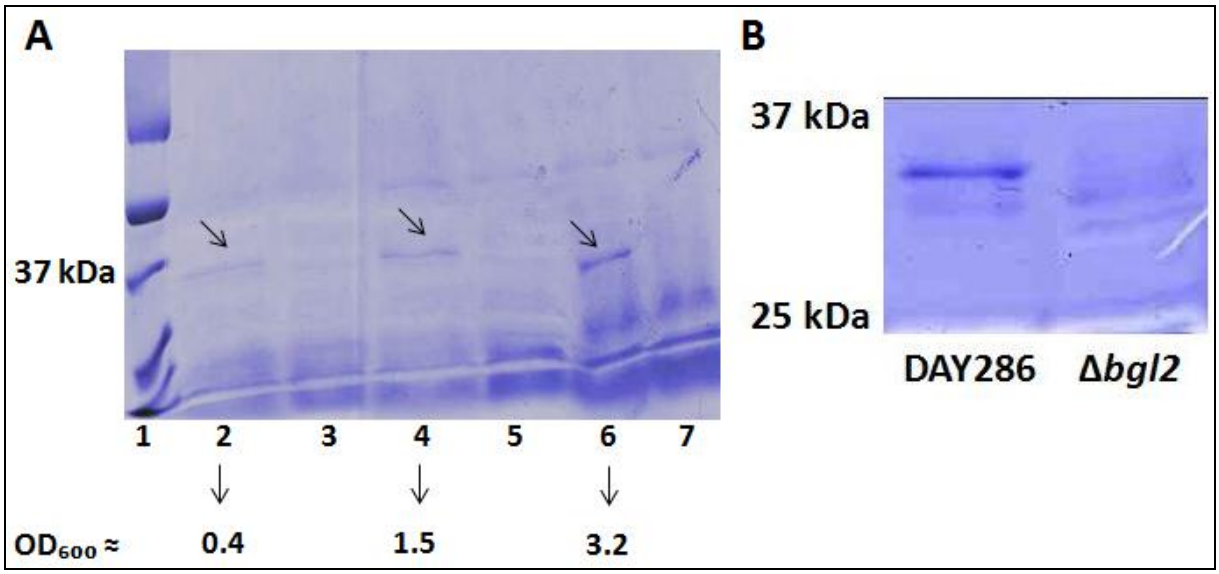

Figure 3.1.2 – Studies on the attachment of Bgl2p to the *C. albicans* cell wall during different growth stages and morphologies.

SDS-PAGE analysis of proteins extracted by heating whole cells of *C. albicans* DAY286 and Δ*bgl2*. (A) Cells were cultivated in YPD medium for different periods until cultures reached the indicated OD_{600} before proteins were extracted. Arrows in the gel indicate Bgl2p. The gel was run for 2 h at 120 V. Lane 1: marker, lanes 2, 4 and 6: DAY286 extracts, lanes 3, 5 and 7: Δ*bgl2* extracts. (B) Cells were cultivated in RPMI medium supplemented with 10% FBS at 37 °C for 3 h for initial hyphal formation. The gel was run for 2 h and 43 min at 120 V (excerpt of the Coomassie stained SDS-gel is shown).

3.1.4 Identification of unique *C. albicans* Bgl2p peptides and generation of anti-Bgl2p monoclonal antibodies

We aimed to identify unique peptides of Bgl2p which could be synthesized and used for immunization in mice for monoclonal antibody production. The identification of suitable peptides was performed in cooperation with projects partners (Yvonne Mayer, Microdiscovery GmbH, Berlin, Germany). Favorable peptides should comply with the following criteria:

(i) Peptides should be 10 – 25 aa long.

(ii) The peptide sequences should be largely conserved among *C. albicans* strains. Furthermore peptide sequences must be specific for *C. albicans* and have low homologies in proteins from non-albicans *Candida* species (NACS).

(iii) Peptides should have low or no homology to proteins from other pathogens or humans.

(iv) The peptides sequence in the protein must be accessible for antibodies.

Only three *C. albicans* strains have been sequenced when the analysis was conducted. These are SC5314, the WO-1 strain and ATCC10261. Multiple sequence alignments (MSA) showed a high conservation of the Bgl2p sequence not only among the three *C. albicans* strains mentioned above, but also among several *Candida spp.* (see Supplemental data 4).

Conserved peptides forming α-helices were analyzed for their ability to serve as target sequences (by Yvonne Mayer). Unfortunately, the 3D-structure of *C. albicans* Bgl2p is not yet elucidated. Thus, *C. albicans* 3D-structure was modeled according to the published 3D-structure 1aq0 of a ß-(1,3)-(1,4)-glucanase from *Hordeum vulgare*. This enzyme showed highest score in paired sequence alignments with Bgl2p, among all known 3D-structures of GH17 members found at the PDB database (http://www.rcsb.org/pdb/home/home.do). However, the identity between both proteins did not exceed 30%, suggesting a poor quality of the obtained model.

Nevertheless, two peptides, termed a10 (SVENAADQWQKGIC) and a7/8 (PAIDAADVVYSNSFSYW), were found identical in all three *C. albicans* strains. a10 was unique for *C. albicans* with only one E246K substitution in *C. dubliniensis* (Figure 3.1.3A). In contrast, a7/8 was conserved in *C. dubliniensis* (Figure 3.1.3B).

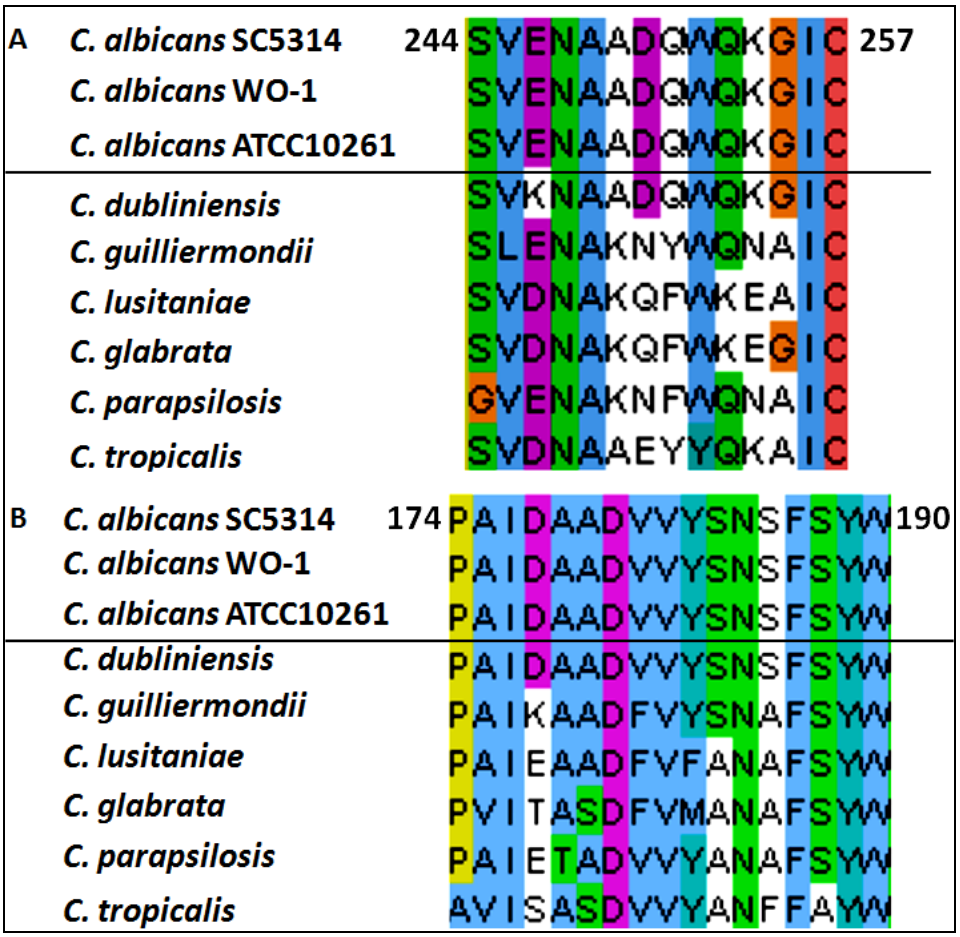

Figure 3.1.3 – Multiple sequence alignment (MSA) of Bgl2p peptides.

MSA were performed for (A) a10 and (B) a7/8 from three different *C. albicans* strains and six different NACS. Alignments were performed using CLUSTALW2 and displayed with the Jalview editor (http://www.ebi.ac.uk/Tools/msa/clustalw2/). Amino acid numbers, lines and species description were added to the Jalview displayed MSA.

A search for similar sequences from bacteria, fungi, archaea and humans was conducted in NCBI (performed by Yvonne Mayer, see Supplemental data 5). For peptide a10, only one relevant hit from *Cellulomonas flavigena* with a score of 52.0 was found. Peptide a7/8 had several hits from different yeasts including *L. elogisporus*, *D. hansenii*, *Pichia stipitis* or *Yarrowia lipolytica*.

The selected peptides must be exposed for binding partners and thus should be present on the proteins outer region rather than being hidden inside the protein fold.

a10 forms an α-helix according to the modeled structure based on 1aq0. The sequence a7/8 should form two short α-helices (Yvonne Mayer, personal communications). α-helices could be located on the proteins surface if they are pre-dominantly made of amino acids with polar side chains. a10 indeed mainly consists of amino acids with polar side chains, in contrast to a7/8, which is mainly made of non-polar or weakly polar side chains (Table 5).

Table 5 – Distribution of amino acids with polar and non-polar side chains in peptides a10 and a7/8 (single letter code for amino acids).

Peptide	**Length (aa)**	**Sequence**	**Polar side chains**	**Non-polar side chains**	**Side chains with weak polarity**
a10	14	SVENAADQWQKGIC	S, E, N, D, Q (2x), K, G, C	V, A (2x), I	W
a7/8	17	PAIDAADVVYSNSFSY W	D (2x), S (2x), N	P, A (3x), I, V (2x), F	Y (2x), W

However, with help of the PyMol v0.99 (DELANO SCIENTIFIC, USA) software, both sequences were predicted to be located in the external parts of the modeled protein (Figure 3.1.4). Antibodies raised against short synthetic peptides have been found to bind the respective sequences in native proteins, if these sequences are present on the surface of the corresponding protein (Lerner, 1982). The peptides a7/8 and a10 were synthesized by Dr. Werner Tegge (CBIO, HZI, Braunschweig, Germany) and used for immunization in Balb/c mice (Dr. Nicole Schliebe, Institute for Biochemistry and Biology, University of Potsdam, Germany, personal communication). Peptide a7/8 was modified at the N-terminus by adding a cysteine residue to allow coupling to carrier proteins. Immunization of mice and selection of positive hybridoma cell culture supernatants was performed by project partners (Prof. Katja Heilmann and co-workers, Institute for Biochemistry and Biology, University of Potsdam).

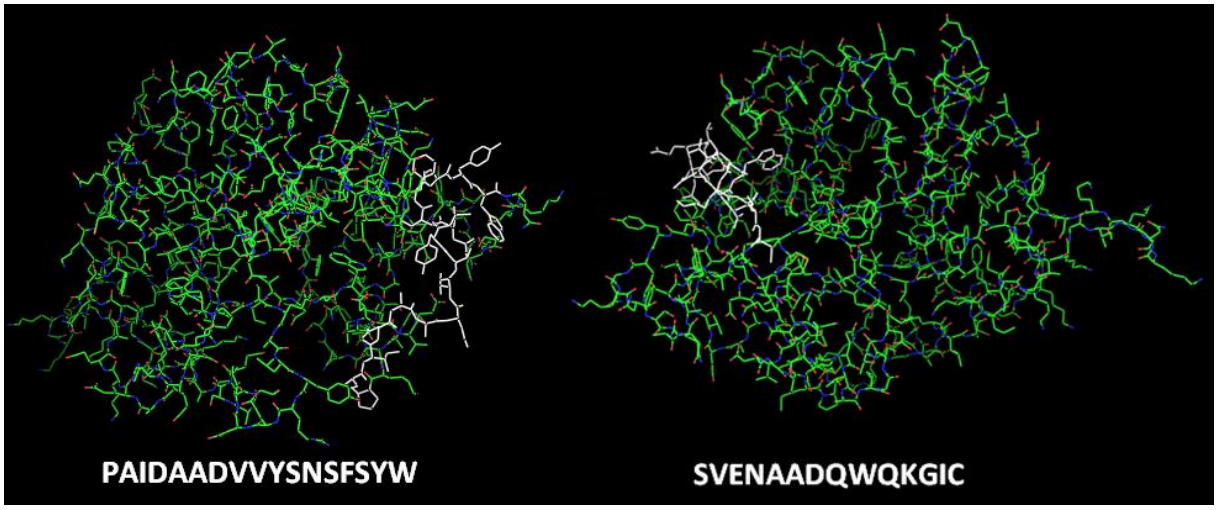

Figure 3.1.4 – Localization of a7/8 and a10 in a modeled structure of *C. albicans* Bgl2p based on the 1aq0 structure of a ß-(1,3)-(1,4) glucanase from *H. vulgare*.

Localization of peptides a7/8 (PAIDAADVVYSNSFSYW) and a10 (SVENAADQWQKGIC) was predicted in a modeled structure based on the structure 1aq0 (http://modbase.compbio.ucsf.edu). a7/8 and a10 are highlighted in white. Note that the protein structure is differentially rotated in each image for proper display of the desired peptides.

3.1.5 Recombinant expression and purification of *C. albicans* rBgl2p-SP under non-denaturing conditions

Generated anti-7/8 or anti-a10 antibodies had to be assessed as to their binding to purified native Bgl2p.The isolation of Bgl2p under non-denaturing conditions was achieved by Zymolyase treatment of *C. albicans* cell walls. However, extracted Bgl2p amounts by Zymolyase digestion of cell walls were judged as relatively low (see Supplemental data 2A), so that further purification steps seemed incapable of providing enough protein. Thus, recombinant protein expression was followed as an alternative strategy. The *C. albicans BGL2* (orf19.4565) sequence was acquired from the Candida Genome Database (CGD) (Inglis et al, 2012). Based on this sequence, a *Ca*Bgl2p encoding gene was designed by Prof. Dr. Peter Müller (RDIF, HZI, Braunschweig) with restriction sites altered by silent nucleotide substitutions to facilitate easier cloning. Furthermore, coding sequences for 3x FLAG- and 8x His-Tags were included at the 3’ end followed by a stop codon. A *NcoI* digestion site was

included after the coding sequence of an 18 aa signal peptide (Angiolella et al, 2009) which allows cloning of two versions of the gene, one which encodes the full length Bgl2p (rBgl2p), while the other encodes Bgl2p lacking the signal peptide (rBgl2p-SP). As the first amino acid after the signal peptide sequence in Bgl2p is methionine, there was no need for insertion of an artificial methionine codon. Figure 3.1.5A shows a schematic illustration of the *Ca_BGL2_FLAG3x_His8x*, encoding recombinant Bgl2p (rBgl2p). See Supplemental data 1 for the sequence of the *Ca_BGL2_FLAG3x_His8x* gene.

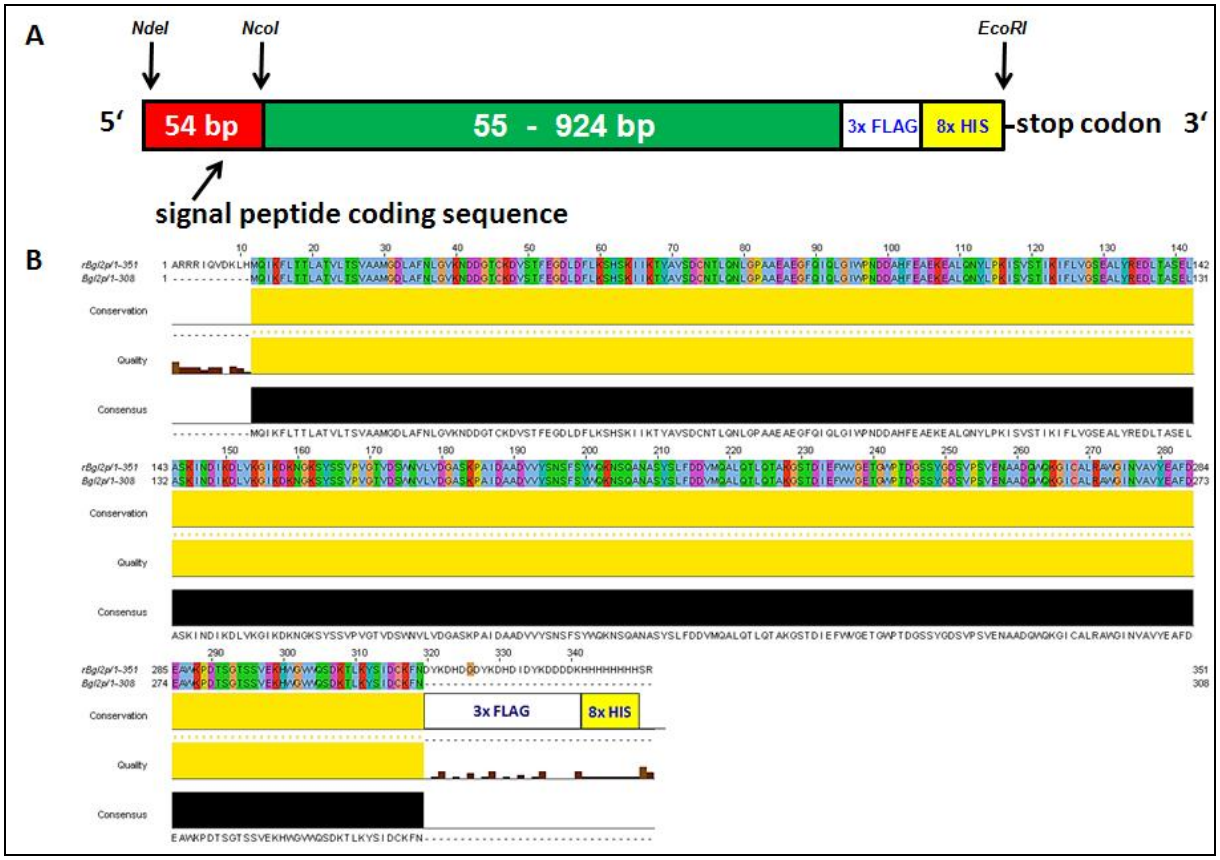

Figure 3.1.5 – Design of *Ca_BGL2_FLAG3x_His8x* encoding recombinant Bgl2p (rBgl2p).

(A) Schematic illustration of *Ca_BGL2_FLAG3x_His8x*, encoding for recombinant Bgl2p (rBgl2p) with respective restriction sites used for cloning of each version. (B) Sequence alignment (ClustalW2; displayed with Jalview) of rBgl2p and the native *C. albicans* Bgl2p sequences. *Ca_BGL2*_FLAG3x_His8x was translated using http://web.expasy.org/translate/. FLAG and HIS tag sequences are indicated.

The resulting amino acid sequence was aligned with Bg2lp sequence obtained from the CGD to confirm correct sequence (Figure 3.1.5B). *Ca_BGL2_FLAG3x_His8x* was synthesized by GENEART AG (Regensburg, Germany).

Experimental work was restricted to *Ca_BGL2*_FLAG3x_His8x_-SP3 so far, as Bgl2p present in the *C. albicans* cell wall lacks a signal peptide (Angiolella et al, 2009).

rBgl2p-SP was expressed from *E. coli Ca_BGL2*_FLAG3x_His8x_-SP3. Four different IPTG concentrations (0, 62.5, 125 and 250 µM) were tested for best expression levels of rBgl2p-SP under non-denaturing conditions. Best expression of the target protein was obtained when no IPTG was added (Figure 3.1.6A). Thus, addition of IPTG was omitted in all later experiments. rBgl2p-SP was successfully purified (> 90%) by means of the N-terminal 8x His-TAG. This was achieved by coupling the selectivity of Ni-NTA beads with separation by molecular weight in a PD-10 sepharose column. Among six analyzed elution fractions, fractions shown in lanes 5 and 6 showed highest rBgl2p-SP content (Figure 3.1.6B), while fractions shown in 3 and 4 showed no content. Fractions shown in lanes 5 – 8 were pooled, concentrated, desalted and eluted with NP buffer by PD-10 columns. The purified protein was concentrated again by Vivaspin6 (3 kDa MWCo) before being applied on SDS-gel. The purified protein was applied twice on the same SDS-gel. After SDS-PAGE, one sample was subjected to coomassie staining, while the other was blotted on a PVDF membrane and probed with anti-FLAG antibody (Figure 3.1.6C and D).

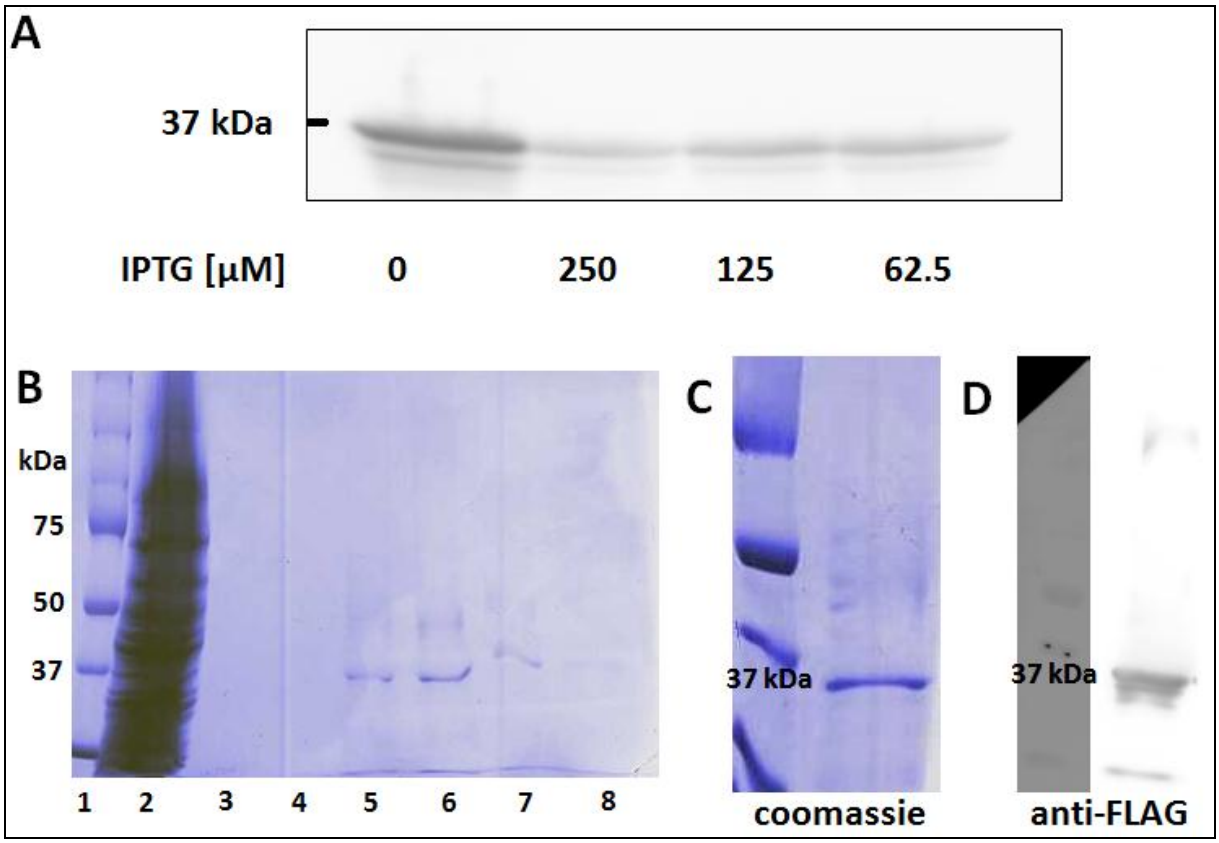

Figure 3.1.6 – Expression and purification of rBgl2p-SP from *E. coli* Rosetta™ 2 (DE3).

(A) Strain *Ca_BGL2*_FLAG3x_His8x_-SP3 was cultivated and cell lysate was prepared as indicated in 2.3.4. Four different IPTG concentrations (0, 62.5, 125 and 250 µM) were tested for best expression levels of rBgl2p-SP under non-denaturing conditions. Lysate was run by SDS-PAGE and proteins were blotted on PVDF membrane. Blot was probed with anti-FLAG for rBgl2p-SP determination. Blot was exposed for 60 seconds. (B) SDS-PAGE (3h, 120 V) followed by Coomassie staining of crude lysate and purified rBgl2p-SP. Lane 1: marker, lane 2: crude lysate, lanes 3 – 8: rBgl2p-SP elution fractions. (C) SDS-PAGE (2h, 120 V) followed by coomassie staining of pooled elution fractions shown in lanes 5 – 8 in (B). Fractions were concentrated, desalted and eluted with NP buffer by PD-10 columns. The sample was concentrated again before being applied on SDS-gel. Identity of Bgl2p band (ca. 36 kDa) was proven by MS/MS analysis. (D) A sample from the same purified rBgl2p-SP shown in (C) was applied on the same gel and then blotted on a PVDF membrane. The membrane was probed with anti-FLAG antibody. The blot was exposed for 50 seconds.

3.1.6 Qualitative evaluation of anti-a7/8 and anti-a10 antibodies for binding to purified rBgl2p-SP

Cell culture supernatants of hybridoma cell lines were evaluated in Enzyme Linked Immunosorbent Assay (ELISA) for binding to the respective antigen (a7/8 or a10) by project partners (Prof. Katja Heilmann and co-workers, Institute for Biochemistry and Biology, University of Potsdam). Supernatants which are named C25 contained antibodies which recognize peptide a10, while those starting with C26 contained antibodies recognizing a7/8 (Natalia Maier, Institute for Biochemistry and Biology, University of Potsdam). Positive supernatants were evaluated for their binding to rBgl2p-SP, expressed and purified under non-denaturing conditions. rBgl2p-SP was dropped on PVDF membranes (dot blot) and membranes were incubated with the respective supernatant and subsequently with an HRP-conjugated secondary antibody. All tested anti-a10 supernatants showed clear binding to rBgl2p-SP, while most anti-a7/8 (e.g. C26FC11F7) did not bind to the protein (Figure 3.1.7 and Supplemental data 6). To confirm presence of the rBgl2p-SP protein, membranes treated with C25JA11B10 or C26FC11F7 were stripped and probed with anti-FLAG antibody (Supplemental data 6).

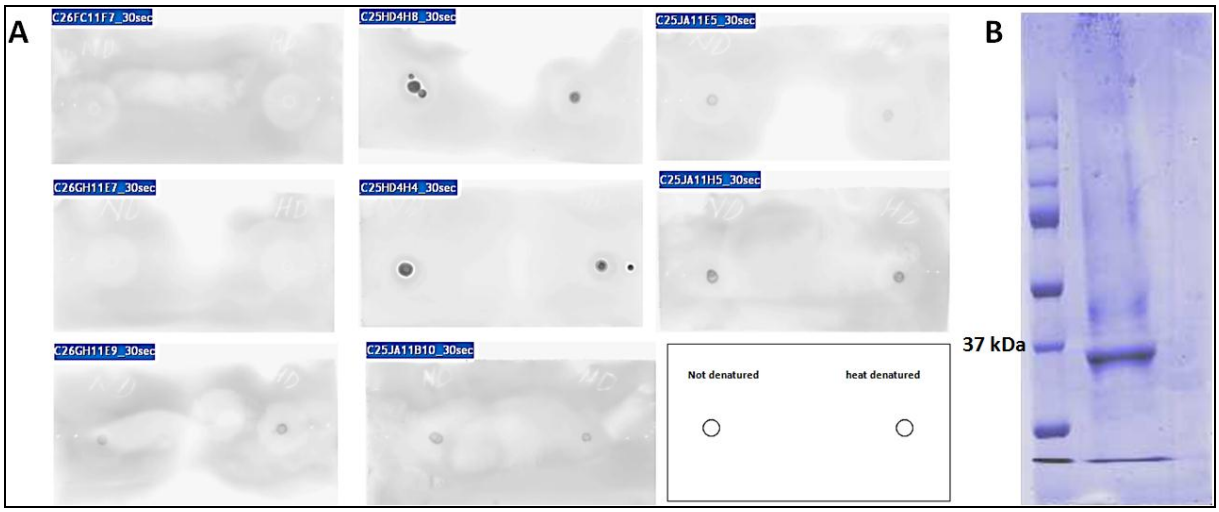

Figure 3.1.7 – Dot blots analysis of binding of several hybridoma cell culture supernatants to rBgl2p-SP.

(A) rBgl2p-SP (ca. 227 ng) was dropped on PVDF membranes. Membranes were blocked, washed with TBS containing 0.05% (v/v) Tween-20 and incubated overnight with the respective hybridoma cell culture supernatants and subsequently with HRP-linked secondary antibody. Blots were exposed for 30 sec each. A scheme of the blots is also shown. rBgl2p-SP used in this experiment derived from a different purification than indicated under Figure 3.1.6. The purification control is shown in (B). (B) SDS-PAGE analysis of rBgl2p-SP purification. Gel ran for 4 h at 120 V. Identity of Bgl2p band (ca. 36 kDa) was proven by MALDI-TOF MS analysis.

Table 6 summarizes the results obtained with the tested supernatants by dot blot detection of rBgl2p-SP.

Table 6 – Binding of antibodies present in tested hybridoma cell culture supernatants to rBgl2p-SP by dot blot analysis.

Supernatant	Bound rBgl2p-SP
C25HD4H4	Yes
C25HD4H8	Yes
C25JA11B10	Yes
C25JA11E5	Yes
C25JA11H5	Yes
C26FC11F7	No
C26GH11E7	No
C26GH11E9	Yes

3.1.7 Evaluation of C25HD4H4 and C25HD4H8 binding to viable *C. albicans* cells

In order to evaluate binding of the anti-a10 antibodies to viable *C. albicans*, flow cytometric analysis of SC5314, DAY286 and Δ*bgl2* strains was performed as indicated in 2.9. As hybridoma cell culture supernatants contained 15% FBS (Dr. Nicole Schliebe, Institute for Biochemistry and Biology, University of Potsdam, personal communication), C25HD4H4 and C25HD4H8 were each concentrated 2.3 fold by Vivaspin columns of 50 kDa MWCo in order to remove lower molecular weight protein contaminants, while enriching the respective antibodies. Binding of C25HD4H4 and C25HD4H8 was evaluated as these supernatants showed the strongest binding to rBgl2p-SP in dot blot analysis (Figure 3.1.7). As Bgl2p content increased during stationary phase of growth (Figure 3.1.2), we first tested the binding of these two supernatants to stationary phase cells.

As can be taken from Figure 3.1.8A, C25HD4H4 and C25HD4H8 bound cells from stationary phase, of both SC5314 and DAY286 (both *BGL2*$^{+}$), but not to Δ*bgl2* cells, as the peak pattern between *BGL2*$^{+}$ and Δ*bgl2* cells was distinct. The histograms of unstained cells (PBS), resembled those of cells which were not bound by fluorescent probes. Cells of all three strains treated only with the secondary antibody (anti-mouse-IgG), showed no unspecific binding by this antibody. Binding of C25HD4H4 was stronger compared to C25HD4H8 as a subpopulation (lower fluorescence range) of SC5314 was not detected by C25HD4H8. As a positive control, SC5314 cell surface proteins were biotinylated and subsequently stained with fluorescently labeled streptavidin (Figure 3.1.8B).

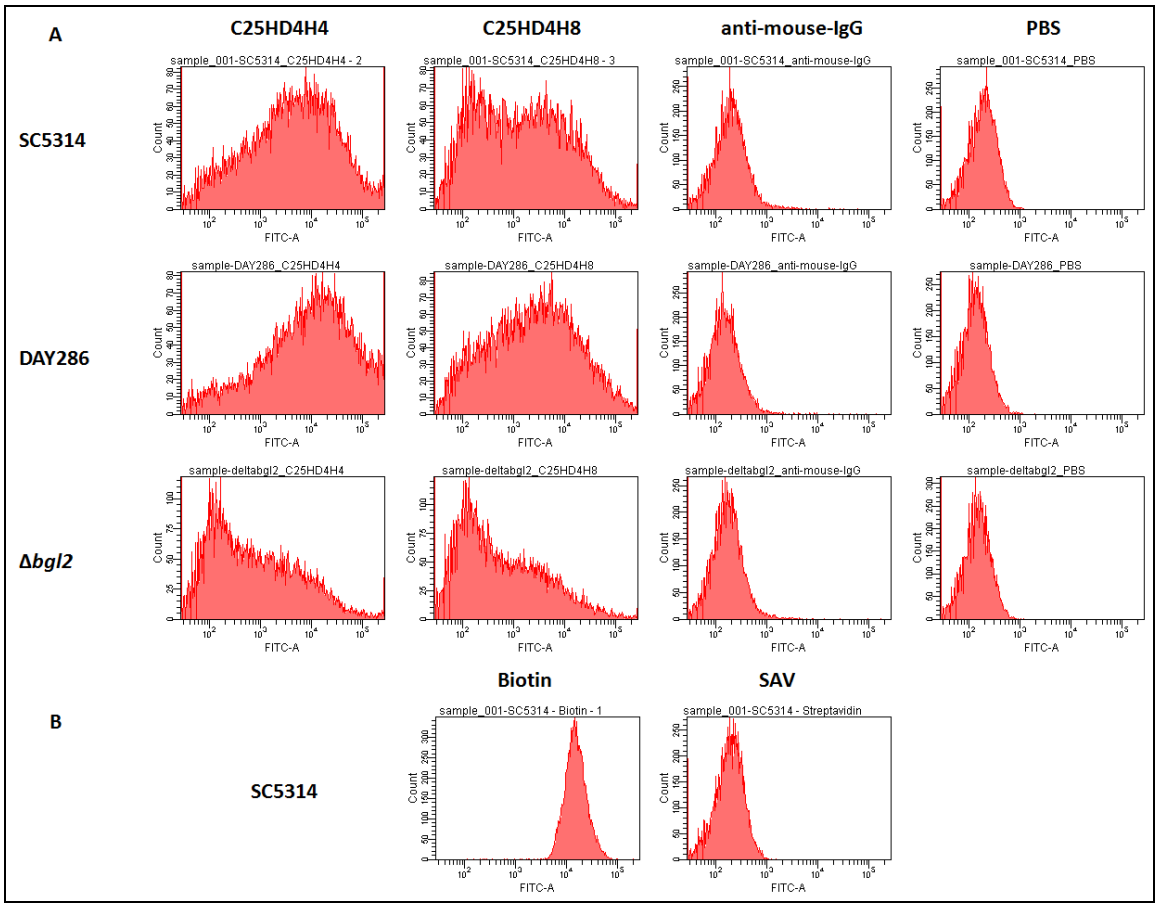

Figure 3.1.8 – Flow cytometric analysis of C25JHD4H4 and C25HD4H8 treated cells.

(A) *C. albicans* SC5314, DAY286 or Δ*bgl2* were incubated with each of the 2.3 fold concentrated mouse hybridoma cell culture supernatants C25HD4H4 or C25HD4H8 containing monoclonal anti-a10 antibodies, followed by incubation with Alexa fluor 488 anti-mouse IgG antibody and analyzed by flow cytometry. For negative controls, supernatants were substituted by the same volume of PBS or only PBS was used during all incubation steps respectively. (B) SC5314 cell surface proteins were biotinylated with 1 mg ml^{-1} EZ-Link Sulfo-NHS-LC-LC-Biotin and subsequently were incubated with Alexa fluor 488 Streptavidin. For negative control, biotin was substituted by the same volume of PBS pH 8.0 and subsequently incubated with Alexa fluor 488 Streptavidin.

3.1.8 Discussion

Numerous *C. albicans* proteins are known for their antigenic properties, however, most of these proteins are either glycolytic enzymes, elongation factors, ribosomal or ribosome associated proteins. Such proteins are highly conserved either among kingdoms, or even among all organism classes. Moreover, the presence of such proteins on the cell surface of *C. albicans* is often disputed (Klis et al, 2009). This would deem such proteins as inappropriate for diagnostic approaches.

Hwp1p is a unique *C. albicans* cell wall protein and parts of this protein were previously used in *C. albicans* diagnostics (Lain et al, 2007). However, this protein is only present in the cell wall during the hyphal morphology (Staab et al, 1996). Yet abundant, such hyphae-specific CWPs were also judged as inappropriate. The yeast morphology is important for dissemination of yeast cells and is thus important during the initial infection process (Saville et al, 2003; Thompson et al, 2011). As rapid detection of *C. albicans* cells during the early stages of infection is of high value; thus, target CWPs present only on the surface of true hyphae could lead to yeast cells being not detected. Patients suffering under early stage Candidiasis would thus not be correctly diagnosed.

Bgl2p is a protein which complies with most of the characteristics mentioned under 3.1.1. We used several methods of cell surface protein extraction from both whole and disrupted cells. Bgl2p was frequently found in almost all of those different extracts, confirming that such observations were not method dependent. Bgl2p could only not be detected in hot SDS extracts. This was surprising, as Bgl2p is known to be a non-covalently bound CWP. Identification of Bgl2p in hot SDS extracts might have been prevented by more abundant proteins of the similar molecular weight in SDS-PAGE, if present in the same gel slice as Bgl2p.

Klis and co-workers had previously suggested that Bgl2p, along with other non-covalently bound CWPs, might be washed away from the cell wall by shaking at 200 rpm (Sorgo et al, 2010). Published Bgl2p extraction methods from *C. albicans* or *S. cerevisiae* included mechanical disruption of cells before subsequent release from the cell wall by heat or Zymolyase treatment (Angiolella et al, 2009; Mrsa et al, 1993, Sarthy et al, 1997). Indeed, our own experiments which involved mechanic disruption of cells by grinding or via a microdismembrator did not lead to satisfying amounts of Bgl2p (see Supplemental data 2), suggesting that Bgl2p was partly lost during disruption of cells and subsequent washing of cytosolic contaminants. Thus, we needed to develop a reliable method to study Bgl2p content of cell walls after different cultivation conditions. We extracted Bgl2p by heating whole cells at 90 °C for 10 min. The high temperatures were sufficient to release Bgl2p from the cell wall without combination of heat with reducing or denaturing agents. As heat disrupts non-covalent bonds (e.g. hydrogen bonds), this correlates with previous knowledge on Bgl2p as a non-covalently bound CWP (Chaffin, 2008). Even though Bgl2p levels markedly increased in stationary phase cells, this protein was found to be permanently attached to the cell wall, which is a prerequisite for accessibility of cells by anti-Bgl2p antibodies. Additionally, Bgl2p was found in extracts derived from cells at initial yeast-to-hyphae switch. This indicates that such cells found during the early phase of infection could also be detectable by anti-Bgl2p antibodies.

Serum anti-Bgl2p antibodies were suggested as diagnostic biomarkers of systemic candidiasis (SC), as the anti-Bgl2p IgG response of SC patients was stronger than of non-SC individuals (Pitarch et al, 2006). This is an indicator of the accessibility of this protein by antibodies during *C. albicans* infection. The same authors suggested that high levels of anti-Bgl2p antibodies represent a defense mechanism against SC and confer protection of the host from SC. Furthermore, these findings indicate that Bgl2p is an appropriate target protein to

distinguish *C. albicans* infection from colonization. Other works have also included Bgl2p among a group of the most antigenic proteins of *C. albicans* (Clancy et al, 2008; Mochon et al, 2010).

The presence of Bgl2p on the cell surface was also experimentally confirmed (Hernaez et al, 2010), as well as being one of the most abundant proteins in the cell wall of *C. albicans* (Angiolella et al, 2009). The function of Bgl2p as an adhesin (Jeng et al, 2005) further confirms its association with the cell surface and implicates a role in pathogenicity. The latter assumption is further strengthened by the reduced pathogenicity of the Δ*bgl2* mutant in a murine model of infection (Sarthy et al, 1997). Thus, Bgl2p appeared to be a strong candidate target protein.

However, members of the Bgl2p family are present in several ascomycetes (Mouyna et al, 1998; Mrsa et al, 1993; Weig et al, 2004). BLAST search also showed a relatively high conservation of this enzyme within *Candida* clade species (see Supplemental data 4). Antisera raised against Bgl2p from *S. cerevisiae* could identify *C. albicans* Bgl2p in western blot experiments (Sarthy et al, 1997). Therefore, epitopes which should be recognized by anti-Bgl2p antibodies in diagnostic approaches had to be unique for *C. albicans* Bgl2p.

The search for unique *C. albicans* Bgl2p epitopes resulted in two peptides, termed a10 and a7/8 respectively. These peptides were found to be conserved in the three *C. albicans* strains mentioned above and had low similarities with sequences from different organismal classes. Furthermore, peptide a10 was unique for *C. albicans* (see Supplemental data 4).

The two peptides a7/8 and a10 were used for antibody production in mice. Anti-peptide antibodies can be highly reactive with the native protein incorporating the same primary amino acid sequence, provided such sequences are not buried within the proteins fold (Lerner, 1982).

In order to evaluate antibody binding to the native protein, Bgl2p had to be extracted and purified under non-denaturing conditions. This was accomplished by Zymolyase digestion of the ß-(1,3)-glucan network of the cell wall. However, extracted amounts of Bgl2p were judged as relatively low after SDS-PAGE analysis so that further purification steps seemed to be unrealistic. We thus decided to recombinantly express Bgl2p and opted for *E. coli* over yeast as expression system. In contrast to yeast, Bgl2p expressed in *E. coli* would lack post-translational modifications such as glycosylation (Lain et al, 2008). However, in yeast expression systems, rBgl2p would be incorporated into the cell wall requiring special treatment for extraction (i.e. Zymolyase digestion), leading to similar problems as in *C. albicans* (see above). Furthermore, overexpression of *ScBGL2* in *S. cerevisiae* led to significant decrease of the growth rate of cells (Mrsa et al, 1993).

Supernatants which contained either anti-a10 or anti-a7/8 antibodies were evaluated for binding against recombinant Bgl2p lacking the signal peptide sequence (rBgl2-SP), expressed and purified under non-denaturing conditions. All five tested anti-a10 supernatants bound rBgl2p-SP in dot blots, while two of three tested anti-a7/8 supernatants did not. An explanation for this behavior could be that peptide a7/8 mostly consists of amino acids with non-polar side chains (Table 5), rendering it less soluble and thus probably hidden inside rBgl2p-SP. In contrast to this, peptide a10 largely consists of amino acids with polar side chains, suggesting that this amino acid sequence might be present on the protein's surface. Thus, more polar alpha-helices are better accessible for antibody binding. However, peptide a7/8 is detectable in principle by antibodies as C26GH11E9 bound rBgl2p. This depends on the localization of the respective epitope which is recognized by each antibody. Modeled structures of *C. albicans* Bgl2p based on 1aq0 from *H. vulgare* suggested that both a7/8 and a10 are largely present in the outer parts of protein. However, because of the low identity (ca. 30%) between *C. albicans* Bgl2p and the *H. vulgare* protein the modeled structure could not

reflect real localization of a7/8 and a10. As the concentration of antibodies in such hybridoma cell culture supernatants is unknown, failure of anti-a7/8 containing supernatants (e.g. C26FC11F7 and C26GH11E7) to bind rBgl2p-SP could also simply be due to low anti-a7/8 titers in those supernatants.

C25HD4H4 and C25HD4H8 showed strongest binding to rBgl2p-SP among all tested supernatants. Previously, these two supernatants showed strong signals when tested in ELISA against a10 (Dr. Nicole Schliebe, Institute for Biochemistry and Biology, University of Potsdam, personal communication). Both C25HD4H4 and C25HD4H8 could bind to *C. albicans* SC5314 (WT) as well as to DAY286 cells. Fluorescence signals from SC5314 and DAY286 were clearly distinct from those of Δ*bgl2* cells treated with the same supernatants, which were similar to the peaks of the negative controls. This indicated that components of the two supernatants could bind to exposed cell surface structures of SC5314 and DAY286 which were missing in Δ*bgl2* cells. The only difference in the genomes of DAY286 and Δ*bgl2* is the lack of the *BGL2* gene in the latter cells (Table 1). This is a strong indicator that Bgl2p is the target of the anti-a10 antibodies present in C25HD4H4 or C25HD4H8. However, the histograms showed background fluorescence resulting probably from unspecific binding of supernatant components to Δ*bgl2*. Hybridoma cell culture supernatants contain a variety of FBS derived proteins, including bovine antibodies which may cross-react with cell surface structures of *C. albicans* cells and might be bound by the fluorescent anti-mouse IgG secondary antibody.

Unfortunately, no purified anti-a10 antibodies were obtained from the project partners within the time of this thesis. This was due to major problems with antibody production and purification. Thus, final conclusions about quality, specificity and sensitivity of anti-a10 antibodies cannot be made until the purified anti-a10 monoclonal antibodies are provided. Future experiments are further discussed in Chapter 4.

3.2 Involvement of the mitogen activated protein kinase Hog1p in the response of *C. albicans* to iron availability

We have isolated proteins belonging to the multicopper ferroxidase (MCFO) class of enzymes from *C. albicans* by heating whole cells (see Supplemental data 2F and section 3.1.2). Members of this class are part of the high affinity iron uptake (HAIU) system which is induced in *C. albicans* during conditions of restricted iron (Lan et al, 2004). However, several components of the HAIU system, including genes encoding MCFO members, were found to be regulated by a variety of factors other than iron availability, such as pH (Bensen et al, 2004) or antimycotic treatment (Liu et al, 2005). Furthermore, several genes encoding HAIU proteins were found to be de-repressed in a Δ*hog1* deletion mutant (Enjalbert et al, 2006) pointing to an involvement of the HOG pathway in regulating iron uptake.

Additionally, the MCFO Fet34p was found among a group of the most serodominant antigenic *C. albicans* proteins together with the ferric reductase Fre10p (Mochon et al, 2010). The state of iron restriction in addition to the physiological pH present in human serum, probably leads to enhanced expression of MCFOs, thus increasing their abundance, which is a requirement for diagnostic target proteins. However, the regulation of MCFO expression seems to be very complex. Moreover, copper dependent ferroxidase proteins are not only present in different fungi, but also in humans (Kosman, 2002), thus complicating their use as target proteins for diagnostic purposes.

However, as the expression of MCFO members was regulated by both, iron availability as well as the final MAP kinase of the HOG pathway Hog1p, we wondered whether a role for Hog1p exists in response to iron availability. Especially, as the role of signaling pathways in the regulation of cellular iron homeostasis was still unknown.

As mentioned in 1.2.6, *C. albicans* Hog1p responds to different stress situations including oxidative stress and oxidative stress conditions are induced by excess of free iron. Furthermore, *C. albicans* has been found to grow well during iron overload conditions as well as associated with iron overload diseases (Caroline et al, 1969; Minn et al, 1997). For these reasons, we were interested in studying the response of *C. albicans* to high iron concentrations with respect to a potential role of Hog1p in this response. The heat extraction method leading to the isolation of MCFOs can thus help to identify regulatory mechanisms of iron uptake in *C. albicans*.

3.2.1 Iron induced *C. albicans* flocculation in a concentration dependent manner

During cultivation of *C. albicans* SC5314 (WT) in RPMI containing different $FeCl_3$ concentrations (0, 1, 5, 7.5, 10, 20 and 30 µM) at 30 °C, we observed flocculation of cells in an iron concentration dependent manner. Flocs of cells could be seen at 5 µM and visibly increased from 7.5 to 30 µM Fe^{3+}. Flocculation was also induced when 30 µM $FeSO_4$ was used as sole iron source instead of $FeCl_3$. However, flocculation in response to $FeSO_4$ was less pronounced at that iron concentration compared to 30 µM $FeCl_3$, as quantified by sedimentation rates (Figure 3.2.1A and B). Quantification of flocculation was accomplished by determination of the sedimentation rate of cells as previously described (see 2.4) (Gregori et al, 2011).

Flocculation was also induced in yeast nitrogen base (YNB) medium containing 30 µM $FeCl_3$ compared to 1.2 µM (basal Fe^{3+} concentration in YNB medium according to the manufacturer), thus showing that the induction of flocculation was independent from the used medium (see Supplemental data 7).

Cells may possess internal iron stores from pre-cultivation in an iron sufficient medium. Thus, we investigated whether the iron content of the medium used during pre-cultivations influenced the dependence of the flocculent phenotype on the iron concentration in RPMI.

C. albicans was either pre-cultivated in a medium with sufficient iron, i.e. the rich yeast extract-peptone-dextrose (YPD) medium, or starved for iron by pre-cultivation in a medium with restricted iron availability (RIM). The RIM resulted from addition of the iron chelator bathophenanthroline disulfonate (BPS) to the YPD medium. As shown in Figure 3.2.1C, sedimentation rates, i.e. flocculation, due to exposure to 30 µM Fe^{3+} were independent on the pre-cultivation medium: WT cells starved for iron by pre-cultivation in RIM flocculated upon exposure to 30 µM Fe^{3+} with a similar sedimentation rate as cells pre-cultivated in YPD. During all later experiments, *C. albicans* was pre-cultivated in YPD and 30 µM $FeCl_3$ were used as iron source in the respective media used for working cultures unless it is mentioned otherwise.

Interactions between cells, which lead to the formation of cell aggregates or flocs, occur via constituents of the cell wall, which favor physical (hydrophobic or electrostatic) or specific biochemical interactions. The cell wall of *C. albicans* comprises proteins which are frequently mannosylated and attached to the backbone of the cell wall formed by glucans and chitin (Chaffin, 2008). To obtain further information on the background of the flocculent phenotype, we inhibited protein biosynthesis by cycloheximide (CHX) 15 min prior to the incubation with iron. A reduction in flocculation was observed after iron addition compared to an equally treated methanol control (Figure 3.2.1D). The requirement of protein synthesis for flocculation was confirmed for the reference strain DAY286 (see Supplemental data 8A and B). Thus, protein synthesis seemed to be required for induction of iron dependent flocculation, indicating the activation of a specific response.

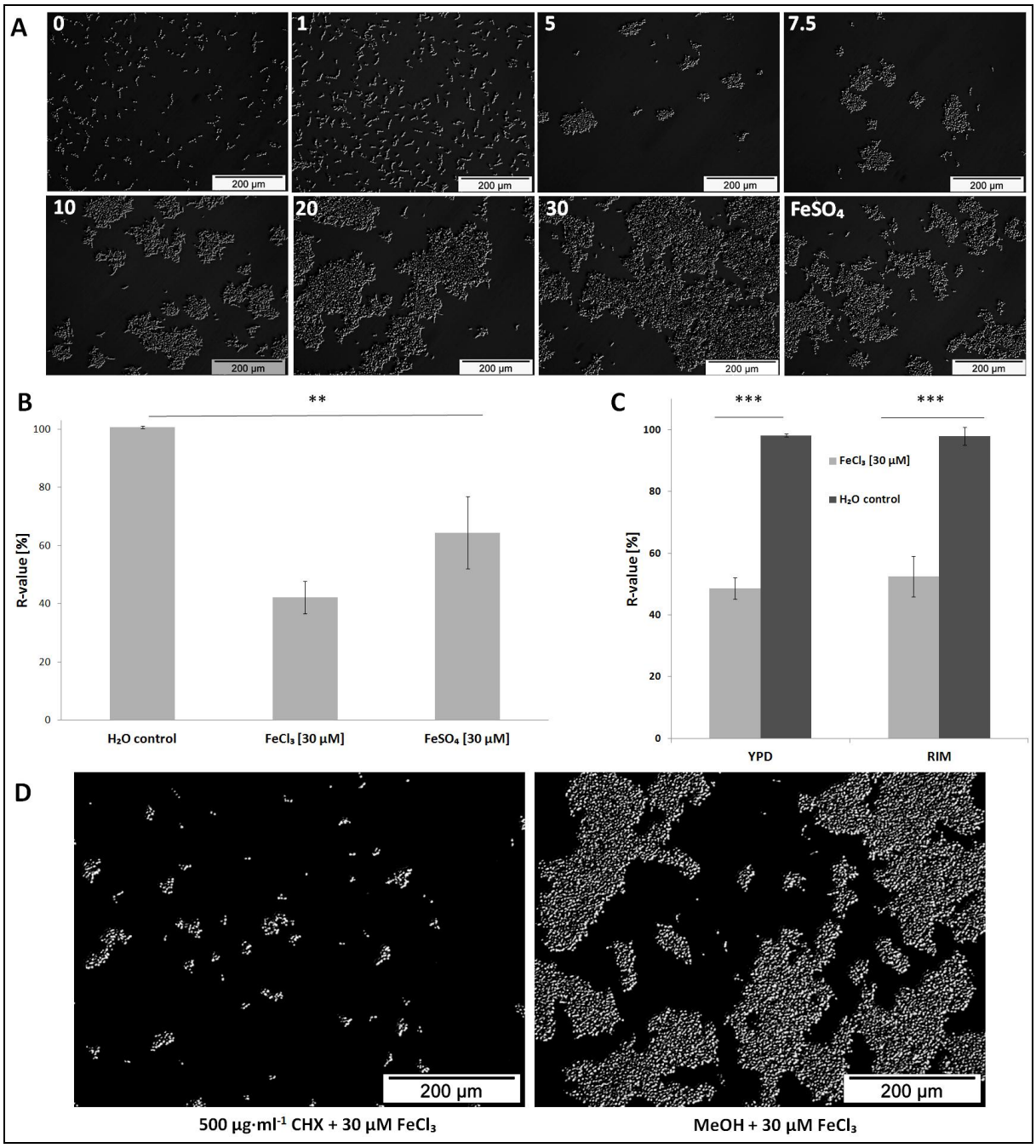

Figure 3.2.1 - Iron induced concentration dependent flocculation of *C. albicans* cells.

(A) Microscopic analysis. *C. albicans* SC5314 (WT) was incubated with different $FeCl_3$ concentrations (indicated at the top left hand of each sub panel) or with 30 µM $FeSO_4$ in RPMI at 30 °C for 2 h. (B) Relative sedimentation rates of WT cells. Flocculation of cells was triggered by 30 µM $FeCl_3$ or 30 µM $FeSO_4$ in RPMI and sedimentation rates were determined after incubation at 30 °C for 2 h. Means and standard deviations of three independent samples are shown (n = 3). ** denotes $P < 0.05$ (student's t-test). (C) Relative sedimentation rates of WT cells pre-cultured in the sufficient iron (YPD) or restricted iron medium (RIM) at 30 °C for 3 h. Flocculation of cells was triggered by 30 µM $FeCl_3$ in RPMI and sedimentation rates were determined after

incubation at 30 °C for 2 h. Means and standard deviations of three independent samples are shown (n = 3). *** denotes $P < 0.001$ (student's t-test). (D) Microscopic analysis of cycloheximide (CHX) or MeOH pre-treated cells. *C. albicans* SC5314 was pre-treated either with 500 µg ml^{-1} CHX or MeOH in RPMI at 30 °C for 15 min. Iron or water were subsequently added and cells were incubated at 30 °C for 2 h.

3.2.2 High extracellular iron levels led to accumulation of intracellular ROS

Iron is a potent inducer of reactive oxygen species (ROS) under aerobic conditions, as ferric iron is efficiently reduced to ferrous iron by superoxide formed as byproduct of respiration. The resulting ferrous iron is oxidized by hydrogen peroxide, resulting in the extremely reactive hydroxyl radical. Thus, uptake of iron leads to the accumulation of toxic ROS and, correspondingly, accumulation of ROS can be used as indicator of iron uptake, if all other conditions are kept constant. ROS levels were determined using CM-H_2DCFDA which is a cell permeable, oxidant sensitive agent widely used for intracellular ROS determination (see 2.5) (Alonso-Monge et al, 2009; Dhamgaye et al, 2012; Lupetti et al, 2002; Pieri et al, 2006). Compared to a water control, exposure of cells to 30 µM (high) but not to 1 µM (low) ferric iron led to an increase in ROS generation by 15 - 40%. This effect could be reversed by the ROS scavenger N-acetyl cysteine (NAC), when added to the cells together with iron (Figure 3.2.2A).

Flocculation is frequently induced in yeasts as a response to stress (Gregori et al, 2011; Verstrepen & Klis, 2006). As we had observed that high iron levels (30 µM) induced both flocculation as well as ROS accumulation while 1 µM Fe^{3+} did not, we investigated whether a relationship exists between the flocculation phenotype and iron induced oxidative stress. We determined the sedimentation rates of cells exposed to 30 µM iron and of cells exposed to the same iron concentration together with NAC. However, NAC did not prevent iron induced flocculation and the same sedimentation rate was obtained from the two data sets (Fig 3.2.2B). Thus, iron induced flocculation and ROS accumulation were not related to each other.

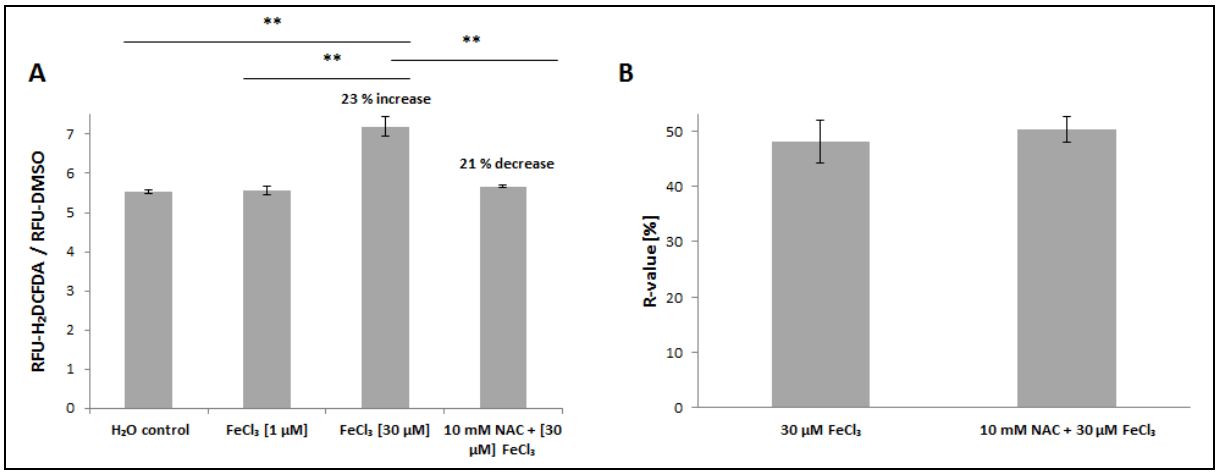

Figure 3.2.2 - High extracellular iron concentrations increased intracellular ROS levels.

(A) Determination of intracellular ROS production. WT cells were exposed to 0 (H_2O control), 1 or 30 µM $FeCl_3$ in RPMI at 30 °C for 10 min. Additionally, cells were exposed to 30 µM $FeCl_3$ together with 10 mM NAC. Means and standard deviations are shown from one representative experiment where all samples were derived from the same pre-culture. ** denotes $P \leq 0.01$ (student's t-test). All experiments were repeated 2 – 4 times from independent pre-cultures with similar results. (B) Influence of ROS on flocculation. Flocculation of cells was triggered by 30 µM $FeCl_3$ in RPMI with or without 10 mM NAC. After 2 h incubation at 30 °C, sedimentation rates were determined as described in the experimental part. Means and standard deviations of three independent samples are shown (n = 3).

3.2.3 *C. albicans* flocculation in response to high iron concentrations was dependent on both Hog1p and Pbs2p kinases

We had observed that high iron concentrations induced a flocculent phenotype in WT cells (Figure 3.2.1). Thus, we investigated whether this phenotype was also dependent on the kinases Hog1p and Pbs2p. Interestingly, microscopic analysis and cell sedimentation assays showed that flocculation was absent in both Δ*hog1* and Δ*pbs2* mutants after exposure to high Fe^{3+}, while it was still induced in the reference strain DAY286 (Figure 3.2.3A and B). When *HOG1* was re-integrated as fusion protein with GFP (strain hAHGI, Table 1), flocculation was restored after exposure to high iron concentrations as shown by measuring cell sedimentation rates (Figure 3.2.3C). Thus, the induction of flocculation was dependent on *HOG1* and *PBS2*. Moreover, we observed flocculation of Δ*hog1*, when RPMI was supplemented with 10% human plasma (see Supplemental data 9). Thus, Δ*hog1* cells still had

the ability to aggregate. These two observations indicated that Hog1p was specifically required for the iron induced flocculent phenotype.

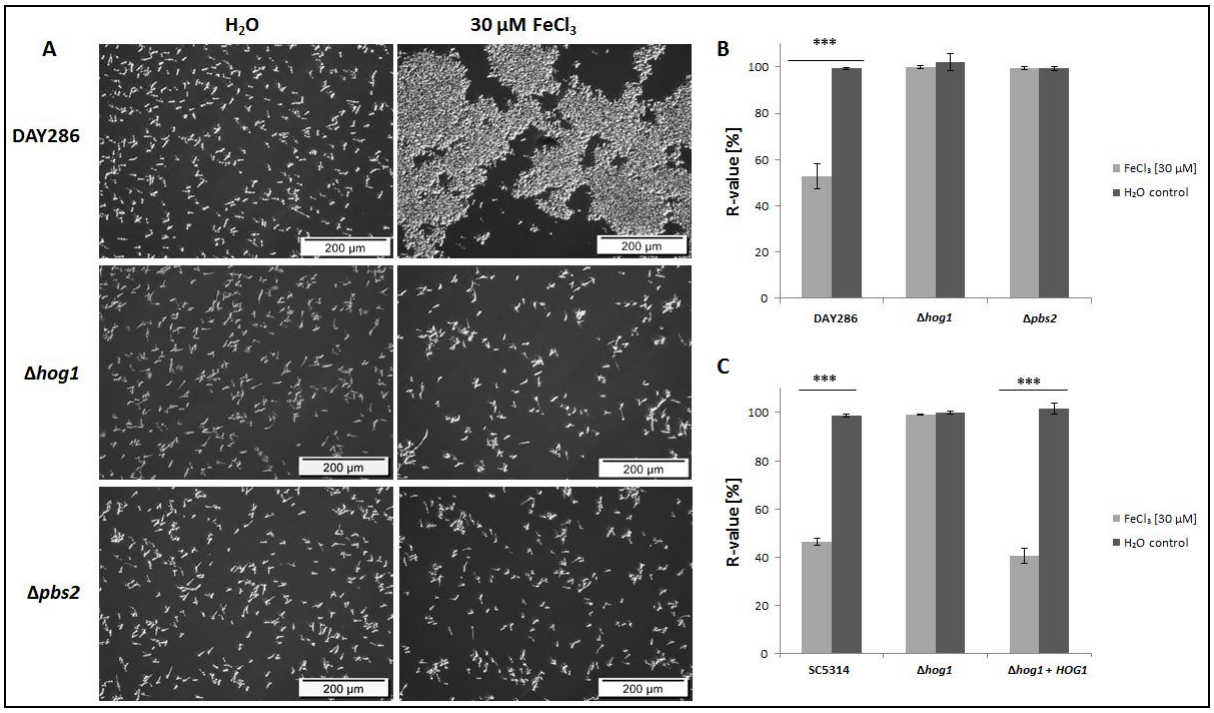

Figure 3.2.3 - High iron mediated flocculation was absent in Δ*hog1* and Δ*pbs2* mutants.

(A) Microscopic analysis of DAY286, Δ*hog1* (JMR114) and Δ*pbs2* (JJH31) upon exposure to 30 µM $FeCl_3$ at 30 °C for 2 h. (B) Relative sedimentation rates of the reference strain (DAY286) and of Δ*hog1* (JMR114) and Δ*pbs2* (JJH31) mutants incubated in RPMI containing 30 µM $FeCl_3$ or water (control) at 30 °C for 2 h. Means and standard deviations of three independent samples are shown (n = 3). *** denotes $P < 0.001$ (student's t-test). (C) Relative sedimentation rates of the WT (SC5314), Δ*hog1* (CNC13) and Δ*hog1* + *HOG1* (hAHGI) incubated in RPMI containing 30 µM $FeCl_3$ or water (control) at 30 °C for 2 h. The hAHGI strain carries the *HOG1* gene fused to *GFP* under control of the *ACT1* promoter and integrated in the *LEU2* locus (Arana et al, 2005). Means and standard deviations of three independent samples are shown (n = 3). *** denotes $P < 0.001$ (student's t-test).

To ensure that iron was taken up by Δ*hog1* and Δ*pbs2* cells, we determined Fe^{3+} levels in culture supernatants of the reference strain DAY286 and the deletion mutants Δ*hog1* and Δ*pbs2* after an incubation time of 15 min. All three strains removed iron with the same efficiency from the growth medium (Table 7). Moreover, we observed increased intracellular ROS generation in Δ*hog1* cells after incubation with 30 µM $FeCl_3$ (see Supplemental data 10), indicating intracellular activity of iron and thus iron uptake by those cells. In agreement with

previous reports (Alonso-Monge et al, 2009), we observed higher basal ROS production in Δ*hog1* cells compared to DAY286 cells.

Table 7 - Fe^{3+} removal from growth medium by *C. albicans* strains.

Strain	**Iron content of supernatant after 15 min at 30 °C [% of starting conditions]**
DAY286	1.8 ± 0.8
Δ*hog1*	1.3 ± 0.47
Δ*pbs2*	2.6 ± 0.2

Starting Fe^{3+} concentrations of 30 µM were set as 100 %.

3.2.4 Hog1p was activated by high iron concentrations

As loss of *HOG1* influenced the response of *C. albicans* to elevated iron concentrations we determined the phosphorylation (i.e. activation) state of Hog1p after exposure to high Fe^{3+} concentrations. As shown in Fig 3.2.4A, we observed significant hyper-phosphorylation of Hog1p when the wild type strain SC5314 was exposed to 30 µM Fe^{3+}. However, Hog1p hyper-phosphorylation was only transient, as maximum phosphorylation was obtained only from 7.5 - 10 min after exposure to high Fe^{3+} (Figure 3.2.4B). Results were similar, when the reference strain DAY286 was used (Figure 3.2.4C, D). Hog1p phosphorylation was almost as strong after exposure to high Fe^{3+} concentrations as after exposure to sorbitol (positive control) (Figure 3.2.4C). But Hog1p was dephosphorylated already 15 min after the exposure to iron, while it was hyper-phosphorylated when sorbitol was used (Figure 3.2.4B and C).

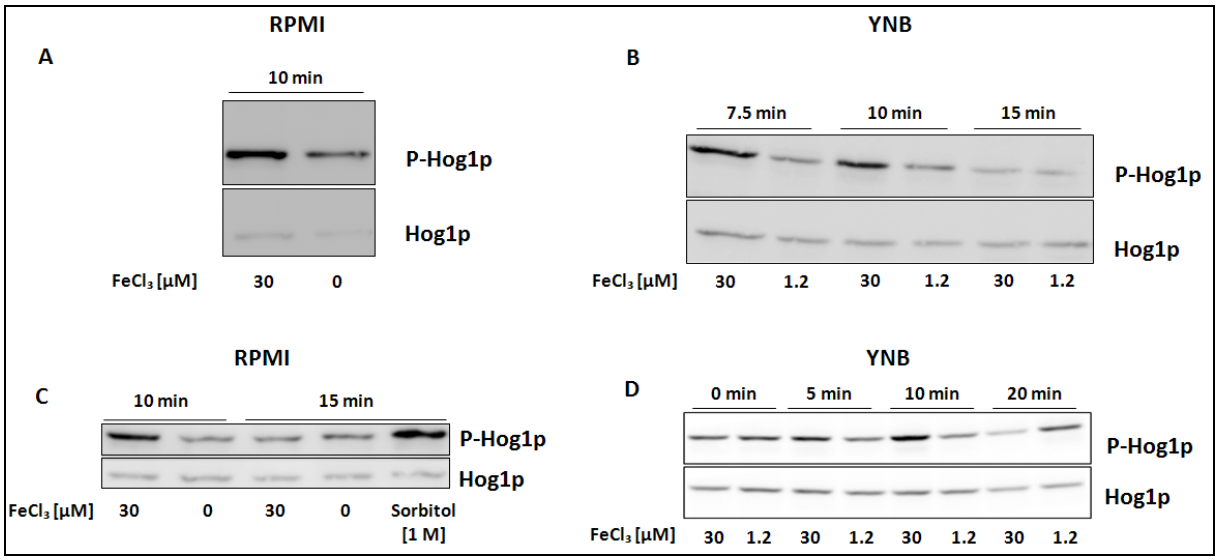

Figure 3.2.4 - The HOG pathway was activated by exposure to high iron levels.

(A) Western blot analysis of phosphorylated Hog1p (P-Hog1p) in *C. albicans* SC5314 (WT) cells exposed to 0 or 30 µM $FeCl_3$ in RPMI at 30 °C for 10 min. 5 µg total protein per sample were separated by SDS-PAGE. Phosphorylated Hog1p was detected by exposure of the membrane for 100 sec (for P-Hog1p) and 130 seconds (for Hog1p) after HRP reaction. (B) Western blot analysis of phosphorylated Hog1p in *C. albicans* SC5314 cells exposed to 30 µM or 1.2 µM $FeCl_3$ in YNB medium for 7.5, 10 or 15 min at 30 °C. 16 µg total protein per sample were separated by SDS-PAGE. Phosphorylated Hog1p was detected by exposure of the membrane for 100 sec (for P-Hog1p) and 130 seconds (for Hog1p) after HRP reaction. (C) Western blot analysis of phosphorylated Hog1p (P-Hog1p) in *C. albicans* DAY286 cells exposed to 0 or 30 µM $FeCl_3$ in RPMI at 30 °C for 10 or 15 min. Sorbitol [1 M] was used as positive control. 12 µg total protein per sample were separated by SDS-PAGE. Phosphorylated Hog1p was detected by exposure of the membrane for 80 sec (for P-Hog1p) and 40 seconds (for Hog1p) after HRP reaction. (D) Western blot analysis of phosphorylated Hog1p in *C. albicans* DAY286 cells exposed to 30 µM or 1.2 µM $FeCl_3$ in YNB medium for 0, 5, 10 or 20 min at 30 °C. Procedures were the same as indicated above except the following: 16 µg protein per sample were loaded on the gel and the membrane was exposed for 20 sec (P-Hog1p) and 30 sec (Hog1p) respectively. The pictures were slightly rotated to obtain almost straight bands.

3.2.5 Hog1p was required for maintenance of *C. albicans* viability under high iron conditions

Since Hog1p appeared to be involved in the response of *C. albicans* to high iron concentrations, we investigated whether Hog1p could have any protecting effect on *C. albicans* against deleterious effects of exposure to high iron levels. Thus, we determined the viability of cells after exposure to 30 µM Fe^{3+} using the alamarBlue® assay, which is an indicator of the metabolic activity of cells (O'Brien et al, 2000). This fluorescence assay has been widely used to determine the viability of different yeasts including *C. albicans* (Fai & Grant, 2009; Pfaller & Barry, 1994; Pfaller et al, 1994). We observed that basal fluorescence signals were always higher for Δ*hog1* cells than for the reference strain DAY286 (see Supplemental data 11). This could be due to the intrinsically enhanced mitochondrial activity of *HOG1* deficient cells (Alonso-Monge et al, 2009).

Cells were exposed to 30 µM $FeCl_3$ in RPMI and incubated at 30 °C for 60 min. A decrease of the reduction rate of alamarBlue®, i.e. of the viability, was observed for all tested strains. However, exposure to high iron levels led to a higher decrease of the signals obtained from the Δ*hog1* mutant (residual viability 46 ± 3%) compared to the reference strain (DAY286) (residual viability 81 ± 9.5%) and the wild type (SC5314) (residual viability 85%). These data indicate that the Δ*hog1* mutant was less resistant to high iron levels than the WT cells. However, after 2 days no apparent growth defects were observed when the strains SC5314 (WT), DAY286 (reference strain), Δ*hog1* and Δ*pbs2* were grown on RPMI agar supplemented with 30 µM $FeCl_3$ compared to cells grown on the same medium containing 0 or 1 µM $FeCl_3$, respectively (see Supplemental data 12). This could indicate that the reduced metabolic activity of the Δ*hog1* mutant observed 1 h after exposure to high iron concentrations did not affect growth of *C. albicans* on the long term.

The lower reduction rate of alamarBlue® after exposure of Δ*hog1* to high Fe^{3+} concentrations was probably not due to the more oxidized intracellular environment after exposure of Δ*hog1* cells to high iron concentrations, as Δ*hog1* cells had a higher basal ROS level than WT cells, but the basal alamarBlue® signals were also higher. Thus, the intracellular oxidation state (indicated by the ROS level) did not directly correlate with alamarBlue® signals.

3.2.6 MCFOs isolated by heat were regulated by iron availability

The expression of genes involved in iron uptake is regulated by iron availability. High affinity iron uptake (HAIU) genes are induced in restricted iron conditions and repressed by high iron concentrations (Lan et al, 2004). As mentioned above, members of the corresponding protein families are present in the plasma membrane of *C. albicans*. Heating whole microbial cells resuspended in phosphate buffers to elevated temperatures was already described as a method for the extraction of proteins associated with the cell wall or with the plasma membrane of different microorganisms (Benz & Schmidt, 1992; Buck et al, 1984; Torres et al, 2002). Indeed, we could isolate members of the multicopper ferroxidase (MCFO) enzyme family by briefly boiling *C. albicans* cells grown in RPMI supplemented with 10% FBS at 30 °C.

Proteins involved in HAIU are expected to be more abundant in cells cultivated in an iron restricted medium, such as RIM, compared to an iron sufficient medium (YPD). To determine whether the MCFO members isolated by heat were regulated by iron availability, we applied the heat extraction method on *C. albicans* SC5314 cells grown either under iron sufficient or iron restricted conditions. The extracted proteins were separated by SDS PAGE and visualized by coomassie staining. A protein band (80 - 100 kDa), which was significantly accumulated in RIM (Figure 3.2.5A), was cut from the gel/ blot and analyzed by MALDI-TOF MS, MS/MS and N-terminal Edman degradation for identification. N-terminal sequencing of the protein extracted from the respective gel band resulted in the identification of the sequence KTHTxYYKTGxVNAN which corresponds to the N-terminal sequence of

the MCFO Fet3p (KTHTWYYKTGWVNAN) after cleavage of a predicted 20 amino acid signal peptide. In the genome of *C. albicans*, five MCFO encoding genes are present. These are *FET3* **(**orf19.4211), *FET31* (orf19.4213), *FET33* (orf19.943), *FET34* (orf19.4215) and *FET99* (orf19.4212). The K21 residue is unique for Fet3p among *C. albicans* MCFOs (Figure 3.2.5B). Additionally, a glutamic acid peak appeared at residue 21, but was less intense than the lysine peak. This is indicative for the MCFOs Fet31p, Fet34p and Fet99p (Figure 3B). MALDI-TOF MS-analysis led to the identification of three peptide peaks specific for Fet34p and two peaks specific for Fet3p in addition to one peak shared between Fet34p and Fet3p, another peak shared between Fet3p, Fet31p and one peak shared between Fet3p, Fet31p and Fet99p (Table 8). MS-MS analysis of the peak appearing at 1384.7 m/z unequivocally confirmed the presence of Fet34p in the excised band. Taken together, these data indicated the presence of at least Fet3p and Fet34p in the protein extract. However, presence of Fet31p and Fet99p is also possible and could neither be confirmed nor excluded. In general, all *C. albicans* MCFOs apart from Fet33p, are highly conserved among each other as Fet31p, Fet34p and Fet99p have an identity ranging between 75 – 83 % compared to Fet3p (Almeida et al, 2009).

Previous gene expression experiments in *C. albicans* had reported that *FET34* expression was regulated by iron availability, as expression of this gene was induced by restricted iron compared to sufficient iron conditions (Hameed et al, 2011; Lan et al, 2004). Thus, we further investigated the dependence of the expression of extracted MCFOs on iron concentration in the growth medium. As RPMI is iron free, we used this medium as basis and added different amounts of $FeCl_3$. Increasing ferric iron concentrations led to significant decreases of MCFOs levels as determined by SDS PAGE and subsequent coomassie staining of proteins (Figure 3.2.5C). When iron concentrations equaled or exceeded 7.5 µM, hardly any protein band was

visible. Taken together, these results confirm that the expression levels of extracted MCFOs were dependent on the iron ion concentration in the growth medium.

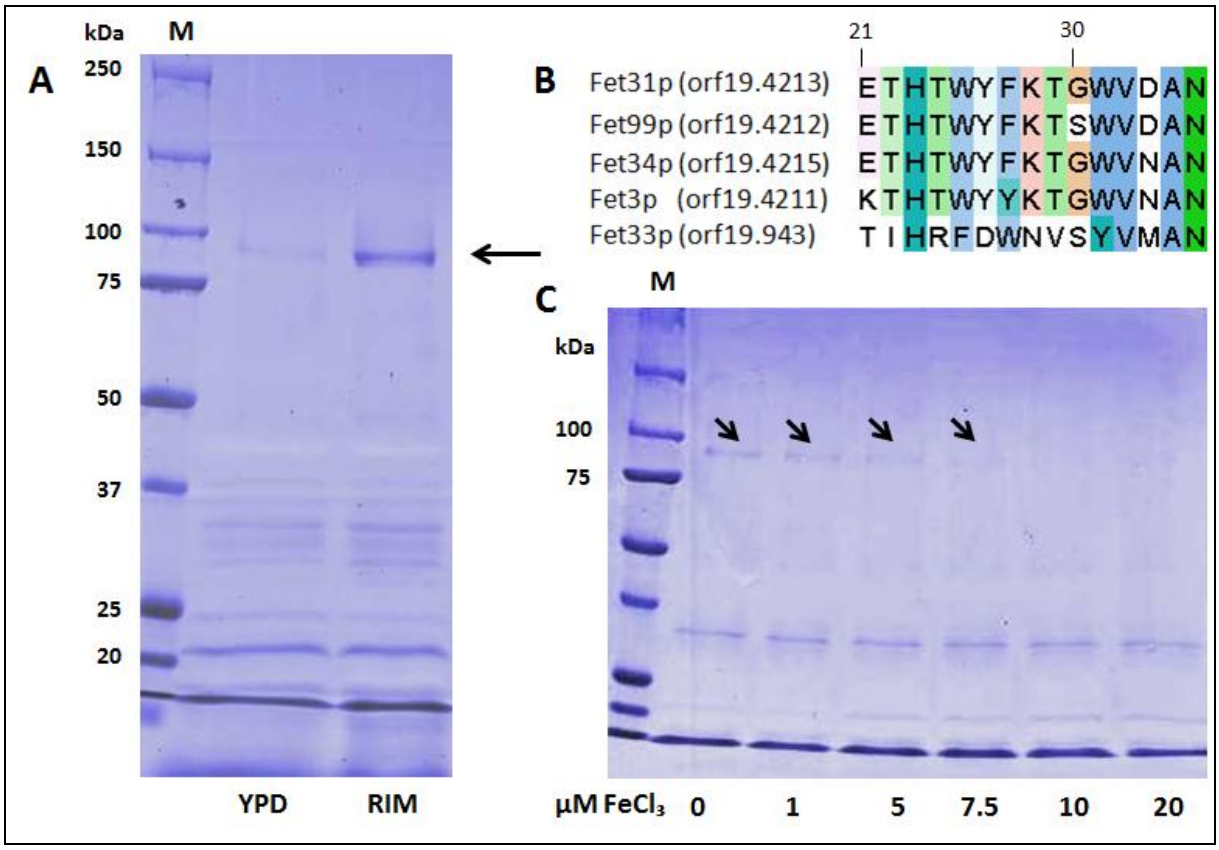

Figure 3.2.5 - MCFOs expression was regulated by iron levels.

(A) SDS-PAGE analysis of proteins extracted by heating whole yeast cells of *C. albicans* SC5314. Cells were cultivated in sufficient iron (YPD) or restricted iron (RIM) medium at 30 °C for 5 h, and proteins were extracted as described in the experimental part. (B) Multiple sequence alignment (MSA) of the first 15 amino acids (aa) (given in the single letter code) after excision of a predicted 20 aa signaling peptide of MCFOs. The alignment was performed using CLUSTALW2 and displayed with the Jalview editor (http://www.ebi.ac.uk/Tools/msa/clustalw2/). The selected proteins are: Fet3p [UniProtKB: Q59NF9**],** Fet31p [UniProtKB: Q59NF7], Fet33 [UniProtKB: Q5A503], Fet34p [UniProtKB: Q59NF5] and Fet99p [UniProtKB: Q59NF8]**.** (C) SDS-PAGE analysis of MCFOs, which were extracted from cells grown in RPMI supplemented with different iron concentrations at 30 °C for 3 h.

Table 8 - Peptide peaks obtained from MS-MALDI-TOF analysis of the MCFOs band.

Peptide peaks [m/z]	MCFO
998.5	Fet3p
1384.7	Fet34p
1389.7	Fet3p
1399.7	Fet34p
1507.8	Fet3p, Fet31p
1726.9	Fet3p, Fet34p
1838.9	Fet34p
1867.0	Fet3p, Fet31p, Fet99p

3.2.7 Deletion of *HOG1* induced components of the HAIU pathway independent of iron availability

Previously, de-repression of genes involved in iron uptake (*FET34*, *FTR1*, *FRE10* and *RBT5*) was reported in the Δ*hog1* mutant by whole genome gene expression profiling of cells grown under sufficient iron conditions (Enjalbert et al, 2006). As the expression of these genes is usually repressed by sufficient iron conditions and induced by restricted iron conditions (Lan et al, 2004) (for MCFOs see Figure 3.2.5), we investigated the function of Hog1p in the response of *C. albicans* to iron. We first confirmed elevated amounts of MCFO proteins in Δ*hog1* and Δ*pbs2* deletion mutants in comparison to the wild type (WT, SC5314) which was best seen in cells grown in YPD overnight (Figure 3.2.6A). The identity of the MCFO proteins was proven by MS/MS analysis of the peptide at 1726.9 m/z (not shown). Increased amounts of MCFOs were observed in two different, independently constructed Δ*hog1* and Δ*pbs2* mutants (see table 3 for the strains used in this study (Arana et al, 2005; San Jose et al, 1996); data are shown for only one of the mutant strains). As proteins, which are usually used as gel loading controls, are cytosolic proteins and not present in the cell wall, we had added BSA to the extracted proteins to demonstrate that all lanes were loaded with the same total

amount of protein. However, the induction of MCFOs by low iron concentrations was not completely eliminated in the Δ*hog1* mutants, as we still observed induction of MCFOs expression (Figure 3.2.6B) when the Δ*hog1* mutant was cultivated in RIM compared to YPD.

As *FRE10*, the major ferric reductase of *C. albicans* (Jeeves et al, 2011), was also reported to be de-repressed in the Δ*hog1* mutant (see above) (Enjalbert et al, 2006), we determined cell surface ferric reductase activity of whole yeast cells using a previously published protocol (Jeeves et al, 2011). As shown in Figure 3.6.2C, ferric reductase activities increased when the wild type (SC5314) and the reference strain (DAY286) were cultivated in RIM compared to YPD. This further highlights the induction of this class of proteins by low iron levels. Moreover, cell surface ferric reductase activity was increased in Δ*hog1* mutants compared to both SC5314 and DAY286 when cultivated in YPD (data are shown for only one of the mutant strains), showing that de-repression of these enzymes in Δ*hog1* mutants led to higher enzyme activities. Similar to the observations made before for MCFO levels, ferric reductase activity of the Δ*hog1* mutant was also increased in RIM compared to YPD. For confirmation, we cultivated all three strains (WT, DAY286 and Δ*hog1*) in RPMI with or without 30 µM $FeCl_3$ and made similar observations. Addition of iron to the RPMI medium led to a decrease in ferric reductase activity in all three strains (Figure 3.6.2D).

Thus deletion of *HOG1* led to both increased MCFOs expression as well as increased cell surface reductase activity, and both were further increased by iron restriction.

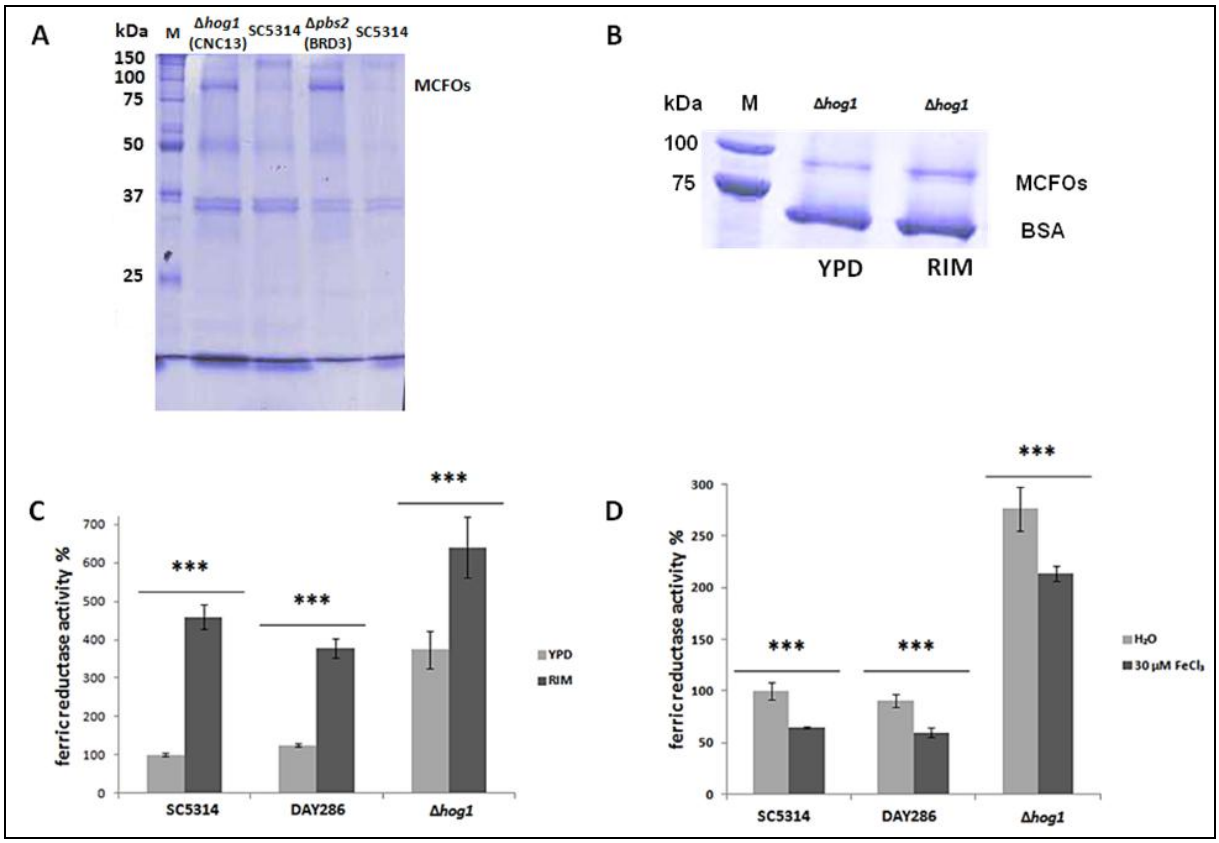

Figure 3.2.6 – Deletion of *HOG1* led to de-repression of MCFOs and to increased ferric reductase activity.

(A) SDS-PAGE analysis of MCFOs extracted from the WT (SC5314), Δ*hog1* (CNC13) and Δ*pbs2* (BRD3) mutants grown in YPD at 30 °C for 17 h. Identity of the MCFOs was confirmed by mass spectrometry. The gel was run for 30 min at 80 V and 90 min at 120 V. (B) SDS-PAGE analysis of MCFOs extracted from Δ*hog1* (JMR114) grown in sufficient iron (YPD) or restricted iron (RIM) medium at 30 °C for 3 h. was run for 3 h at 120 V (excerpt of the Coomassie stained SDS-gel is shown). (C) Cell surface ferric reductase activity of SC5314 (WT), DAY286 (reference strain) and Δ*hog1* (JMR114) under both restricted iron (RIM) and sufficient iron (YPD) conditions. Mean values and standard deviations of three independent experiments (n = 3) are shown. *** denotes $P < 0.001$ (student's t-test). The ferric reductase of activity of the WT strain (SC5314) grown in YPD was set as 100%. (D) Cell surface ferric reductase activity of SC5314 (WT), DAY286 (reference strain) and Δ*hog1* (JMR114) under no iron (H_2O) and high iron (30 µM $FeCl_3$) conditions. Mean values and standard deviations of three independent experiments (n = 3) are shown. *** denotes $P < 0.001$ (student's t-test). The ferric reductase of activity of the WT strain (SC5314) grown in YPD was set as 100%.

3.3.8 Identification of factors involved in the response to iron downstream of Hog1p

Our data suggested that high iron induced flocculation of *C. albicans* cells was dependent on both, an intact HOG pathway and the synthesis of new proteins. The induction of flocculation suggests alterations of cell wall molecular organization. Flocculation was induced in *C. albicans* in response to the antimycotic compound caspofungin, which targets ß-(1,3)-glucan synthesis. This flocculent phenotype was dependent on the transcription factor Efg1p, which was required to activate the flocculine Als1p in response to caspofungin (Gregori et al, 2011). On the other hand, Tup1p is a transcriptional co-repressor known for inhibition of filamentous growth (Braun & Johnson, 1997), as well as an involvement in iron dependent responses of the cell (Knight et al, 2002).

We investigated the phenotypic behavior of both Δ*efg1* and Δ*tup1* compared to the reference strain WT-arg. Both WT-arg and Δ*tup1* flocculated in response to 30 µM Fe^{3+} in a similar way as the WT. However, flocculation upon exposure to the same iron concentration was completely absent in Δ*efg1* (Figure 3.2.7), suggesting that Efg1p was required for induction of flocculation upon iron exposure, similar to Hog1p and Pbs2p.

To confirm that Δ*efg1* had no iron uptake deficiency, we determined iron concentration in cell culture supernatants (see 2.6) of the reference strain WT-arg, Δ*efg1* and Δ*tup1* 15 min after iron exposure. All three strains removed almost all iron from the supernatant with the same efficiency (not shown).

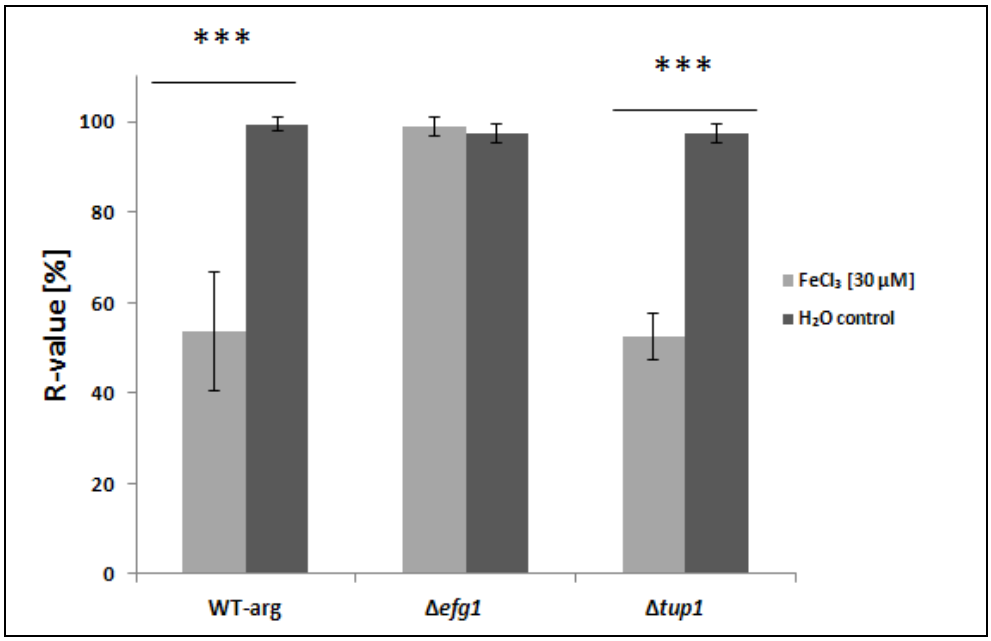

Figure 3.2.7 - High iron mediated flocculation was present in Δ*tup1* but absent in Δ*efg1* mutants.

Relative sedimentation rates of the reference strain (WT-arg) and of Δ*efg1* (TF156) and Δ*tup1* (TF117) mutants incubated in RPMI containing 30 µM $FeCl_3$ or water (control) at 30 °C for 2 h. Mean values and standard deviations of three independent samples are shown (n = 3). *** denotes $P < 0.001$ (student's t-test).

3.2.9 Discussion

Previous studies on Δ*hog1* mutants from *C. albicans* and *Cryptococcus neoformans* showed that deletion of *HOG1* led to the de-repression of several genes known to be upregulated under restricted iron conditions (Enjalbert et al, 2006; Ko et al, 2009). In *C. albicans*, this group of genes included *RBT5*, *FRE10*, *FTR1*, *FET34*, orf19.251, *PMH7*, *ECM331*, *CAT1*, *DDR48*, *YOR009* and *HSP12* (Chen et al, 2011; Enjalbert et al, 2006; Lan et al, 2004).

Whether this phenotype was due to a direct involvement of Hog1p in the regulation of the iron responsive network or due to indirect effects, such as perturbations of copper metabolism, which may have impaired the functionality of iron uptake proteins was not yet studied.

As expected, high levels of extracellular iron increased the formation of intracellular ROS. Thus, we used intracellular ROS levels together with the removal of iron from growth

medium as indicators of iron entry into the cells. We detected increased basal ROS levels in the Δ*hog1* mutants, as previously reported (Alonso-Monge et al, 2009). These ROS levels were further increased by exposure to 30 µM Fe^{3+} confirming that iron was taken up by Δ*hog1* cells. Moreover, iron ions were removed from the growth medium with the same efficiency by Δ*hog1* as by the reference (DAY286) cells. Thus, Hog1p dependent phenotypes of the *C. albicans* response to iron were not due to iron uptake deficiencies, but could be rather due to the involvement of Hog1p in the response to iron availability. This is supported by our data on the transient hyper-phosphorylation of Hog1p during exposure of cells to high iron concentrations.

Elevated iron concentrations induced a flocculent phenotype of *C. albicans*, which was dependent on the presence of both Hog1p and Pbs2p, as well as on protein synthesis. As high iron concentrations led to increased phosphorylation of Hog1p, this could induce the synthesis of proteins of which some mediate cell aggregation. This iron triggered activation of Hog1p was likely not related to oxidative stress, as the potent radical scavenger NAC did not prevent the flocculent phenotype upon exposure to high iron concentrations, while it decreased intracellular ROS levels. For the closely related yeast *S. cerevisiae*, a function of *Sc*Hog1p in cell aggregation was reported, in that hyperactive *Sc*Hog1p mutants resulted in increased flocculation (Bell et al, 2001). Furthermore, the induction of flocculation is an indicator to changes in molecular organization of the cell wall. In a previous work (Gregori et al, 2011), the transcription factor Efg1p induced expression of Als1p leading to a flocculent phenotype in response to caspofungin exposure. Similarly, Efg1p was found in this work to be required for iron induced flocculation.

It has still to be elucidated if Hog1p translocates to the nucleus upon hyper-activation by iron and whether iron activated Hog1p directly influences transcription and synthesis of new

proteins. Particularly, Efg1p could be activated by Hog1p and is thus a potential downstream factor in the network responsive to high iron concentrations.

First hints on an involvement of Hog1p in the response of *C. albicans* to iron came from the observation of the de-repression of several iron uptake genes in the Δ*hog1* mutant under otherwise repressive conditions (Enjalbert et al, 2006). In agreement with these gene expression data, we observed increased MCFOs protein levels and ferric reductase activity in Δ*hog1* mutants. Furthermore we found that MCFOs were also de-repressed in Δ*pbs2* mutants, indicating that the *HOG1* mediated regulation of MCFOs was dependent on *PBS2*. Remarkably, induction of MCFOs and ferric reductases in RIM was not strictly dependent on Hog1p, as this induction was also observed in the Δ*hog1* mutant. Thus deletion of *HOG1* de-repressed components of the iron uptake system, and this elevated basal level was further enhanced when iron availability was limited.

Mass spectrometric and N-terminal sequencing analysis of protein bands in gels obtained from heat extracts of *C. albicans* identified at least Fet3p and Fet34p among the five possible MCFO gene products. The extracted MCFOs were collectively found to be regulated by iron availability, which is in line with data obtained from transcription analysis, as *FET3* and *FET34* were found to be upregulated during iron restriction in contrast to the other MCFO encoding genes (Cheng et al, 2013).

Hog1p was shown to be essential for *C. albicans* under oxidative stress conditions (Alonso-Monge et al, 2003). Our data indicated that the absence of *HOG1* reduced the metabolic activity of the cells after exposure to high iron concentrations compared to wild type cells. Taking into account that exposure of Δ*hog1* cells to high iron concentrations further increased the comparably high basal intracellular ROS levels in the mutant, the decreased viability of the Δ*hog1* mutant under such conditions could be due to elevated oxidative stress. However, other mechanisms independent from Hog1p were also described for the initiation of oxidative

stress responses (Gonzalez-Parraga et al, 2010). These mechanisms could allow also the mutant strains to adapt to the stress conditions so that the reduced viability was observed only as immediate response and did not lead to significant growth defects on the long term.

It has yet to be elucidated which elements downstream of Hog1p provide the link between the HOG pathway and factors which regulate reductive iron uptake. As many Hog1p repressed genes, including those involved in iron uptake (*FET34*, *FRE10*, *FTR1* and *RBT5*), were also found to be repressed by Tup1p (Enjalbert et al, 2006), a role for this global co-repressor downstream of Hog1p could be assumed. Indeed, a role of Tup1p in regulating iron uptake has been reported (Knight et al, 2002). However, the details remain to be elucidated.

In this study, we used several single gene deletion mutants which were generated by different approaches (Arana et al, 2005; Davis et al, 2002; Nobile & Mitchell, 2009; San Jose et al, 1996). All mutant strains with exception of TF117, TF156 and WT-arg were descendants of the strain CAI-4 (Fonzi & Irwin, 1993), in which both copies of *IRO1* are deleted. Additionally, all strains ectopically express *URA3.*

IRO1 is a gene that encodes a transcription factor with a potential role in iron utilization. Expression of *IRO1* in a Δ*aft1 S. cerevisiae* strain restored growth in iron depleted media. However, a role of *IRO1* in *C. albicans* iron metabolism is not confirmed (Garcia et al, 2001). Ectopic expression of *URA3* has been shown to affect several features of *C. albicans*, such as hyphal morphology, adhesion, virulence and cellular proteome in addition to Ura3p activity (Brand et al, 2004; Cheng et al, 2003).

In all our experiments, the DAY286 reference strain behaved similar to the WT SC5314. Additionally, CNC13 and JMR114 (Δ*hog1*) as well as BRD3 and JJH31 (Δ*pbs2*) showed similar features. Thus, no effects of the ectopic expression of *URA3* or the absence of *IRO1* were observed.

3.3 Effect of antifungal treatment on reductive iron uptake components of *C. albicans* with a special focus on fludioxonil

3.3.1 Treatment of *C. albicans* cells by fludioxonil and iprodione repressed RIUP components independent of the HOG pathway

As we found that Hog1p responds to changes in extracellular iron ion concentration on one hand and as RIUP components were de-repressed in Δ*hog1* cells on the other hand, we wondered whether the activation of Hog1p results in repression of iron uptake proteins expression. The repression of HAIU components under iron restricted conditions could be of high importance in fighting *C. albicans* infections. To study the effect of Hog1p activation on the RIUP system, represented by MCFOs expression and ferric reductase activity, we activated Hog1p by treatment of *C. albicans* DAY286 with the fungicides fludioxonil and iprodione (Figure 3.3.1A). Fludioxonil (a phenylpyrrole) and iprodione (a dicarboximide), target the histidine kinase (HK) Cos1p of *C. albicans*, which is upstream of the Hog1p MAPK module. Treatment of *S. cerevisiae* expressing *C. albicans* Cos1p with both antifungals has led to the activation of Hog1p in this yeast (Buschart et al, 2012b). Moreover, fludioxonil physically interacts with *C. albicans* Cos1p, confirming that this HK is a receptor of fludioxonil (Mohammed El-Mowafy, BISA, personal communication).

Addition of 20 µg ml^{-1} of each antifungal to YPD as well as to RIM, led to a significant repression of MCFOs expression (Figure 3.3.1B and C). However, addition of fludioxonil to RIM decreased MCFO levels also in Δ*hog1* cells (Figure 3.3.1D).

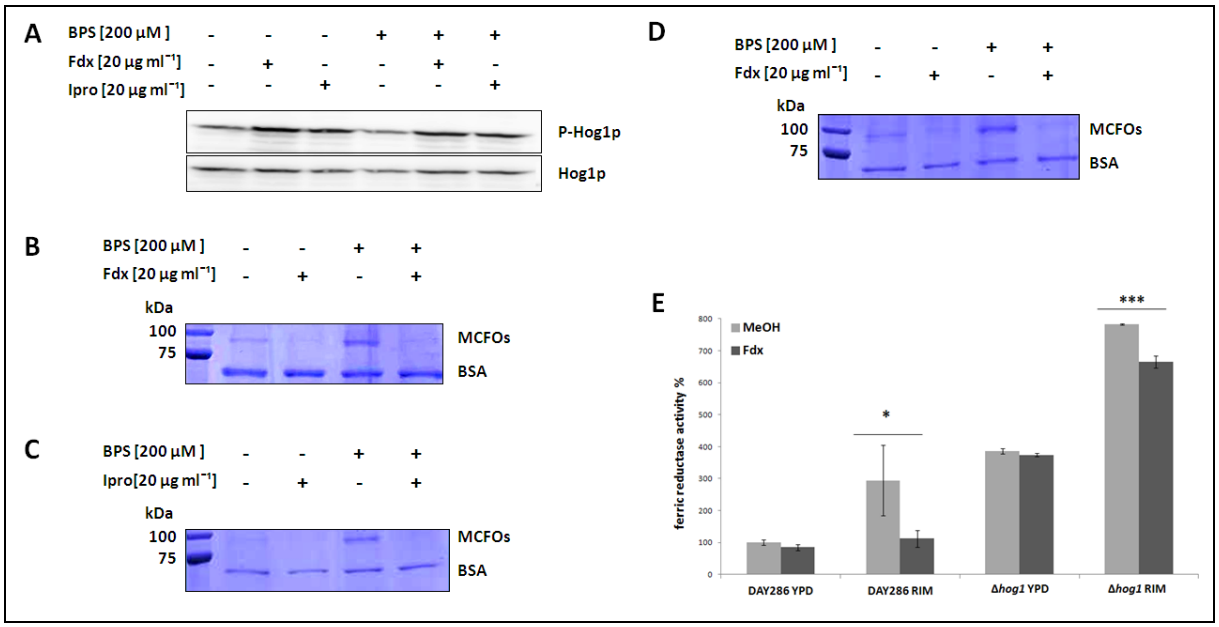

Figure 3.3.1 – Treatment of *C. albicans* with fludioxonil or iprodione led to repression of RIUP components independently of Hog1p.

RIM was prepared by adding 200 µM BPS to YPD resulting in iron restricted conditions. (A) Western blot analysis of phosphorylated Hog1p in *C. albicans* DAY286 treated with fludioxonil or iprodione (at 20 µg ml^{-1} final concentration each) or MeOH (solvent control; i.e. without the addition of fludioxonil or iprodione) in both YPD (iron sufficient) and RIM (iron restricted) at 30 °C. Blot was exposed for 10 sec (P-Hog1p) and 20 sec (Hog1p) respectively. (B) Excerpt of coomassie stained SDS gel showing MCFOs from *C. albicans* DAY286 cells treated with fludioxonil [20 µg ml^{-1}] or MeOH in both YPD and RIM (3 h at 30 °C). The gel was run for 3 h at 120 V. (C) Excerpt of coomassie stained SDS gel showing MCFOs from *C. albicans* DAY286 cells treated with iprodione [20 µg ml^{-1}] or MeOH in both YPD and RIM (3 h at 30 °C). The gel was run for 3 h at 120 V. (D) Excerpt of coomassie stained SDS gel showing MCFOs from *C. albicans* Δ*hog1* cells (JMR114) treated with fludioxonil [20 µg ml^{-1}] or MeOH in both YPD and RIM (3 h at 30 °C). The gel was run for 3 h at 120 V. (E) Cell surface ferric reductase activity of *C. albicans* DAY286 and Δ*hog1* (JMR114) treated with fludioxonil [20 µg ml^{-1}], or MeOH. Mean values and standard deviations of three independent experiments (n = 3) are shown. * denotes $P \leq 0.05$ (student's t-test). The ferric reductase of activity of the MeOH (solvent) treated reference strains (DAY286) grown in YPD was set as 100%. Fdx: fludioxonil; Ipro: iprodione. Bovine serum albumin (BSA) was added to protein extracts shown in B - D as internal standard to serve as a loading control.

Furthermore, fludioxonil treatment decreased ferric reductase activity of cells in both, the sufficient iron (YPD) and the restricted iron medium (RIM). This was observed for both, the reference strain (DAY286) as well as the Δ*hog1* mutant (Figure 3.3.1E).

To confirm that such observations were independent of genetic background of DAY286 cells, ferric reductase activity of SC5314 cells was determined in RIM. Fludioxonil was found to decrease ferric reductase activity by ca. 50% (see Supplemental data 13).

These results indicated that fludioxonil targeted reductive iron uptake pathway (RIUP) components independent on Hog1p.

To determine whether repression of RIUP components by the antifungals occurred in a Cos1p independent manner, we analyzed ferric reductase activity and MCFO levels in a Δ*cos1* deletion mutant after fludioxonil or iprodione treatment. Total surface ferric reductase activity of Δ*cos1* cells was significantly decreased by fludioxonil in RIM (See Supplemental data 14A). Furthermore, treatment of Δ*cos1* cells with fludioxonil and iprodione repressed MCFOs expression under both, iron sufficient (YPD) and iron restricted (RIM) conditions (See Supplemental data 14B). These results clearly showed that fludioxonil and iprodione acted on the RIUP in a Cos1p independent manner.

A number of antifungal compounds of different classes, including the azole antifungal ketoconazole, were reported to cause downregulation of genes encoding iron uptake proteins (Liu et al, 2005). Combination of the azole antifungal fluconazole with several iron binding molecules or serum has been widely reported to increase antifungal activity of fluconazole on *C. albicans* (Fiori & Van Dijck, 2012; Kobayashi et al, 2011; Minn et al, 1997; Wakabayashi et al, 1998). Thus, we determined ferric reductase activity of fluconazole treated cells. Fluconazole (20 μg ml^{-1}) significantly decreased ferric reductase activity of cells in RIM compared to MeOH control (See Supplemental data 13), while having no apparent effect on growth during incubation time (not shown). In a different experiment, a lower fluconazole concentration (10 μg ml^{-1}) also decreased ferric reductase activity as did fludioxonil and iprodione (See Supplemental data 15).

3.3.2 Repression of RIUP components by fludioxonil was independent on Sfu1p

We wondered whether fludioxonil perturbed cellular iron homeostasis thus simulating conditions of iron overload as suggested for amphotericin B (Liu et al, 2005). Sfu1p is the negative transcriptional regulator of several iron uptake genes, including MCFO and ferric reductase encoding genes (Lan et al, 2004; Homann et al, 2009; Chen et al, 2011) and is believed to act as iron sensor (Pelletier et al, 2007). Therefore, we analyzed MCFO levels of the Δ*sfu1* mutant in RIM medium after fludioxonil treatment. Fludioxonil was found to repress MCFOs expression under these conditions in the Δ*sfu1* mutant as well as the in corresponding reference strain WT-arg (Figure 3.3.2). Furthermore, MCFOs were de-repressed in Δ*sfu1*cells (in comparison with WT-arg), complying with previous knowledge on the role of Sfu1p in repressing HAIU components (Lan et al, 2004; Chen et al, 2011). This experiment indicated that repression of MCFOs expression by fludioxonil was not dependent on Sfu1p.

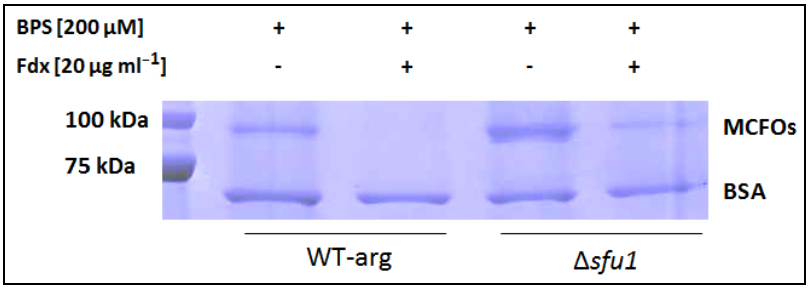

Figure 3.3.2 – Repression of MCFOs by fludioxonil was independent of Sfu1p transcriptional repressor.

(A) Excerpt of coomassie stained SDS gel showing MCFOs from *C. albicans* Δ*cos1* cells treated with fludioxonil [20 µg ml^{-1}] or MeOH in RIM (3 h at 30 °C). Fdx: fludioxonil. Bovine serum albumin (BSA) was added to protein extracts as internal standard to serve as a loading control. Gel was run for 3 h and 15 min at 120 V. This experiment was performed only once.

3.3.3 Fludioxonil reduced growth of *C. albicans* SC5314 under iron restricted conditions

As fludioxonil repressed RIUP components even under iron restricted conditions, where these components are normally induced, we speculated whether fludioxonil treatment would have any effect on *C. albicans* growth under conditions of iron restriction. *C. albicans* SC5314 was pre-cultivated in YPD (iron repleted) or YPD + 400 µM BPS (iron depleted) before cells were dropped on agar plates of different media comprising a fermentable (glucose or galactose) or a non-fermentable (glycerol) carbon source. The agar plates were incubated at 30 °C for 16 h. Figure 3.3.3 summarizes the results of *C. albicans* SC5314 under these conditions. Fludioxonil alone had little effect on *C. albicans* growth in YPD. Restricting iron availability by 200 µM BPS slightly reduced *C. albicans* growth compared to YPD. However, addition of fludioxonil led to a significant growth reduction. No differential behavior was observed between cells which were pre-cultivated under iron depleted or repleted conditions (Figure 3.3.3A). When glucose was substituted by galactose (YP-galactose medium), no clear reduction in growth was observed in fludioxonil treated cells compared to solvent control. In contrast to this, iron restriction significantly reduced growth and addition of fludioxonil almost prevented growth, especially of cells which were pre-cultivated in iron depleted medium (Figure 3.3.3B). Similarly to galactose, cells exhibited a significant decrease of growth under iron restricted conditions when grown on glycerol as carbon source. Fludioxonil further aggravated the effect of iron restriction on *C. albicans* growth under iron restricted conditions, while it had again no clear effect when under sufficient iron conditions (Figure 3.3.3C). Taken together these results indicate that fludioxonil treatment enhanced the effect of iron restriction on *C. albicans* growth, probably by repression of high affinity iron uptake (HAIU) components which are required under such conditions. This effect was independent from the ability of *C. albicans* to use the available carbon source for fermentation.

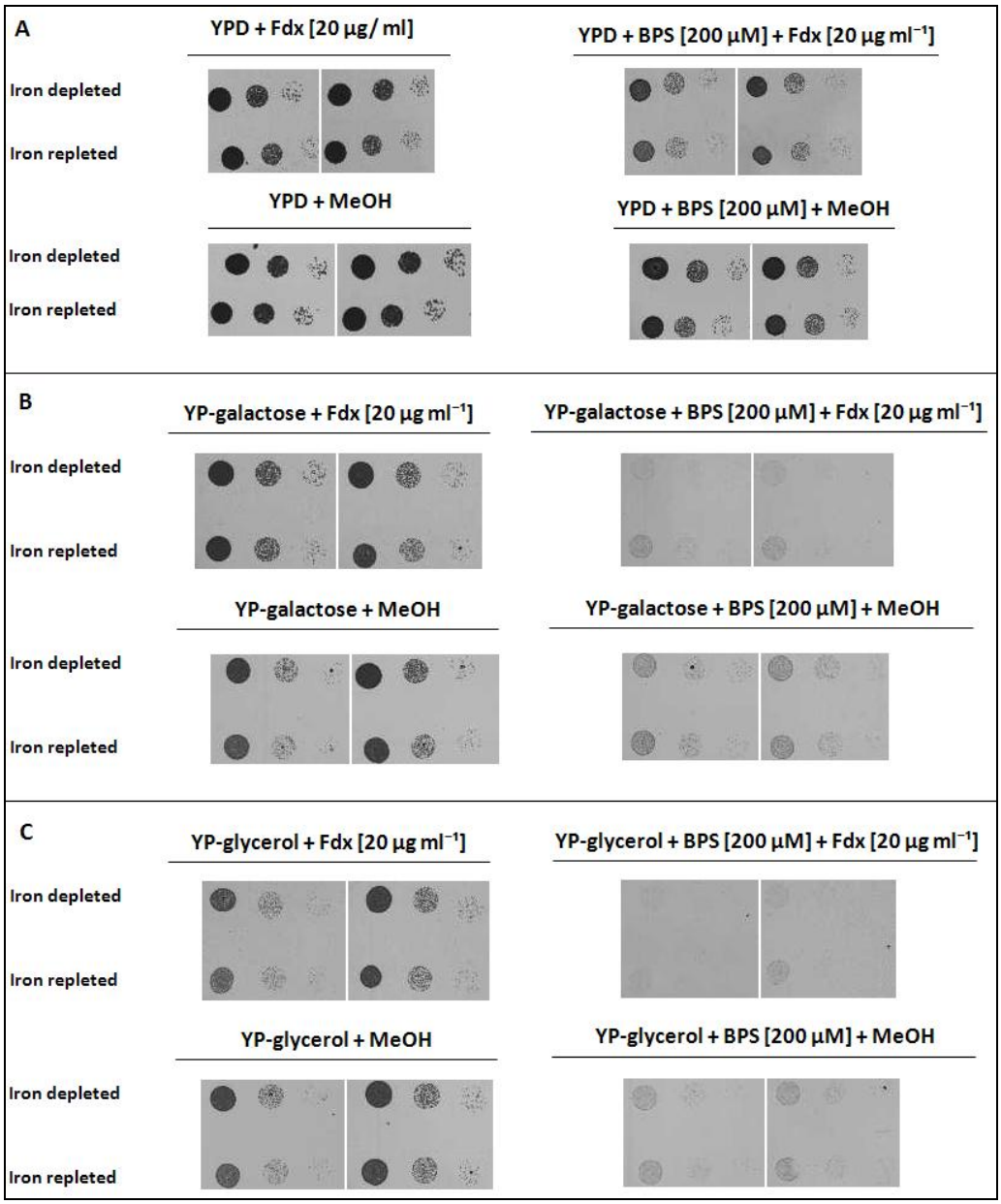

Figure 3.3.3 – Fludioxonil treatment aggravated the effect of iron restriction on *C. albicans* growth.

(A) Growth test of *C. albicans* SC5314 on YPD agar plates supplemented with either the phenylpyrrole antifungal fludioxonil (Fdx; 20 µg ml^{-1}) or the iron chelator BPS (200 µM) or both. (B) Growth test of *C. albicans* SC5314 on YP-galactose agar plates supplemented either with fludioxonil (Fdx; 20 µg ml^{-1}) or BPS (200 µM) or both. (C) Growth test of *C. albicans* SC5314 on YP-glycerol agar plates supplemented either with fludioxonil (Fdx; 20 µg ml^{-1}) or BPS (200 µM) or both. All plates were incubated at 30 °C for 16 h. Two replicate plates for each treatment are shown. Only first three serial dilutions (1:1 – $1:10^2$) of cells are shown. "Iron depleted" refers to the cells being pre-cultivated in YPD + 400 µM BPS at 30 °C for 7 h, while "iron repleted" refers to the cells being pre-cultivated in YPD at 30 °C for 7 h.

3.3.4 Fludioxonil induced flocculation of *C. albicans*

The repression of RIUP components by fludioxonil under iron restricted conditions could reduce the availability of HAIU proteins on the cell surface and thus lead to decreased iron uptake. To determine whether fludioxonil treatment caused reduced iron uptake, we investigated the effect of fludioxonil on the uptake of iron from transferrin, the major iron binding protein in human serum. The RIUP of *C. albicans* was previously shown to be required for iron uptake from transferrin (Knight et al, 2005). However, experiments could not be properly performed, as fludioxonil induced flocculation of cells in RPMI medium after ca. 3 h of incubation at 30 °C. This prevented correct counting of cell numbers in order to calculate relative iron uptake pro cell.

Induction of flocculation by fludioxonil was found to be dependent on Hog1p as Δ*hog1* cells lost the ability to form flocs in contrast to SC5314 and DAY286 cells (Figure 3.3.4). However, although flocs were formed in SC5314 and DAY286 after fludioxonil treatment, the influence of fludioxonil concentration on flocculation was not reproducible. In some cases, same fludioxonil concentrations led to visibly different degrees of flocculation in independent tests (not shown).

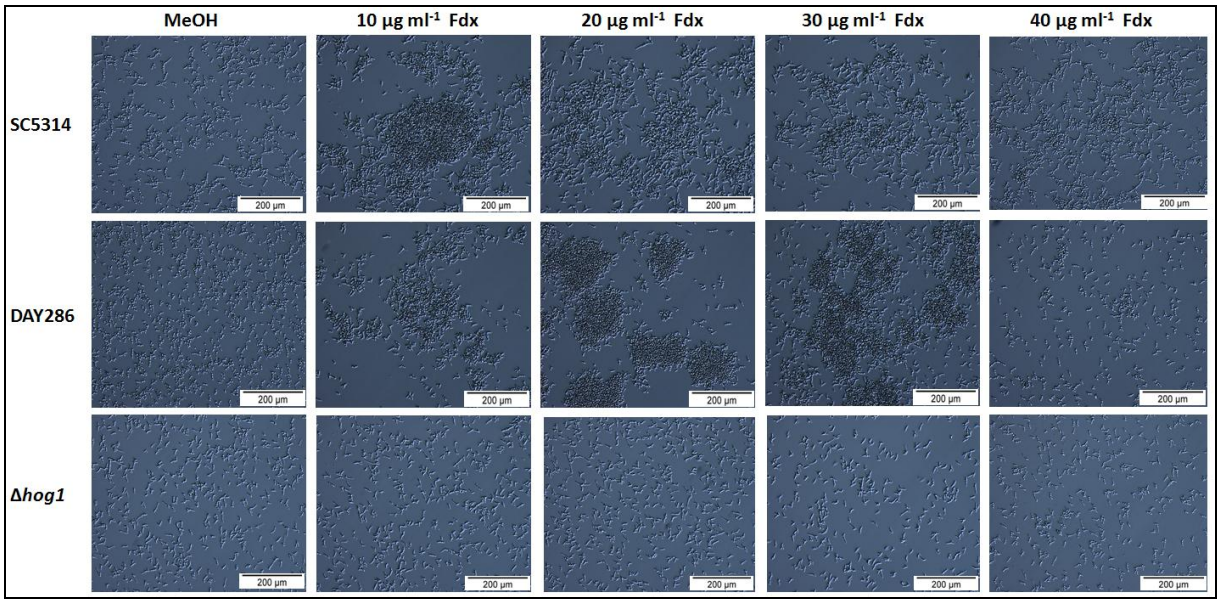

Figure 3.3.4 – Fludioxonil treatment induced flocculation of *C. albicans*.

Microscopic analysis of SC5314, DAY286 and Δ*hog1* (JMR114) after exposure to different fludioxonil (Fdx) concentrations in RPMI medium at 30 °C for 4 h (starting OD_{600} = 0.32). Figure represents one single experiment.

3.3.5 Discussion

Fludioxonil treatment of DAY286 led to reduced MCFO levels and ferric reductase activity. Remarkably, the same observation was made in Δ*hog1* and Δ*cos1* deletion mutants pointing to fludioxonil mediated effects independent of the HOG pathway.

The existence of Cos1p- (and thus HOG pathway) independent effects of fludioxonil were recently reported by our group (Buschart et al, 2012a). However, it is still elusive why fludioxonil and iprodione behaved similarly in Δ*cos1* or Δ*hog1* deletion mutants, as both antifungals potentially share the intracellular target, Cos1p (Buschart et al, 2012b), but belong to different compound classes. Fluconazole had a similar decreasing effect on ferric reductase activity of WT cells as fludioxonil and iprodione. Other compounds, such as amphotericin B ketoconazole or casponfungin, have been shown to downregulate iron uptake genes at the transcriptional level (Liu et al, 2005). This points to influences which are not specific for a certain chemical class of compounds, as most of these compounds are chemically not related

to each other and have different modes of action. Fluconazole inhibits the activity of the cytochrome P450 dependent Lanosterol 14-alpha-demethylase (P450-DM), which is responsible for ergosterol synthesis in *C. albicans* (Vanden Bossche et al, 1995). In *C. albicans*, P450-DM is the gene product of *ERG11*. Iron restriction has been shown to downregulate *ERG11* leading to a decrease in ergosterol content of cell membranes thus increasing membrane fluidity (Prasad et al, 2006). Furthermore, P450-DM activity requires heme iron (Vanden Bossche et al, 1995). It has been reported that combination of iron binding molecules or serum with fluconazole treatment has led to increased susceptibility of *C. albicans* to fluconazole (Fiori & Van Dijck, 2012; Kobayashi et al, 2011; Minn et al, 1997; Wakabayashi et al, 1998). As *C. albicans* upregulates *ERG11* as a defense mechanism upon exposure to fluconazole (Henry et al, 2000), it is likely that iron restriction reverses this effect by Hap43p mediated repression of iron utilizing genes (Chen et al, 2011) leading to increased fluconazole susceptibility. Furthermore, the decrease of ferric reductase activity by fluconazole (Supplemental data 13) suggests a decrease of the high affinity iron uptake capacity, which is required during restricted iron conditions. Thus, increased susceptibility of *C. albicans* to fluconazole could be due to additive factors which reduce both iron uptake and ergosterol synthesis.

Furthermore, it should be noted that if membrane properties are altered by the combined effect of iron restriction and fluconazole treatment, this could lead to the improper integration of membrane associated proteins into the membrane, such as RIUP components (Figure 1.4). For this reason, potential regulation of RIUP components by fluconazole should be studied at the transcriptional level.

The action of fludioxonil under restricted iron conditions could be, at least in part, analogous to that of fluconazole. However, currently no other target of fludioxonil than Cos1p is known in *C. albicans* and our results suggest a Cos1p independent effect of fludioxonil in repressing

RIUP components. Fludioxonil reversed induction of RIUP components under restricted iron conditions. Repression of MCFOs by fludioxonil also occurred in Δ*sfu1* cells suggesting that fludioxonil treatment did not simulate a situation of intracellular iron overload. In agreement of previous knowledge at the transcriptional level (Chen et al, 2011; Homann et al, 2009), the de-repression of MCFOs in Δ*sfu1* cells compared to the reference strain (WT-arg) was observed in solvent (MeOH) treated cells. This reduces the probability of improper integration of MCFOs into the cell membrane by fludioxonil treatment.

The fludioxonil mediated repression of RIUP components reduces the availability of proteins involved in high affinity iron uptake. As such proteins are induced under iron restricted conditions, this suggests that fludioxonil treated cells may suffer from decreased iron uptake during iron limitation. This could explain the slightly reduced growth of *C. albicans* on BPS and fludioxonil supplemented plates. However, effects of fludioxonil on growth of iron deprived cells were more apparent when cells grew on glycerol, which is a non-fermentable carbon source (Askew et al, 2009). In this case, cells would be dependent on respiration for providing energy, and restricted iron conditions lead to the Hap43p mediated downregulation of genes of iron utilizing proteins, including genes of the respiratory chain. This would explain the poor growth of *C.albicans* on BPS supplemented YP-glycerol plates. Similar observations were also made with growth on galactose. The poor growth of *C. albicans* YP-galactose supplemented with BPS may in this case point to an effect similar to the "Kluyver-effect", known from other yeasts, which describes poor metabolization of galactose or other sugars under anaerobic conditions (Goffrini et al, 2002). Furthermore, the expression of *GAL1*, encoding for the first enzyme in galactose metabolism (Askew et al, 2009), was found to be repressed by Hap43p under iron restricted conditions (Singh et al, 2011). Fludioxonil treatment reduced growth further, as fewer proteins with high affinity to iron would be available on the cell surface leading to decreased iron uptake. This hypothesis is further

strengthened by the slightly protective effect of pre-cultivating cells in iron repleted conditions (YPD), compared to iron depleted conditions (YPD + 400 µM BPS) seen upon growth on galactose and to a lesser extent on glycerol while being absent upon growth on glucose (Figure 3.3.3).

The induction of flocculation by fludioxonil points to altered cell wall organization. As in the case of iron, fludioxonil dependent flocculation seemed to be dependent on Hog1p. However, flocculation in response to 20 µg ml^{-1} fludioxonil in RPMI medium could only be observed after 3 – 4 h of incubation at 30 °C. Unfortunately, no concentration dependent effects could be observed as intensity of flocculation visibly changed for the same concentration between different cultivations. The irreproducibility of results regarding concentration dependency prevented further characterization of this phenomenon. However, fludioxonil mediated flocculation could be therapeutically useful if flocs cause a reduced adhesion of *C. albicans* cells to host tissues.

Chapter 4 Conclusion and outlook

We have produced two synthetic peptides (a10 and a7/8) resembling predicted alpha-helices in the antigenic *C. albicans* cell wall protein Bgl2p, which were used for monoclonal antibody production by immunization in Balb/c mice. We have expressed and purified a recombinant variant of Bgl2p lacking the signal peptide (rBgl2p-SP) in *E. coli* under non- denaturing conditions. This variant of the protein could be bound by anti-a10 or anti-a7/8 antibodies present in hybridoma cell culture supernatants. Moreover, anti-a10 antibodies from two supernatants, C25HD4H4 and C25HD4H8, could bind to SC5314, DAY286 cells but not to Δ*bgl2* cells as determined by flow cytometry analysis. Thus, the anti-a10 antibodies contained in C25HD4H4 or C25HD4H8 provide promising tools for early clinical diagnosis of *C. albicans* cells. However, full evaluation of the specificity and sensitivity of the two antibodies described above was not possible within the time of this thesis. Once purified anti-a10 antibodies are available, flow cytometric analysis should be repeated and the antibodies should be tested with other pathogens to determine potential cross reactivities. Conditional expression of Bgl2p in Δ*bgl2* cells (Park & Morschhauser, 2005) and subsequent analysis of antibody binding to transformants should also confirm the specificity of antibodies for Bgl2p.

This thesis reports for the first time in fungi, that the conserved stress activated MAPK Hog1p of *C. albicans* is involved in the response to changes in extracellular iron levels. Previous studies had only shown that deletion of *HOG1* led to the de-repression of HAIU components in this fungus under otherwise repressive conditions. We found that repression of high affinity iron uptake (HAIU) components of the reductive pathway by Hog1p occurs independently of environmental iron availability. Exposure of *C. albicans* to high iron concentrations renders Hog1p hyper-phosphorylated. Thus, these results suggest that Hog1p plays a dual role in *C. albicans* iron homeostasis: on the one hand basal Hog1p activity permanently reduces

expression of HAIU components and on the other hand hyper-activity of Hog1p leads to the activation of a specific response towards high iron concentrations. It has yet to be elucidated which elements downstream of Hog1p provide the link between the HOG pathway and factors which regulate reductive iron uptake, with Efg1p appearing as a putative component.

Figure 4.1.1 summarizes the currently known intracellular events upon exposure of *C. albicans* to high iron concentrations.

This thesis further describes new findings related to the effect of fludioxonil on *C. albicans* growth under iron restricted conditions as well as on expression and activity of RIUP components. This could be of high value for *C. albicans* treatment, as targeting iron uptake pathways is considered as an attractive approach for fighting microbial pathogens.

Combination of therapeutically applied iron binding molecules, such as lactoferrin, deferroxamine or genistein, with fludioxonil or iprodione could be investigated for its effect on *C. albicans* growth. The main idea behind this is to create conditions of iron restriction while simultaneously preventing *C. albicans* from full utilization of its high affinity iron uptake machinery. This could be of great importance for patients suffering from iron overload, which are at high risk of acquiring *C. albicans* infections.

The repression of RIUP components by fludioxonil occurred independently of Sfu1p. This indicates a complex regulation of these iron uptake proteins. This would lead to the conclusion that MCFOs are not suitable targets for diagnostic approaches.

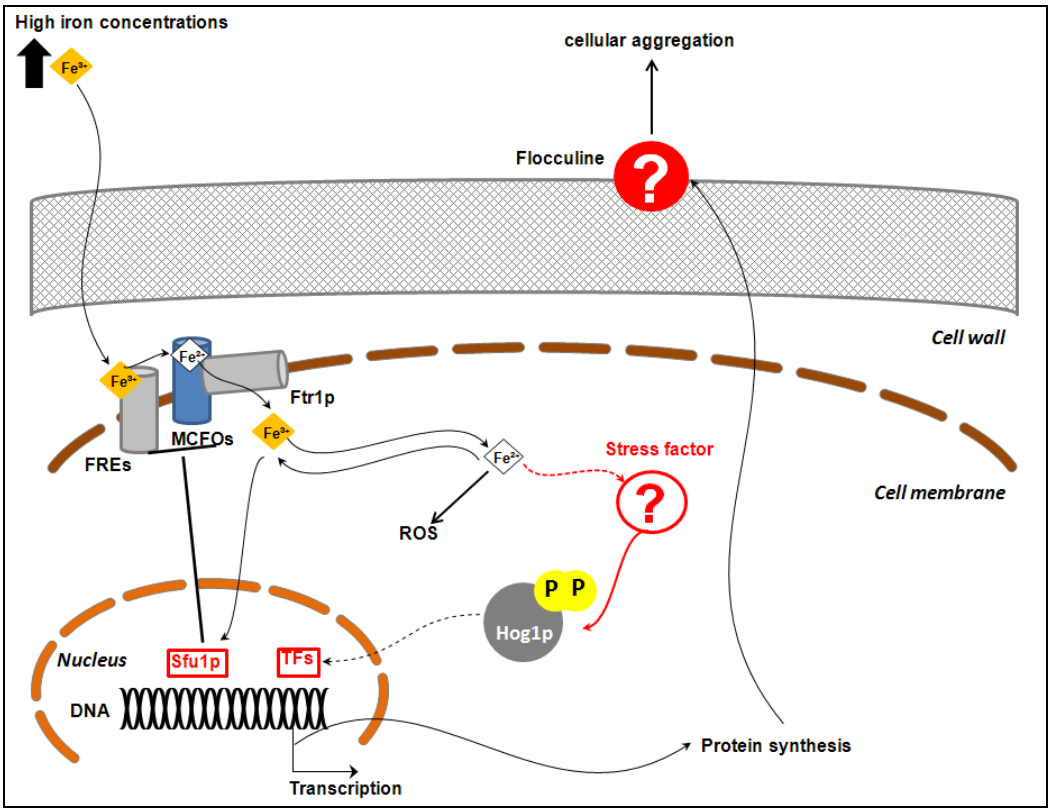

Figure 4.1.1 – Exposure of *C. albicans* to high iron concentrations.

Current knowledge of intracellular events upon exposure of *C. albicans* to high iron concentrations (30 µM Fe^{3+}) is summarized herewith. Fe^{3+} is rapidly removed from the growth medium (within 15 minutes) and enters the cell leading to accumulation of reactive oxygen species (ROS). This means that Fe^{3+} is, at least partly, intracellularly reduced to Fe^{2+}. Genes encoding high affinity iron uptake proteins are repressed by Sfu1p (Chen et al, 2011) which is thought to act as an iron sensor (Pelletier et al, 2007). High iron concentrations induce hyper-phosphorylation of the MAPK Hog1p. It is still unknown whether this happens in a direct or indirect fashion. The high iron concentrations lead to the induction of flocculation of *C. albicans* cells. This is dependent on an intact HOG pathway as well as on synthesis of new proteins, but is rather not related to ROS accumulation. Transcription factors (TFs) and flocculins that could mediate flocculation are still to be identified. One potential transcription factor downstream of Hog1 could be Efg1p (not included in the figure), as Efg1p was also required for iron induced flocculation.

Effects of fludioxonil on the regulation of RIUP components should be studied at the transcriptional level. This could help to ascertain whether fludioxonil mediated repression of MCFOs and decrease of ferric reductase activity, are due post-transcriptional regulation, such as blocking of trafficking or proper integration of the respective proteins to the cell

membrane. However, an initial experiment on the Δ*sfu1* mutant did not support this suggestion (3.3.2).

Dissecting changes which occur in the cell wall upon exposure to high iron or to fludioxonil, leading to the induction of flocculation are of great interest. The induction of flocculation by fludioxonil could be interesting because it may inhibit or decrease *C. albicans* adhesion to host cells, as binding sites of adhesins of may be occupied or shielded by floc formation.

Chapter 5 Supplemental data

Supplemental data 1

Ca_BGL2_ FLAG3x_His8x sequence (*Ca_BGL2*) in alignment with the *BGL2* WT nucleotide sequence (>orf19.4565|BGL2).

>orf19.4565|BGL2 was obtained from the CGD (www.candidagenome.org). Alignment was performed using ClustalW2 and displayed with Jalview. Stop codon, restriction sites used for cloning and signal peptide coding sequence are indicated.

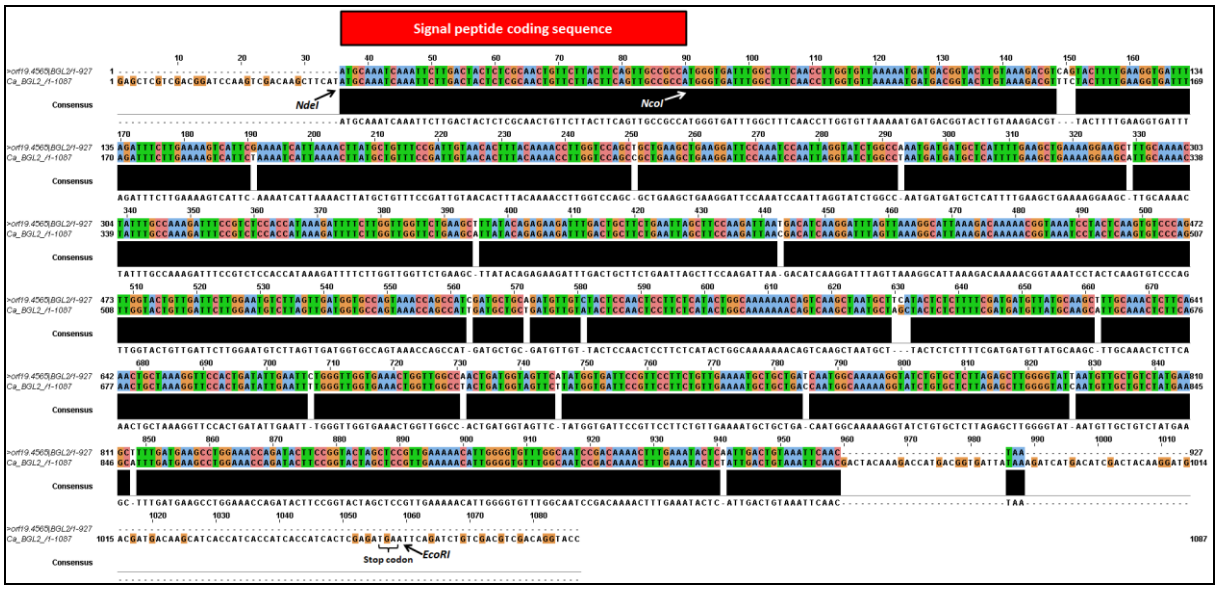

Supplemental data 2

Extraction of cell surface proteins by several methods from both whole and disrupted cells.

SDS-PAGE analysis of coomassie stained *C. albicans* cell surface proteins. (A) proteins extracted from CAF2-1 cell walls by Zymolyase treatment (20 U ml^{-1}). 48 µg total protein was loaded on gel. Gel ran for 25 min at 80 V and 3 h 17 min at 120 V. three Bgl2p peaks were identified by MALDI-TOF MS analysis: 1142.5 m/z, 1267.69 m/z and 3057.441 m/z. (B) proteins extracted from cell walls by Zymolyase treatment. Lane 1: extracts from DAY286. Lane 2: extracts from Δ*bgl2* (FB63-3). 43 µg total protein was loaded on gel for each extract. Gel ran for 1 h at 80 V and 1 h at 120 V. Bgl2p was identified in DAY286 extract by comparison with an equally treated extract from Δ*bgl2* in addition to molecular size. (C) Proteins extracted from cell walls by treatment with 12 M urea at 90 °C. Lane 1: extracts from DAY286. Lane 2: extracts from Δ*bgl2* (FB63-1). 50 µg total protein was loaded on gel for each extract. Gel ran for 3 h and 20 min at 80 V. Bgl2p was identified in DAY286 extract by comparison with an equally treated extract from Δ*bgl2* in addition to molecular size. (D) Proteins extracted from CAF2-1 cell walls by treatment with 2% SDS in 5 mM Tris HCl pH 7.5 at 90 °C. 15 µg total protein was loaded on gel. Presence of Bgl2p could not be confirmed by MALDI-TOF MS or MS/ MS analysis. Following proteins could be identified by MALDI-TOF MS and subsequent mascot search (http://www.matrixscience.com/) instead: Tef1p (orf19.1435; peaks 1364.7 m/z, 1560.8 m/z, 1677.9 and 2493.1 m/z), Adh1p (orf19.3997; peaks 1103.6 m/z, and 1271.6 m/z), Atp1p (orf19.6854; peaks 1273.7 m/z and 1553.8 m/z), Tdh3p (orf19.6814; peaks 1145.6 m/z, 1500.8 m/z and 1766.8 m/z) and Rps4p (orf19.5341; peak1199.6 m/z). (E) Proteins extracted from CAF2-1 cell walls at 90 °C in 5 mM Tris HCl pH 7.5. 24 µg total protein was loaded on gel. Presence of Bgl2p could be confirmed by MS/ MS analysis. (F) Proteins extracted from whole SC5314 cells (grown in RPMI + 10% FBS at 30 °C for 5 h) at 90 °C in PBS. 38 µg total protein was loaded on gel. Gel ran for 2 h and 20 min at 120 V. Presence of multicopper ferroxidase (MCFO) members was confirmed by MALDI-TOF-MS analysis (see below) and N-terminal sequencing (KTHTWYYKTGxV).

Peptide peaks [m/z]	**MCFO**
1384.7	Fet34p
1726.9	Fet3p, Fet34p
1838.9	Fet34p
1867.0	Fet3p, Fet31p, Fet99p
3107.5	Fet3p
4056.9	Fet34p

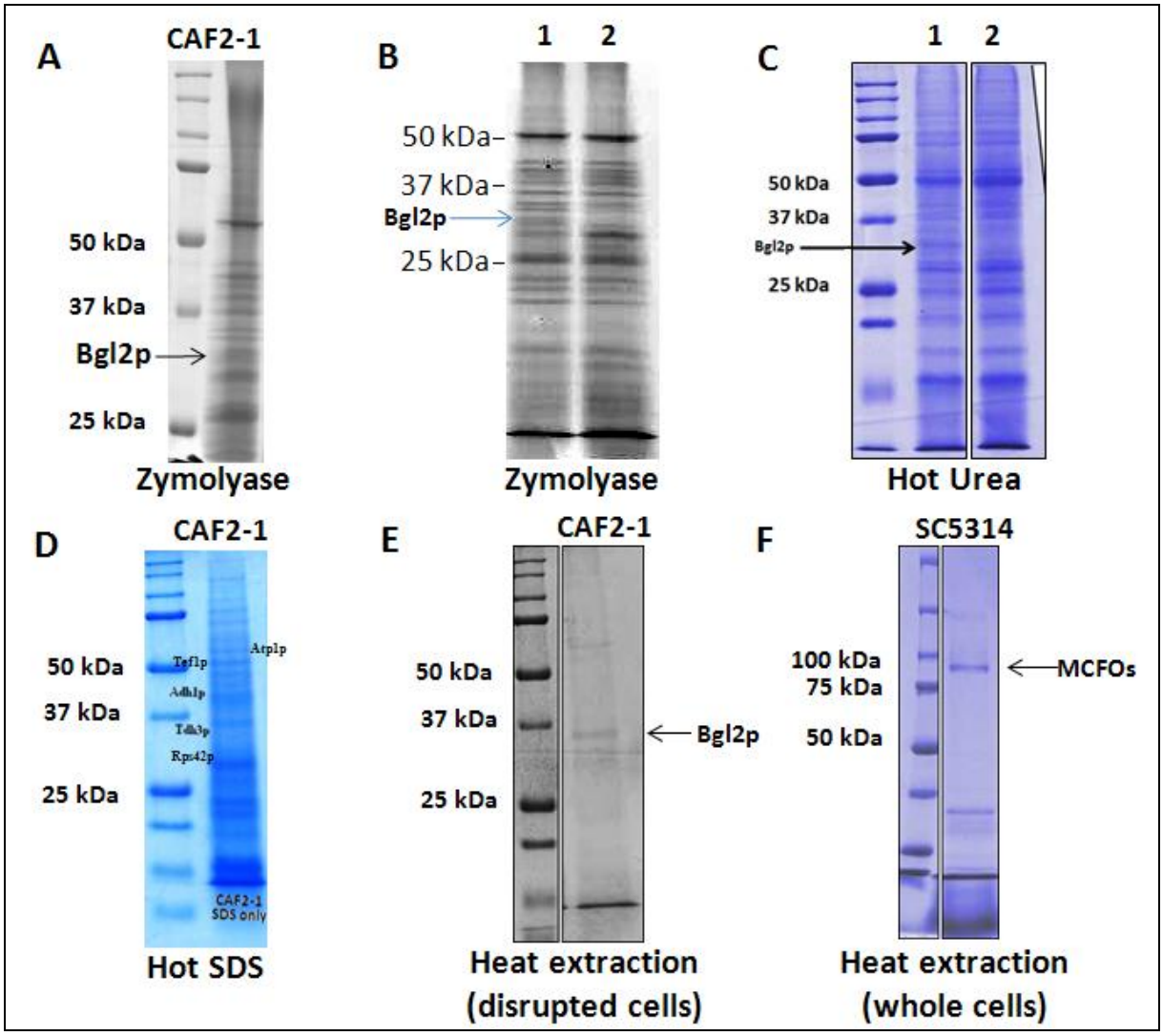
A
CAF2-1
50 kDa
37 kDa
Bgl2p
25 kDa
Zymolyase
B
1
2
50 kDa
37 kDa
Bgl2p
25 kDa
Zymolyase
C
1
2
50 kDa
37 kDa
Bgl2p
25 kDa
Hot Urea
D
CAF2-1
50 kDa
37 kDa
25 kDa
Tef1p
Adh1p
Tdh3p
Rps42p
Atp1p
CAF2-1 SDS only
Hot SDS
E
CAF2-1
50 kDa
37 kDa
25 kDa
Bgl2p
Heat extraction (disrupted cells)
F
SC5314
100 kDa
75 kDa
50 kDa
MCFOs
Heat extraction (whole cells)

Supplemental data 3

Microscopic analysis of *C. albicans* DAY286 grown in RPMI + 10% FBS at 37 °C for 3 h.

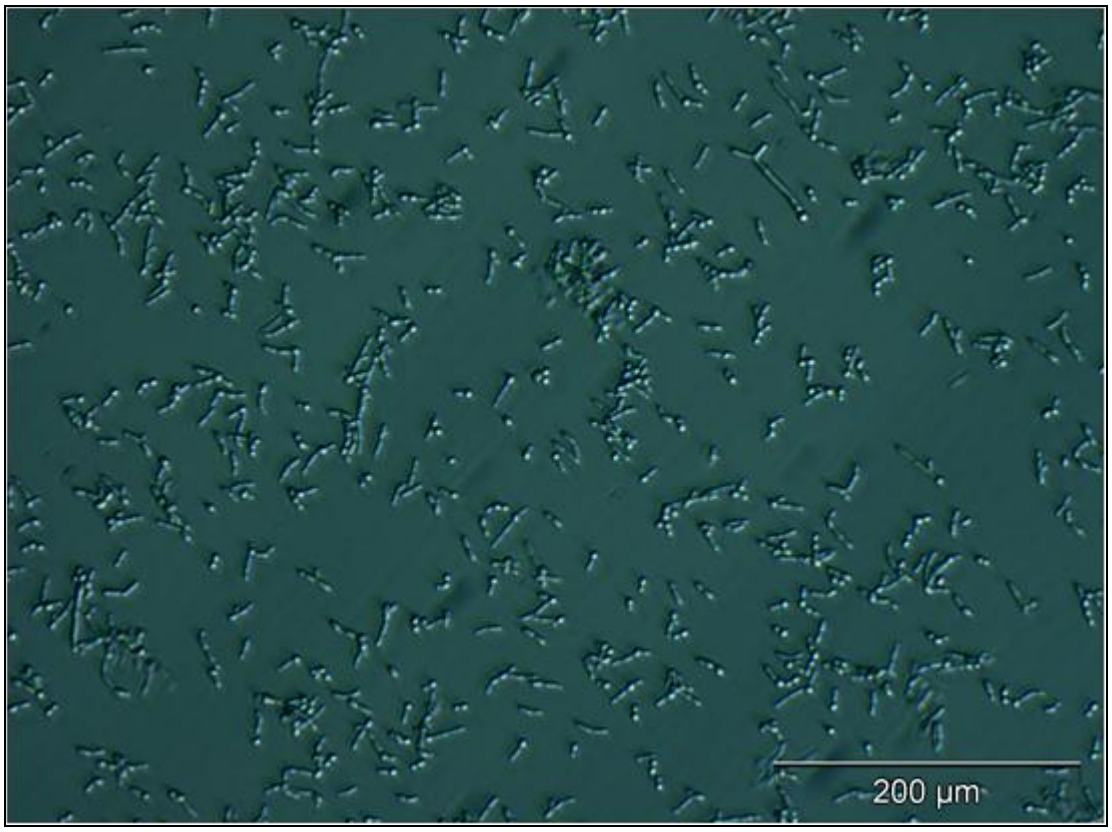

Supplemental data 4

Multiple sequence alignment (MSA) of Bgl2p orthologues from three different *C. albicans* strains (SC5314, WO-1 and ATCC10261) and six different non-albicans *Candida* species.

Cdu: *C. dubliniensis*, Cgl: *C. glabrata*, Ctr: *C. tropicalis*, Cgu: *C. guilliermondii*, Clu: *C. lusitaniae* (Clu), Cpa: *C. parapsilosis*. See 2.10 for details. Alignment was performed with ClustalW2 (http://www.ebi.ac.uk/Tools/msa/clustalw2/) (default settings) and displayed with Jalview.

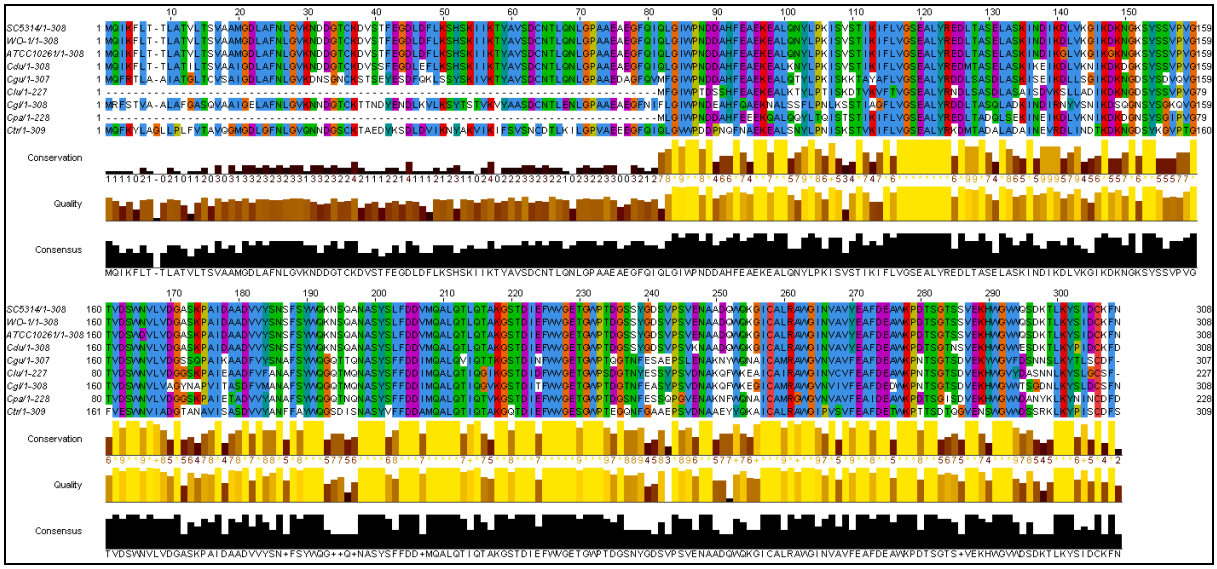

Alignment scores are listed in the table below compared to the sequence of the *C. albicans* SC5314 orthologue. Note that N-terminal fragments of the *C. lusitaniae* and *C. parapsilosis* orthologues were missing*.

Strain/ Organism	Length (aa)	Alignment score
SC5314	308	100
WO-1	308	100
ATCC10261	308	99
C. dubliniensis	308	95
C. parapsilosis	228*	74
C. guilliermondii	307	70
C. lusitaniae	227*	70
C. glabrata	308	65
C. tropicalis	309	60

Supplemental data 5

NCBI basic local alignment search tool (BLAST) results for peptides a10 and a7/8 respectively in bacteria, fungi (excluding the *Candida* clade*), archaea and humans.

Following criteria were applied to determine a relevant hit:

(i) No gaps were allowed between peptide and hit-sequence in the alignment
(ii) Query coverage (QC) between peptide and hit-sequence must be at least 80%.
(iii) Identity (I) and similarity (S) between peptide and hit-sequence must be at least 80%.
(iv) The E-value was set at 1000.
(v) The score was calculated according to the PAM-30 substitution matrix.

BLAST was performed by Yvonne Mayer (Microdiscovery GmbH, Berlin).

Hits for peptide a10						
Organism	**Protein ID**	**QC**	**I**	**S**	**E-Value**	**Score**
Cellulomonas flavigena DSM 20109	YP 003635918: glycoside hydrolase family 10	93	54	85	613.16	52.0
Hits for peptide a7/8						
Organism	**Protein ID**	**QC**	**I**	**S**	**E-Value**	**Score**
Lodderomyces elongisporus NRRL YB-4239	XP 001524413: glucan 1,3-beta-glucosidase precursor	100	82	82	2.38719E-5	110.0
Scheffersomyces stipitis CBS 6054, *Pichia stipitis* CBS 6054	XP 001387556: Glycoside hydrolase, family 17	100	82	82	4.29787E-5	108.0
Pichia guilliermondii ATCC 6260	EDK38288: hypothetical protein PGUG 02386	100	82	82	6.05893E-4	99.0
Meyerozyma guilliermondii ATCC 6260	XP 001484657: hypothetical protein PGUG 02386	100	82	82	6.05893E-4	99.0
Debaryomyces hansenii CBS767, *Debaryomyces hansenii*	XP 462355: DEHA2G18766p	100	76	82	0.00109084	97.0
Yarrowia lipolytica	XP 500465: YALI0B03564p	100	71	82	0.00263517	94.0
Clavispora lusitaniae ATCC 42720	XP 002614964: hypothetical protein CLUG 04979	100	71	82	0.00636586	91.0

Please note that *Lodderomyces elongisporus*, *Pichia* (*Meyerozyma*) (*Candida*) *guilliermondii*, *Debaryomyces hansenii* and *Clavispora* (*Candida*) *lusitaniae* belong to the *Candida* clade (see Figure 1.1).

Supplemental data 6

Dot blot analysis of supernatants binding to rBgl2-SP

rBgl2p-SP was expressed and purified under non-denaturing conditions and 96 ng were dropped on PVDF membranes. Membranes were blocked and washed with TBS containing 0.05% (v/v) Tween-20. Membranes were incubated overnight with C25JA11B10 or C26FC11F7 and subsequently with HRP-linked secondary antibody. Membranes were later stripped and treated with anti-FLAG antibody. Blots were exposed for 100 sec each.

Supplemental data 7

Microscopic analysis of the reference strain (DAY286) after exposure to 30 µM or 1.2 µM $FeCl_3$ in YNB. Cells were incubated at 30 °C for 2 h.

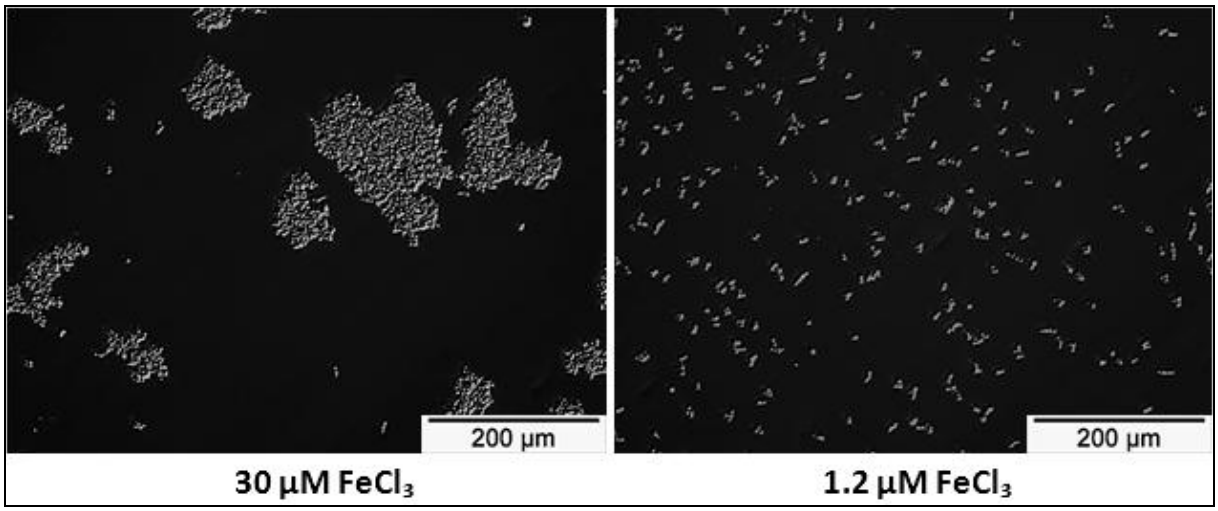

Supplemental data 8

Synthesis of new proteins is required for induction of flocculation in DAY286 upon exposure to 30 µM Fe^{3+}.

(A) Relative sedimentation rates of DAY286 cells treated with cycloheximide (CHX) *C. albicans* DAY286 was pre-treated either with 500 µg ml^{-1} CHX or MeOH in RPMI at 30 °C for 15 min. Iron or water were subsequently added and cells were incubated at 30 °C for 2 h. Sedimentation rates were determined as described in the experimental part. Means and standard deviations of three independent samples are shown (n = 3). ** denotes $P \leq 0.01$ (student's t-test). (B) Microscopic analysis of CHX or MeOH pre-treated cells (see A).

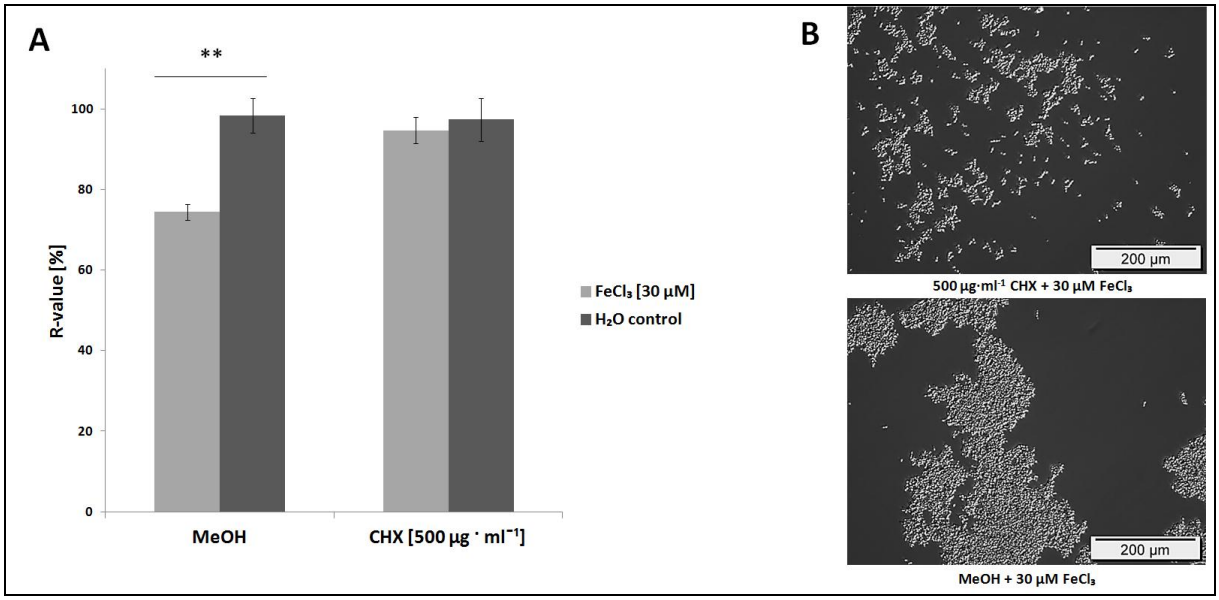

Supplemental data 9

Flocculation is induced in the Δ*hog1* mutant by exposure to 10% human plasma.

Microscopic analysis of DAY286 or Δ*hog1* (JMR114) cells incubated in RPMI supplemented with 10% human plasma at 30 °C for 2 h 30 min.

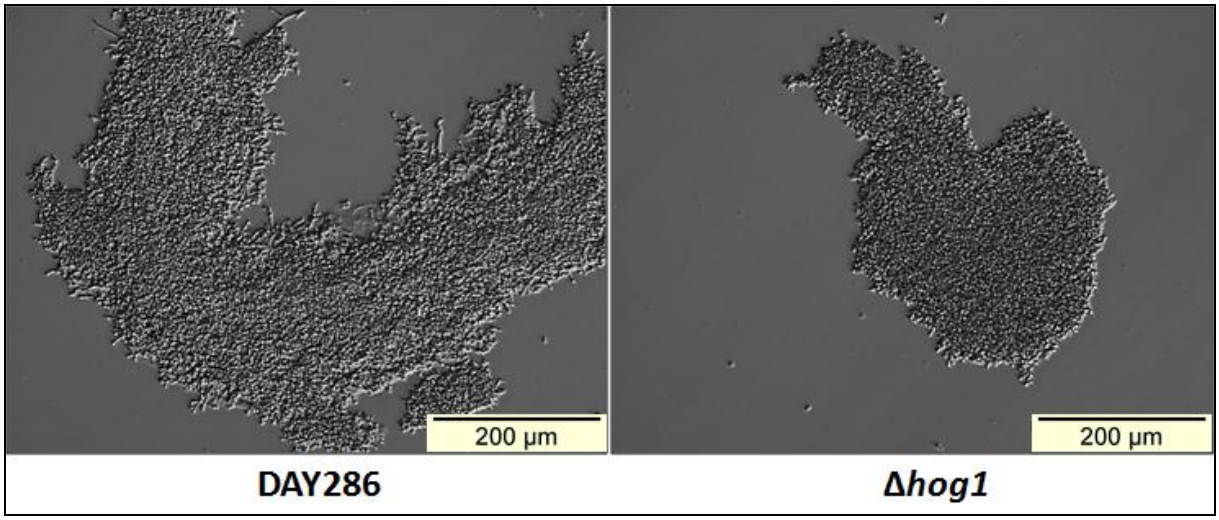

Supplemental data 10

Exposure to high iron concentrations led to intracellular ROS accumulation in Δ*hog1* cells.

Experiments for ROS accumulation in Δ*hog1* cells were performed twice (n = 2). Means and standard deviations are shown of one representative experiment where all samples were derived from the same pre-culture. *** denotes $P < 0.001$ (student's t-test).

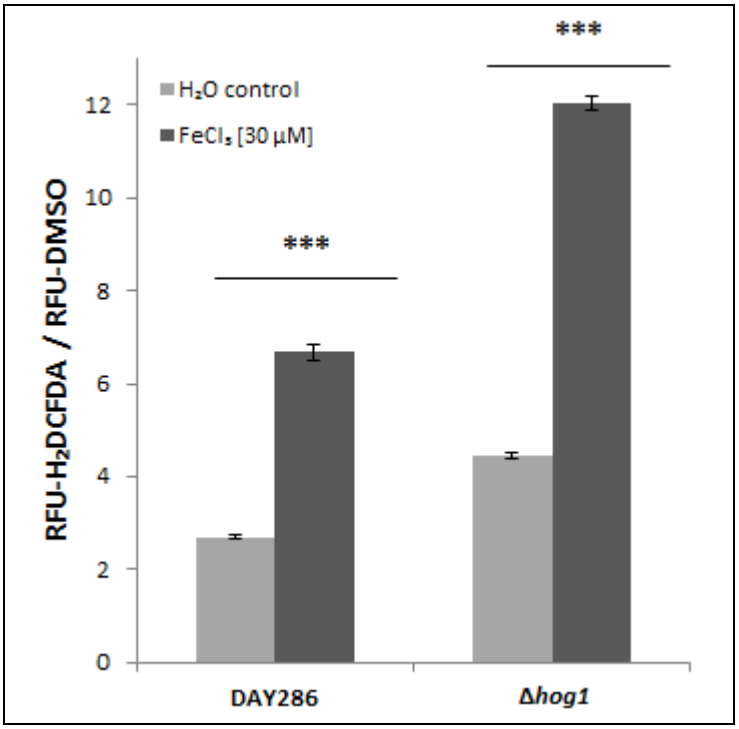

Supplemental data 11

Cell viability measurement by alamarBlue®

Relative fluorescence units (RFU) obtained for SC5314, DAY286 and Δ*hog1* (JMR114) 1 h after exposure to 30 µM $FeCl_3$ or H_2O control at 30 °C. Results for DAY286 and Δ*hog1* (JMR114) are shown as means of three independent experiments. Experiment for SC5314 was performed only once.

Sample	**RFU**
SC5314 H_2O control	6207.67
SC5314 30 µM $FeCl_3$	5302.67
DAY286 H_2O control	4656.44 ± 358.51
DAY286 30 µM $FeCl_3$	3777.22 ± 428
Δ*hog1* H_2O control	9424.66 ± 758.8
Δ*hog1* 30 µM $FeCl_3$	4370.55 ± 358.5

Supplemental data 12

Growth tests of several *C. albicans* strains of solid RPMI medium containing different concentrations.

The WT (SC5314), the reference strain (DAY286), and the Δ*hog1* (JMR114) and Δ*pbs2* (JJH31) mutants were diluted in YPD each to ca. $0.5 \cdot 10^6$ cells ml^{-1} and further diluted in 1:10 steps. 5 µl of each cell suspension were dropped on RPMI agar plates containing 0 (RPMI), 1 or 30 µM $FeCl_3$. Plates were incubated for 2 d at 30 °C before pictures were taken. All plates were prepared in triplicates and one representative for each plate is shown.

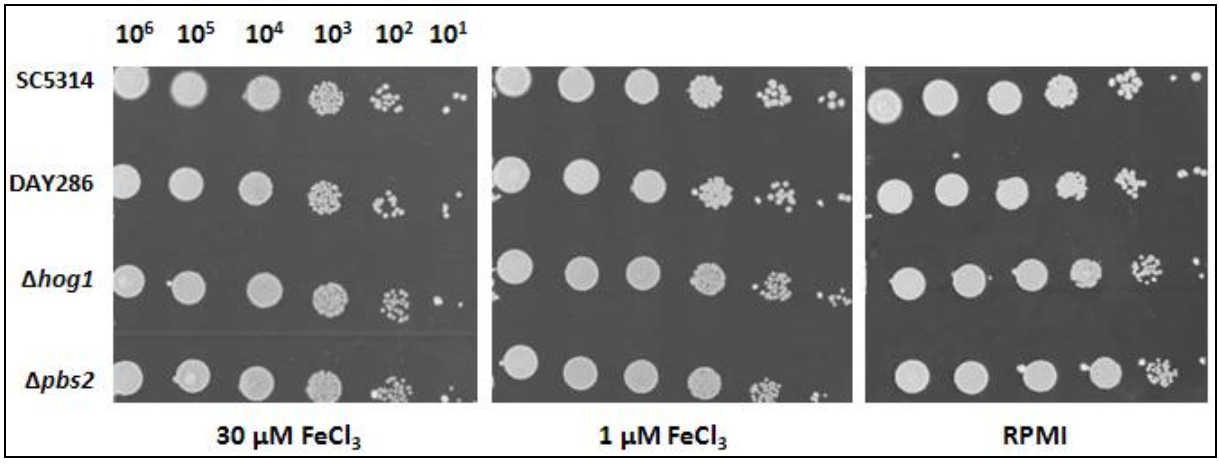

Supplemental data 13

Ferric reductase activity was decreased in SC5314 after fludioxonil treatment under restricted iron conditions

Cell surface ferric reductase activity of *C. albicans* SC5314 treated with MeOH, fludioxonil or fluconazole in RIM medium. Mean values and standard deviations of three independent experiments (n = 3) are shown. *** denotes $P \leq 0.001$ (student's t-test). The ferric reductase of activity of the MeOH (solvent) treated culture set as 100%.

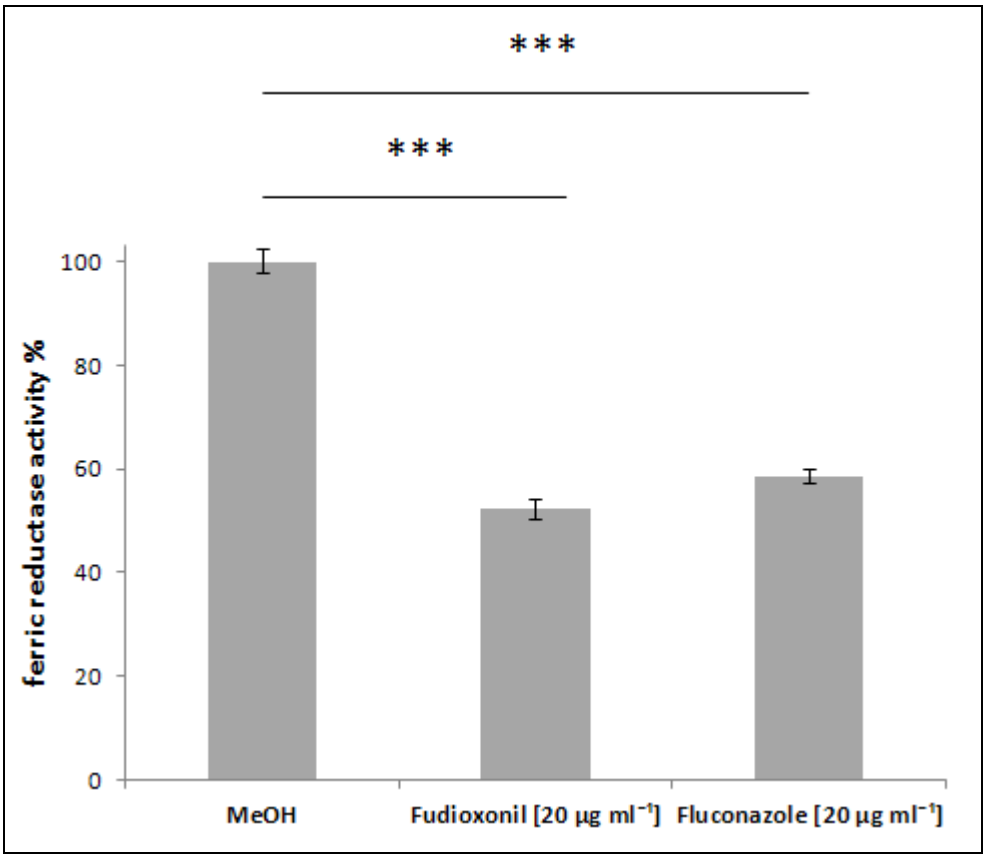

Supplemental data 14

Repression of RIUP components by fludioxonil is independent of the fludioxonil receptor, histidine kinase Cos1p.

(A) Cell surface ferric reductase activity of *C. albicans* Δ*cos1* (JJH37) treated with fludioxonil [20 µg ml^{-1}], or MeOH in RIM medium. Mean values and standard deviations of three independent experiments (n = 3) are shown. *** denotes $P \leq 0.001$ (student's t-test). The ferric reductase of activity of the MeOH (solvent) treated culture set as 100%. (B) Excerpt of coomassie stained SDS gel showing MCFOs from *C. albicans* Δ*cos1* cells treated with fludioxonil or iprodione [each at 20 µg ml^{-1} final concentration] or MeOH in both YPD and RIM (3 h at 30 °C). Fdx: fludioxonil; ipro: iprodione. Bovine serum albumin (BSA) was added to protein extracts shown in B as internal standard to serve as a loading control. Gel ran for 3 h at 120 V.

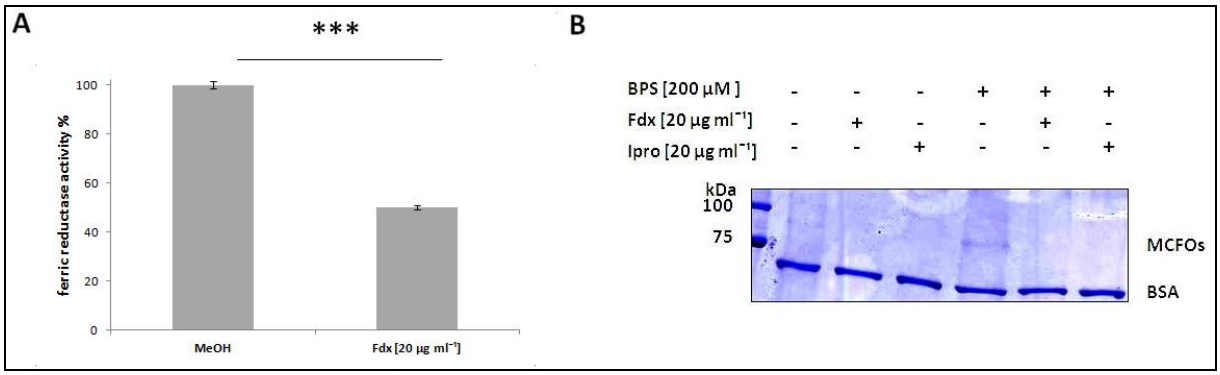

Supplemental data 15

Ferric reductase activity of SC5314 treated with MeOH, fludioxonil, iprodione or fluconazole under restricted iron conditions

Cell surface ferric reductase activity of *C. albicans* SC5314 treated with MeOH, fludioxonil (Fdx), iprodione (Ipro) or fluconazole (Flu) in RIM medium. Cells were resuspended in 1.5 ml RIM supplemented with the respective antifungal/ MeOH and cultivated in a 24 well plate (30 °C, 3 h, 550 rpm) in an Eppendorf comfort 5355R thermomixer. Experiment was performed only once.

Antifungal [concentration]	**Ferric reductase activity (% of RIM + MeOH)**
YPD + MeOH	40.28
RIM + MeOH	100
RIM + Fdx [20 µg ml^{-1}]	64.28
RIM + Ipro [20 µg ml^{-1}]	74.14
RIM + Flc [10 µg ml^{-1}]	47.24

References

Alby K, Bennett RJ (2010) Sexual reproduction in the *Candida* clade: cryptic cycles, diverse mechanisms, and alternative functions. *Cell Mol Life Sci* **67:** 3275-3285

Almeida RS, Brunke S, Albrecht A, Thewes S, Laue M, Edwards JE, Filler SG, Hube B (2008) the hyphal-associated adhesin and invasin Als3 of *Candida albicans* mediates iron acquisition from host ferritin. *PLoS Pathog* **4:** e1000217

Almeida RS, Wilson D, Hube B (2009) *Candida albicans* iron acquisition within the host. *FEMS Yeast Res* **9:** 1000-1012

Alonso-Monge R, Carvaihlo S, Nombela C, Rial E, Pla J (2009) The Hog1 MAP kinase controls respiratory metabolism in the fungal pathogen *Candida albicans*. *Microbiology* **155:** 413-423

Alonso-Monge R, Navarro-Garcia F, Roman E, Negredo AI, Eisman B, Nombela C, Pla J (2003) The Hog1 mitogen-activated protein kinase is essential in the oxidative stress response and chlamydospore formation in *Candida albicans*. *Eukaryot Cell* **2:** 351-361

Alonso-Monge R, Roman E, Arana DM, Prieto D, Urrialde V, Nombela C, Pla J (2010) The Sko1 protein represses the yeast-to-hypha transition and regulates the oxidative stress response in *Candida albicans*. *Fungal Genet Biol* **47:** 587-601

Angiolella L, Micocci MM, D'Alessio S, Girolamo A, Maras B, Cassone A (2002) Identification of major glucan-associated cell wall proteins of *Candida albicans* and their role in fluconazole resistance. *Antimicrob Agents Chemother* **46:** 1688-1694

Angiolella L, Vitali A, Stringaro A, Mignogna G, Maras B, Bonito M, Colone M, Palamara AT, Cassone A (2009) Localisation of Bgl2p upon antifungal drug treatment in *Candida albicans*. *Int J Antimicrob Agents* **33:** 143-148

Arana DM, Nombela C, Alonso-Monge R, Pla J (2005) The Pbs2 MAP kinase kinase is essential for the oxidative-stress response in the fungal pathogen Candida albicans. *Microbiology* **151:** 1033-1049

Arias CA, Weisner J, Blackburn JM, Reynolds PE (2000) Serine and alanine racemase activities of VanT: a protein necessary for vancomycin resistance in *Enterococcus gallinarum* BM4174. *Microbiology* **146 (Pt 7):** 1727-1734

Askew C, Sellam A, Epp E, Hogues H, Mullick A, Nantel A, Whiteway M (2009) Transcriptional regulation of carbohydrate metabolism in the human pathogen *Candida albicans*. *PLoS pathogens* **5:** e1000612

Barnett JA (2004) A history of research on yeasts 8: taxonomy. *Yeast* **21:** 1141-1193

Bell M, Capone R, Pashtan I, Levitzki A, Engelberg D (2001) Isolation of hyperactive mutants of the MAPK p38/Hog1 that are independent of MAPK kinase activation. *J Biol Chem* **276:** 25351-25358

Bensen ES, Martin SJ, Li M, Berman J, Davis DA (2004) Transcriptional profiling in *Candida albicans* reveals new adaptive responses to extracellular pH and functions for Rim101p. *Mol Microbiol* **54:** 1335-1351

Benz I, Schmidt MA (1992) Isolation and serologic characterization of AIDA-I, the adhesin mediating the diffuse adherence phenotype of the diarrhea-associated *Escherichia coli* strain 2787 (O126:H27). *Infect Immun* **60:** 13-18

Bianchi DE (1964) Flocculation of Lag Phase Yeast Cells of *Candida albicans*. *Antonie Van Leeuwenhoek* **30:** 401-411

Brand A, MacCallum DM, Brown AJ, Gow NA, Odds FC (2004) Ectopic expression of *URA3* can influence the virulence phenotypes and proteome of *Candida albicans* but can be overcome by targeted reintegration of *URA3* at the *RPS10* locus. *Eukaryot Cell* **3:** 900-909

Braun BR, Johnson AD (1997) Control of filament formation in *Candida albicans* by the transcriptional repressor *TUP1*. *Science* **277:** 105-109

Braun BR, van Het Hoog M, d'Enfert C, Martchenko M, Dungan J, Kuo A, Inglis DO, Uhl MA, Hogues H, Berriman M, Lorenz M, Levitin A, Oberholzer U, Bachewich C, Harcus D, Marcil A, Dignard D, Iouk T, Zito R, Frangeul L, Tekaia F, Rutherford K, Wang E, Munro CA, Bates S, Gow NA, Hoyer LL, Kohler G, Morschhauser J, Newport G, Znaidi S, Raymond M, Turcotte B, Sherlock G, Costanzo M, Ihmels J, Berman J, Sanglard D, Agabian N, Mitchell AP, Johnson AD, Whiteway M, Nantel A (2005) A human-curated annotation of the *Candida albicans* genome. *PLoS Genet* **1:** 36-57

Brawner DL, Cutler JE (1986) Variability in expression of cell surface antigens of *Candida albicans* during morphogenesis. *Infect Immun* **51:** 337-343

Brown AJ, Haynes K, Quinn J (2009) Nitrosative and oxidative stress responses in fungal pathogenicity. *Current opinion in microbiology* **12:** 384-391

Buck GE, Smith JS, Parshall KA (1984) Composition of the antigenic material removed from *Campylobacter jejuni* by heat. *J Clin Microbiol* **20:** 1094-1098

Bullen JJ, Rogers HJ, Spalding PB, Ward CG (2006) Natural resistance, iron and infection: a challenge for clinical medicine. *J Med Microbiol* **55:** 251-258

Buschart A, Burakowska A, Bilitewski U (2012a) The fungicide fludioxonil antagonizes fluconazole activity in the human fungal pathogen *Candida albicans*. *J Med Microbiol*

Buschart A, Gremmer K, El-Mowafy M, van den Heuvel J, Mueller PP, Bilitewski U (2012b) A novel functional assay for fungal histidine kinases group III reveals the role of HAMP domains for fungicide sensitivity. *Journal of biotechnology* **157:** 268-277

Butler G, Rasmussen MD, Lin MF, Santos MA, Sakthikumar S, Munro CA, Rheinbay E, Grabherr M, Forche A, Reedy JL, Agrafioti I, Arnaud MB, Bates S, Brown AJ, Brunke S, Costanzo MC, Fitzpatrick DA, de Groot PW, Harris D, Hoyer LL, Hube B, Klis FM, Kodira C, Lennard N, Logue ME, Martin R, Neiman AM, Nikolaou E, Quail MA, Quinn J, Santos MC, Schmitzberger FF, Sherlock G, Shah P, Silverstein KA, Skrzypek MS, Soll D, Staggs R, Stansfield I, Stumpf MP, Sudbery PE, Srikantha T, Zeng Q, Berman J, Berriman M, Heitman J, Gow NA, Lorenz MC, Birren BW, Kellis M, Cuomo CA (2009) Evolution of pathogenicity and sexual reproduction in eight *Candida* genomes. *Nature* **459:** 657-662

Caroline L, Rosner F, Kozinn PJ (1969) Elevated serum iron, low unbound transferrin and candidiasis in acute leukemia. *Blood* **34:** 441-451

Chaffin WL (2008) *Candida albicans* cell wall proteins. *Microbiol Mol Biol Rev* **72:** 495-544

Chaffin WL, Lopez-Ribot JL, Casanova M, Gozalbo D, Martinez JP (1998) Cell wall and secreted proteins of *Candida albicans*: identification, function, and expression. *Microbiol Mol Biol Rev* **62:** 130-180

Cheetham J, MacCallum DM, Doris KS, da Silva Dantas A, Scorfield S, Odds F, Smith DA, Quinn J (2011) MAPKKK-independent regulation of the Hog1 stress-activated protein kinase in *Candida albicans*. *The Journal of biological chemistry* **286:** 42002-42016

Chen C, Noble SM (2012) Post-transcriptional regulation of the Sef1 transcription factor controls the virulence of *Candida albicans* in its mammalian host. *PLoS Pathog* **8:** e1002956

Chen C, Pande K, French SD, Tuch BB, Noble SM (2011) An iron homeostasis regulatory circuit with reciprocal roles in *Candida albicans* commensalism and pathogenesis. *Cell Host Microbe* **10:** 118-135

Cheng S, Nguyen MH, Zhang Z, Jia H, Handfield M, Clancy CJ (2003) Evaluation of the roles of four *Candida albicans* genes in virulence by using gene disruption strains that express *URA3* from the native locus. *Infect Immun* **71:** 6101-6103

Cheng X, Xu N, Yu Q, Qian K, Ding X, Zhao Q, Wang Y, Zhang B, Xing L, Li M (2013) Novel insight into the expression and function of the multicopper oxidases in *Candida albicans*. *Microbiology*

Clancy CJ, Nguyen ML, Cheng S, Huang H, Fan G, Jaber RA, Wingard JR, Cline C, Nguyen MH (2008) Immunoglobulin G responses to a panel of *Candida albicans* antigens as accurate and early markers for the presence of systemic candidiasis. *J Clin Microbiol* **46:** 1647-1654

Cleary IA, MacGregor NB, Saville SP, Thomas DP (2012) Investigating the function of Ddr48p in *Candida albicans*. *Eukaryot Cell* **11:** 718-724

Cornelis P, Wei Q, Andrews SC, Vinckx T (2011) Iron homeostasis and management of oxidative stress response in bacteria. *Metallomics* **3:** 540-549

Costa-de-Oliveira S, Silva AP, Miranda IM, Salvador A, Azevedo MM, Munro CA, Rodrigues AG, Pina-Vaz C (2013) Determination of chitin content in fungal cell wall: An alternative flow cytometric method. *Cytometry A*

Crampin H, Finley K, Gerami-Nejad M, Court H, Gale C, Berman J, Sudbery P (2005) *Candida albicans* hyphae have a Spitzenkorper that is distinct from the polarisome found in yeast and pseudohyphae. *J Cell Sci* **118:** 2935-2947

Crowe JD, Sievwright IK, Auld GC, Moore NR, Gow NA, Booth NA (2003) *Candida albicans* binds human plasminogen: identification of eight plasminogen-binding proteins. *Mol Microbiol* **47:** 1637-1651

Davis DA, Bruno VM, Loza L, Filler SG, Mitchell AP (2002) *Candida albicans* Mds3p, a conserved regulator of pH responses and virulence identified through insertional mutagenesis. *Genetics* **162:** 1573-1581

de Groot PW, de Boer AD, Cunningham J, Dekker HL, de Jong L, Hellingwerf KJ, de Koster C, Klis FM (2004) Proteomic analysis of *Candida albicans* cell walls reveals covalently bound carbohydrate-active enzymes and adhesins. *Eukaryotic cell* **3:** 955-965

Dhamgaye S, Devaux F, Manoharlal R, Vandeputte P, Shah AH, Singh A, Blugeon C, Sanglard D, Prasad R (2012) In vitro effect of malachite green on *Candida albicans* involves

multiple pathways and transcriptional regulators UPC2 and STP2. *Antimicrob Agents Chemother* **56:** 495-506

Dongari-Bagtzoglou A, Kashleva H, Dwivedi P, Diaz P, Vasilakos J (2009) Characterization of mucosal *Candida albicans* biofilms. *PloS one* **4:** e7967

Dujon B, Sherman D, Fischer G, Durrens P, Casaregola S, Lafontaine I, De Montigny J, Marck C, Neuveglise C, Talla E, Goffard N, Frangeul L, Aigle M, Anthouard V, Babour A, Barbe V, Barnay S, Blanchin S, Beckerich JM, Beyne E, Bleykasten C, Boisrame A, Boyer J, Cattolico L, Confanioleri F, De Daruvar A, Despons L, Fabre E, Fairhead C, Ferry-Dumazet H, Groppi A, Hantraye F, Hennequin C, Jauniaux N, Joyet P, Kachouri R, Kerrest A, Koszul R, Lemaire M, Lesur I, Ma L, Muller H, Nicaud JM, Nikolski M, Oztas S, Ozier-Kalogeropoulos O, Pellenz S, Potier S, Richard GF, Straub ML, Suleau A, Swennen D, Tekaia F, Wesolowski-Louvel M, Westhof E, Wirth B, Zeniou-Meyer M, Zivanovic I, Bolotin-Fukuhara M, Thierry A, Bouchier C, Caudron B, Scarpelli C, Gaillardin C, Weissenbach J, Wincker P, Souciet JL (2004) Genome evolution in yeasts. *Nature* **430:** 35-44

Edman P, Begg G (1967) A protein sequenator. *Eur J Biochem* **1:** 80-91

El-Kirat-Chatel S, Beaussart A, Alsteens D, Sarazin A, Jouault T, Dufrene YF (2013) Single-molecule analysis of the major glycopolymers of pathogenic and non-pathogenic yeast cells. *Nanoscale*

Enjalbert B, Smith DA, Cornell MJ, Alam I, Nicholls S, Brown AJ, Quinn J (2006) Role of the Hog1 stress-activated protein kinase in the global transcriptional response to stress in the fungal pathogen *Candida albicans*. *Mol Biol Cell* **17:** 1018-1032

Enoch DA, Ludlam HA, Brown NM (2006) Invasive fungal infections: a review of epidemiology and management options. *Journal of medical microbiology* **55:** 809-818

Ernst JF, Pla J (2011) Signaling the glycoshield: maintenance of the *Candida albicans* cell wall. *International journal of medical microbiology : IJMM* **301:** 378-383

Eroles P, Sentandreu M, Elorza MV, Sentandreu R (1997) The highly immunogenic enolase and Hsp70p are adventitious *Candida albicans* cell wall proteins. *Microbiology* **143 (Pt 2):** 313-320

Fai PB, Grant A (2009) A comparative study of *Saccharomyces cerevisiae* sensitivity against eight yeast species sensitivities to a range of toxicants. *Chemosphere* **75:** 289-296

Fanning S, Mitchell AP (2012) Fungal biofilms. *PLoS pathogens* **8:** e1002585

Fidel PL, Jr., Vazquez JA, Sobel JD (1999) *Candida glabrata*: review of epidemiology, pathogenesis, and clinical disease with comparison to C. albicans. *Clinical microbiology reviews* **12:** 80-96

Fiori A, Van Dijck P (2012) Potent synergistic effect of doxycycline with fluconazole against *Candida albicans* is mediated by interference with iron homeostasis. *Antimicrobial agents and chemotherapy* **56:** 3785-3796

Fonzi WA, Irwin MY (1993) Isogenic strain construction and gene mapping in *Candida albicans*. *Genetics* **134:** 717-728

Fratti RA, Belanger PH, Ghannoum MA, Edwards JE, Jr., Filler SG (1998) Endothelial cell injury caused by *Candida albicans* is dependent on iron. *Infect Immun* **66:** 191-196

Fu Y, Ibrahim AS, Sheppard DC, Chen YC, French SW, Cutler JE, Filler SG, Edwards JE, Jr. (2002) *Candida albicans* Als1p: an adhesin that is a downstream effector of the *EFG1* filamentation pathway. *Molecular microbiology* **44:** 61-72

Fu Y, Rieg G, Fonzi WA, Belanger PH, Edwards JE, Jr., Filler SG (1998) Expression of the *Candida albicans* gene *ALS1* in *Saccharomyces cerevisiae* induces adherence to endothelial and epithelial cells. *Infection and immunity* **66:** 1783-1786

Galaris D, Pantopoulos K (2008) Oxidative stress and iron homeostasis: mechanistic and health aspects. *Crit Rev Clin Lab Sci* **45:** 1-23

Gantner BN, Simmons RM, Underhill DM (2005) Dectin-1 mediates macrophage recognition of *Candida albicans* yeast but not filaments. *Embo J* **24:** 1277-1286

Garcia MG, O'Connor JE, Garcia LL, Martinez SI, Herrero E, del Castillo Agudo L (2001) Isolation of a *Candida albicans* gene, tightly linked to *URA3*, coding for a putative transcription factor that suppresses a *Saccharomyces cerevisiae aft1* mutation. *Yeast* **18:** 301-311

Gaur NK, Klotz SA (1997) Expression, cloning, and characterization of a *Candida albicans* gene, *ALA1*, that confers adherence properties upon *Saccharomyces cerevisiae* for extracellular matrix proteins. *Infection and immunity* **65:** 5289-5294

Gil-Navarro I, Gil ML, Casanova M, O'Connor JE, Martinez JP, Gozalbo D (1997) The glycolytic enzyme glyceraldehyde-3-phosphate dehydrogenase of *Candida albicans* is a surface antigen. *J Bacteriol* **179:** 4992-4999

Gillum AM, Tsay EY, Kirsch DR (1984) Isolation of the *Candida albicans* gene for orotidine-5'-phosphate decarboxylase by complementation of *S. cerevisiae ura3* and *E. coli pyrF* mutations. *Mol Gen Genet* **198:** 179-182

Goffrini P, Ferrero I, Donnini C (2002) Respiration-dependent utilization of sugars in yeasts: a determinant role for sugar transporters. *Journal of bacteriology* **184:** 427-432

Goldman RC, Sullivan PA, Zakula D, Capobianco JO (1995) Kinetics of beta-1,3 glucan interaction at the donor and acceptor sites of the fungal glucosyltransferase encoded by the *BGL2* gene. *Eur J Biochem* **227:** 372-378

Gonzalez-Parraga P, Alonso-Monge R, Pla J, Arguelles JC (2010) Adaptive tolerance to oxidative stress and the induction of antioxidant enzymatic activities in *Candida albicans* are independent of the Hog1 and Cap1-mediated pathways. *FEMS Yeast Res* **10:** 747-756

Gow NA, van de Veerdonk FL, Brown AJ, Netea MG (2012) *Candida albicans* morphogenesis and host defence: discriminating invasion from colonization. *Nature reviews Microbiology* **10:** 112-122

Gozalbo D, Roig P, Villamon E, Gil ML (2004) *Candida* and candidiasis: the cell wall as a potential molecular target for antifungal therapy. *Curr Drug Targets Infect Disord* **4:** 117-135

Granger BL, Flenniken ML, Davis DA, Mitchell AP, Cutler JE (2005) Yeast wall protein 1 of *Candida albicans*. *Microbiology* **151:** 1631-1644

Gregori C, Glaser W, Frohner IE, Reinoso-Martin C, Rupp S, Schuller C, Kuchler K (2011) Efg1 Controls caspofungin-induced cell aggregation of *Candida albicans* through the adhesin Als1. *Eukaryot Cell* **10:** 1694-1704

Gutierrez J, Maroto C, Piedrola G, Martin E, Perez JA (1993) Circulating *Candida* antigens and antibodies: useful markers of candidemia. *J Clin Microbiol* **31:** 2550-2552

Haas H (2012) Iron - A Key Nexus in the Virulence of Aspergillus fumigatus. *Front Microbiol* **3:** 28

Haas H, Zadra I, Stoffler G, Angermayr K (1999) The *Aspergillus nidulans* GATA factor SREA is involved in regulation of siderophore biosynthesis and control of iron uptake. *J Biol Chem* **274:** 4613-4619

Hameed S, Dhamgaye S, Singh A, Goswami SK, Prasad R (2011) Calcineurin signaling and membrane lipid homeostasis regulates iron mediated multidrug resistance mechanisms in *Candida albicans*. *PLoS One* **6:** e18684

Hameed S, Prasad T, Banerjee D, Chandra A, Mukhopadhyay CK, Goswami SK, Lattif AA, Chandra J, Mukherjee PK, Ghannoum MA, Prasad R (2008) Iron deprivation induces *EFG1*-mediated hyphal development in *Candida albicans* without affecting biofilm formation. *FEMS Yeast Res* **8:** 744-755

Harris WR (2012) Anion binding properties of the transferrins. Implications for function. *Biochim Biophys Acta* **1820:** 348-361

Hartland RP, Emerson GW, Sullivan PA (1991) A secreted beta-glucan-branching enzyme from Candida albicans. *Proc Biol Sci* **246:** 155-160

Hawksworth DL, Rossman AY (1997) Where are all the undescribed fungi? *Phytopathology* **87:** 888-891

Heilmann CJ, Sorgo AG, Siliakus AR, Dekker HL, Brul S, de Koster CG, de Koning LJ, Klis FM (2011) Hyphal induction in the human fungal pathogen *Candida albicans* reveals a characteristic wall protein profile. *Microbiology* **157:** 2297-2307

Heintz-Buschart A, Eickhoff H, Hohn E, Bilitewski U (2012) Identification of inhibitors of yeast-to-hyphae transition in *Candida albicans* by a reporter screening assay. *J Biotechnol*

Henry KW, Nickels JT, Edlind TD (2000) Upregulation of ERG genes in *Candida* species by azoles and other sterol biosynthesis inhibitors. *Antimicrobial agents and chemotherapy* **44:** 2693-2700

Hentze MW, Muckenthaler MU, Andrews NC (2004) Balancing acts: molecular control of mammalian iron metabolism. *Cell* **117:** 285-297

Hernaez ML, Ximenez-Embun P, Martinez-Gomariz M, Gutierrez-Blazquez MD, Nombela C, Gil C (2010) Identification of *Candida albicans* exposed surface proteins in vivo by a rapid proteomic approach. *Journal of proteomics* **73:** 1404-1409

Heymann P, Gerads M, Schaller M, Dromer F, Winkelmann G, Ernst JF (2002) The siderophore iron transporter of *Candida albicans* (Sit1p/Arn1p) mediates uptake of ferrichrome-type siderophores and is required for epithelial invasion. *Infect Immun* **70:** 5246-5255

Hickman MA, Zeng G, Forche A, Hirakawa MP, Abbey D, Harrison BD, Wang YM, Su CH, Bennett RJ, Wang Y, Berman J (2013) The 'obligate diploid' *Candida albicans* forms mating-competent haploids. *Nature* **494:** 55-59

Hiller E, Heine S, Brunner H, Rupp S (2007) *Candida albicans* Sun41p, a putative glycosidase, is involved in morphogenesis, cell wall biogenesis, and biofilm formation. *Eukaryot Cell* **6:** 2056-2065

Hiller E, Zavrel M, Hauser N, Sohn K, Burger-Kentischer A, Lemuth K, Rupp S (2011) Adaptation, adhesion and invasion during interaction of *Candida albicans* with the host--focus on the function of cell wall proteins. *Int J Med Microbiol* **301:** 384-389

Homann OR, Dea J, Noble SM, Johnson AD (2009) A phenotypic profile of the *Candida albicans* regulatory network. *PLoS Genet* **5:** e1000783

Hoyer LL, Green CB, Oh SH, Zhao X (2008) Discovering the secrets of the *Candida albicans* agglutinin-like sequence (ALS) gene family--a sticky pursuit. *Med Mycol* **46:** 1-15

Hsu PC, Yang CY, Lan CY (2011) *Candida albicans* Hap43 is a repressor induced under low-iron conditions and is essential for iron-responsive transcriptional regulation and virulence. *Eukaryot Cell* **10:** 207-225

Hull CM, Johnson AD (1999) Identification of a mating type-like locus in the asexual pathogenic yeast *Candida albicans*. *Science* **285:** 1271-1275

Hull CM, Raisner RM, Johnson AD (2000) Evidence for mating of the "asexual" yeast *Candida albicans* in a mammalian host. *Science* **289:** 307-310

Hunter RL, Bennett B, Towns M, Vogler WR (1984) Transferrin in disease II: defects in the regulation of transferrin saturation with iron contribute to susceptibility to infection. *American journal of clinical pathology* **81:** 748-753

Inglis DO, Arnaud MB, Binkley J, Shah P, Skrzypek MS, Wymore F, Binkley G, Miyasato SR, Simison M, Sherlock G (2012) The *Candida* genome database incorporates multiple *Candida* species: multispecies search and analysis tools with curated gene and protein information for *Candida albicans* and *Candida glabrata*. *Nucleic acids research* **40:** D667-674

Jansons VK, Nickerson WJ (1970) Induction, morphogenesis, and germination of the chlamydospore of *Candida albicans*. *J Bacteriol* **104:** 910-921

Jeeves RE, Mason RP, Woodacre A, Cashmore AM (2011) Ferric reductase genes involved in high-affinity iron uptake are differentially regulated in yeast and hyphae of *Candida albicans*. *Yeast* **28:** 629-644

Jeng HW, Holmes AR, Cannon RD (2005) Characterization of two *Candida albicans* surface mannoprotein adhesins that bind immobilized saliva components. *Med Mycol* **43:** 209-217

Jung WH, Sham A, White R, Kronstad JW (2006) Iron regulation of the major virulence factors in the AIDS-associated pathogen *Cryptococcus neoformans*. *PLoS Biol* **4:** e410

Jurado RL (1997) Iron, infections, and anemia of inflammation. *Clin Infect Dis* **25:** 888-895

Kaba HE, Nimtz M, Muller PP, Bilitewski U (2013) Involvement of the mitogen activated protein kinase Hog1p in the response of *Candida albicans* to iron availability. *BMC Microbiol* **13:** 16

Kamaya T (1969) Flocculation phenomenon of *Candida albicans* by lysozyme. *Mycopathol Mycol Appl* **37:** 320-330

Khan FA, Fisher MA, Khakoo RA (2007) Association of hemochromatosis with infectious diseases: expanding spectrum. *Int J Infect Dis* **11:** 482-487

Klebl F, Tanner W (1989) Molecular cloning of a cell wall exo-beta-1,3-glucanase from *Saccharomyces cerevisiae*. *Journal of bacteriology* **171:** 6259-6264

Klis FM, Sosinska GJ, de Groot PW, Brul S (2009) Covalently linked cell wall proteins of *Candida albicans* and their role in fitness and virulence. *FEMS yeast research* **9:** 1013-1028

Klotz SA, Gaur NK, Lake DF, Chan V, Rauceo J, Lipke PN (2004) Degenerate peptide recognition by *Candida albicans* adhesins Als5p and Als1p. *Infection and immunity* **72:** 2029-2034

Knight SA, Lesuisse E, Stearman R, Klausner RD, Dancis A (2002) Reductive iron uptake by Candida albicans: role of copper, iron and the TUP1 regulator. *Microbiology* **148:** 29-40

Knight SA, Vilaire G, Lesuisse E, Dancis A (2005) Iron acquisition from transferrin by *Candida albicans* depends on the reductive pathway. *Infect Immun* **73:** 5482-5492

Ko YJ, Yu YM, Kim GB, Lee GW, Maeng PJ, Kim S, Floyd A, Heitman J, Bahn YS (2009) Remodeling of global transcription patterns of *Cryptococcus neoformans* genes mediated by the stress-activated HOG signaling pathways. *Eukaryot Cell* **8:** 1197-1217

Kobayashi T, Kakeya H, Miyazaki T, Izumikawa K, Yanagihara K, Ohno H, Yamamoto Y, Tashiro T, Kohno S (2011) Synergistic antifungal effect of lactoferrin with azole antifungals against *Candida albicans* and a proposal for a new treatment method for invasive candidiasis. *Japanese journal of infectious diseases* **64:** 292-296

Kofla G, Ruhnke M (2011) Pharmacology and metabolism of anidulafungin, caspofungin and micafungin in the treatment of invasive candidosis: review of the literature. *Eur J Med Res* **16:** 159-166

Kojic EM, Darouiche RO (2004) *Candida* infections of medical devices. *Clin Microbiol Rev* **17:** 255-267

Kosman DJ (2002) FET3P, ceruloplasmin, and the role of copper in iron metabolism. *Advances in protein chemistry* **60:** 221-269

Kragelund C, Kieffer-Kristensen L, Reibel J, Bennett EP (2013) Oral candidosis in lichen planus: the diagnostic approach is of major therapeutic importance. *Clinical oral investigations* **17:** 957-965

Lain A, Elguezabal N, Amutio E, Fernandez de Larrinoa I, Moragues MD, Ponton J (2008) Use of recombinant antigens for the diagnosis of invasive candidiasis. *Clinical & developmental immunology* **2008:** 721950

Lain A, Elguezabal N, Brena S, Garcia-Ruiz JC, Del Palacio A, Moragues MD, Ponton J (2007) Diagnosis of invasive candidiasis by enzyme-linked immunosorbent assay using the N-terminal fragment of *Candida albicans* hyphal wall protein 1. *BMC microbiology* **7:** 35

Lan CY, Rodarte G, Murillo LA, Jones T, Davis RW, Dungan J, Newport G, Agabian N (2004) Regulatory networks affected by iron availability in *Candida albicans*. *Mol Microbiol* **53:** 1451-1469

Lerner RA (1982) Tapping the immunological repertoire to produce antibodies of predetermined specificity. *Nature* **299:** 593-596

Lesuisse E, Knight SA, Camadro JM, Dancis A (2002) Siderophore uptake by *Candida albicans*: effect of serum treatment and comparison with Saccharomyces cerevisiae. *Yeast* **19:** 329-340

Lew MA, Siber GR, Donahue DM, Maiorca F (1982) Enhanced detection with an enzyme-linked immunosorbent assay of candida mannan in antibody-containing serum after heat extraction. *The Journal of infectious diseases* **145:** 45-56

Liu TT, Lee RE, Barker KS, Lee RE, Wei L, Homayouni R, Rogers PD (2005) Genome-wide expression profiling of the response to azole, polyene, echinocandin, and pyrimidine antifungal agents in *Candida albicans*. *Antimicrobial agents and chemotherapy* **49:** 2226-2236

Lopez-Ribot JL, Alloush HM, Masten BJ, Chaffin WL (1996) Evidence for presence in the cell wall of Candida albicans of a protein related to the hsp70 family. *Infect Immun* **64:** 3333-3340

Lupetti A, Paulusma-Annema A, Senesi S, Campa M, Van Dissel JT, Nibbering PH (2002) Internal thiols and reactive oxygen species in candidacidal activity exerted by an N-terminal peptide of human lactoferrin. *Antimicrob Agents Chemother* **46:** 1634-1639

Machner MP, Isberg RR (2006) Targeting of host Rab GTPase function by the intravacuolar pathogen *Legionella pneumophila*. *Developmental cell* **11:** 47-56

Magee BB, Magee PT (2000) Induction of mating in *Candida albicans* by construction of MTLa and MTLalpha strains. *Science* **289:** 310-313

Martinez JP, Gil ML, Lopez-Ribot JL, Chaffin WL (1998) Serologic response to cell wall mannoproteins and proteins of *Candida albicans*. *Clin Microbiol Rev* **11:** 121-141

Mayer FL, Wilson D, Hube B (2013) *Candida albicans* pathogenicity mechanisms. *Virulence* **4:** 119-128

McCluskey K, Wiest A, Plamann M (2010) The Fungal Genetics Stock Center: a repository for 50 years of fungal genetics research. *J Biosci* **35:** 119-126

Minn Y, Brummer E, Stevens DA (1997) Effect of iron on fluconazole activity against *Candida albicans* in presence of human serum or monocyte-derived macrophages. *Mycopathologia* **138:** 29-35

Mochon AB, Jin Y, Kayala MA, Wingard JR, Clancy CJ, Nguyen MH, Felgner P, Baldi P, Liu H (2010) Serological profiling of a *Candida albicans* protein microarray reveals permanent host-pathogen interplay and stage-specific responses during candidemia. *PLoS Pathog* **6:** e1000827

Monge RA, Roman E, Nombela C, Pla J (2006) The MAP kinase signal transduction network in *Candida albicans*. *Microbiology* **152:** 905-912

Morrissey JA, Williams PH, Cashmore AM (1996) *Candida albicans* has a cell-associated ferric-reductase activity which is regulated in response to levels of iron and copper. *Microbiology* **142 (Pt 3):** 485-492

Morschhauser J (2010a) Regulation of multidrug resistance in pathogenic fungi. *Fungal Genet Biol* **47:** 94-106

Morschhauser J (2010b) Regulation of white-opaque switching in *Candida albicans*. *Medical microbiology and immunology* **199:** 165-172

Mouyna I, Hartland RP, Fontaine T, Diaquin M, Simenel C, Delepierre M, Henrissat B, Latge JP (1998) A 1,3-beta-glucanosyltransferase isolated from the cell wall of *Aspergillus fumigatus* is a homologue of the yeast Bgl2p. *Microbiology* **144 (Pt 11):** 3171-3180

Mrsa V, Klebl F, Tanner W (1993) Purification and characterization of the *Saccharomyces cerevisiae BGL2* gene product, a cell wall endo-beta-1,3-glucanase. *Journal of bacteriology* **175:** 2102-2106

Murciano C, Moyes DL, Runglall M, Tobouti P, Islam A, Hoyer LL, Naglik JR (2012) Evaluation of the role of *Candida albicans* agglutinin-like sequence (Als) proteins in human oral epithelial cell interactions. *PLoS One* **7:** e33362

Musallam KM, Cappellini MD, Wood JC, Taher AT (2012) Iron overload in non-transfusion-dependent thalassemia: a clinical perspective. *Blood reviews* **26 Suppl 1:** S16-19

Nairz M, Schroll A, Sonnweber T, Weiss G (2010) The struggle for iron - a metal at the host-pathogen interface. *Cell Microbiol* **12:** 1691-1702

Nather K, Munro CA (2008) Generating cell surface diversity in *Candida albicans* and other fungal pathogens. *FEMS Microbiol Lett* **285:** 137-145

Neely LA, Audeh M, Phung NA, Min M, Suchocki A, Plourde D, Blanco M, Demas V, Skewis LR, Anagnostou T, Coleman JJ, Wellman P, Mylonakis E, Lowery TJ (2013) T2 magnetic resonance enables nanoparticle-mediated rapid detection of candidemia in whole blood. *Science translational medicine* **5:** 182ra154

Nilsson UA, Bassen M, Savman K, Kjellmer I (2002) A simple and rapid method for the determination of "free" iron in biological fluids. *Free Radic Res* **36:** 677-684

Nobile CJ, Mitchell AP (2009) Large-scale gene disruption using the *UAU1* cassette. *Methods Mol Biol* **499:** 175-194

Nobile CJ, Nett JE, Hernday AD, Homann OR, Deneault JS, Nantel A, Andes DR, Johnson AD, Mitchell AP (2009) Biofilm matrix regulation by *Candida albicans* Zap1. *PLoS biology* **7:** e1000133

O'Brien J, Wilson I, Orton T, Pognan F (2000) Investigation of the Alamar Blue (resazurin) fluorescent dye for the assessment of mammalian cell cytotoxicity. *Eur J Biochem* **267:** 5421-5426

Ochiai N, Fujimura M, Oshima M, Motoyama T, Ichiishi A, Yamada-Okabe H, Yamaguchi I (2002) Effects of iprodione and fludioxonil on glycerol synthesis and hyphal development in Candida albicans. *Bioscience, biotechnology, and biochemistry* **66:** 2209-2215

Odds FC, Brown AJ, Gow NA (2004) *Candida albicans* genome sequence: a platform for genomics in the absence of genetics. *Genome Biol* **5:** 230

Ollert MW, Calderone RA (1990) A monoclonal antibody that defines a surface antigen on *Candida albicans* hyphae cross-reacts with yeast cell protoplasts. *Infect Immun* **58:** 625-631

Ostrosky-Zeichner L, Alexander BD, Kett DH, Vazquez J, Pappas PG, Saeki F, Ketchum PA, Wingard J, Schiff R, Tamura H, Finkelman MA, Rex JH (2005) Multicenter clinical evaluation of the (1-->3) beta-D-glucan assay as an aid to diagnosis of fungal infections in humans. *Clinical infectious diseases : an official publication of the Infectious Diseases Society of America* **41:** 654-659

Park YN, Morschhauser J (2005) Tetracycline-inducible gene expression and gene deletion in *Candida albicans*. *Eukaryotic cell* **4:** 1328-1342

Pelletier B, Beaudoin J, Mukai Y, Labbe S (2002) Fep1, an iron sensor regulating iron transporter gene expression in *Schizosaccharomyces pombe*. *J Biol Chem* **277:** 22950-22958

Pelletier B, Mercier A, Durand M, Peter C, Jbel M, Beaudoin J, Labbe S (2007) Expression of *Candida albicans* Sfu1 in fission yeast complements the loss of the iron-regulatory transcription factor Fep1 and requires Tup co-repressors. *Yeast* **24:** 883-900

Pfaller MA (2012) Antifungal drug resistance: mechanisms, epidemiology, and consequences for treatment. *Am J Med* **125:** S3-13

Pfaller MA, Barry AL (1994) Evaluation of a novel colorimetric broth microdilution method for antifungal susceptibility testing of yeast isolates. *J Clin Microbiol* **32:** 1992-1996

Pfaller MA, Diekema DJ (2007) Epidemiology of invasive candidiasis: a persistent public health problem. *Clinical microbiology reviews* **20:** 133-163

Pfaller MA, Grant C, Morthland V, Rhine-Chalberg J (1994) Comparative evaluation of alternative methods for broth dilution susceptibility testing of fluconazole against *Candida albicans*. *J Clin Microbiol* **32:** 506-509

Pieri L, Bucciantini M, Nosi D, Formigli L, Savistchenko J, Melki R, Stefani M (2006) The yeast prion Ure2p native-like assemblies are toxic to mammalian cells regardless of their aggregation state. *J Biol Chem* **281:** 15337-15344

Pitarch A, Jimenez A, Nombela C, Gil C (2006) Decoding serological response to *Candida* cell wall immunome into novel diagnostic, prognostic, and therapeutic candidates for systemic candidiasis by proteomic and bioinformatic analyses. *Mol Cell Proteomics* **5:** 79-96

Pitarch A, Pardo M, Jimenez A, Pla J, Gil C, Sanchez M, Nombela C (1999) Two-dimensional gel electrophoresis as analytical tool for identifying *Candida albicans* immunogenic proteins. *Electrophoresis* **20:** 1001-1010

Prasad T, Chandra A, Mukhopadhyay CK, Prasad R (2006) Unexpected link between iron and drug resistance of *Candida spp.*: iron depletion enhances membrane fluidity and drug diffusion, leading to drug-susceptible cells. *Antimicrob Agents Chemother* **50:** 3597-3606

Pryce TM, Kay ID, Palladino S, Heath CH (2003) Real-time automated polymerase chain reaction (PCR) to detect *Candida albicans* and *Aspergillus fumigatus* DNA in whole blood from high-risk patients. *Diagnostic microbiology and infectious disease* **47:** 487-496

Ramanan N, Wang Y (2000) A high-affinity iron permease essential for *Candida albicans* virulence. *Science* **288:** 1062-1064

Rico H, Carrillo C, Aguado C, Mormeneo S, Sentandreu R (1997) Initial steps of wall protoplast regeneration in *Candida albicans*. *Research in microbiology* **148:** 593-603

Roman E, Cottier F, Ernst JF, Pla J (2009) Msb2 signaling mucin controls activation of Cek1 mitogen-activated protein kinase in *Candida albicans*. *Eukaryot Cell* **8:** 1235-1249

Ruiz-Herrera J, Elorza MV, Valentin E, Sentandreu R (2006) Molecular organization of the cell wall of *Candida albicans* and its relation to pathogenicity. *FEMS Yeast Res* **6:** 14-29

San Jose C, Monge RA, Perez-Diaz R, Pla J, Nombela C (1996) The mitogen-activated protein kinase homolog *HOG1* gene controls glycerol accumulation in the pathogenic fungus *Candida albicans*. *J Bacteriol* **178:** 5850-5852

Santos MA, Tuite MF (1995) The CUG codon is decoded in vivo as serine and not leucine in *Candida albicans*. *Nucleic acids research* **23:** 1481-1486

Sarthy AV, McGonigal T, Coen M, Frost DJ, Meulbroek JA, Goldman RC (1997) Phenotype in *Candida albicans* of a disruption of the *BGL2* gene encoding a 1,3-beta-glucosyltransferase. *Microbiology* **143 (Pt 2):** 367-376

Sasse C, Hasenberg M, Weyler M, Gunzer M, Morschhauser J (2013) White-opaque switching of *Candida albicans* allows immune evasion in an environment-dependent fashion. *Eukaryotic cell* **12:** 50-58

Saville SP, Lazzell AL, Monteagudo C, Lopez-Ribot JL (2003) Engineered control of cell morphology *in vivo* reveals distinct roles for yeast and filamentous forms of *Candida albicans* during infection. *Eukaryotic cell* **2:** 1053-1060

Schaible UE, Kaufmann SH (2004) Iron and microbial infection. *Nat Rev Microbiol* **2:** 946-953

Siddique A, Kowdley KV (2012) Review article: the iron overload syndromes. *Alimentary pharmacology & therapeutics* **35:** 876-893

Singh RP, Prasad HK, Sinha I, Agarwal N, Natarajan K (2011) Cap2-HAP complex is a critical transcriptional regulator that has dual but contrasting roles in regulation of iron homeostasis in *Candida albicans*. *The Journal of biological chemistry* **286:** 25154-25170

Slutsky B, Staebell M, Anderson J, Risen L, Pfaller M, Soll DR (1987) "White-opaque transition": a second high-frequency switching system in *Candida albicans*. *Journal of bacteriology* **169:** 189-197

Smaldone GT, Revelles O, Gaballa A, Sauer U, Antelmann H, Helmann JD (2012) A Global Investigation of the *Bacillus subtilis* Iron-Sparing Response Identifies Major Changes in Metabolism. *J Bacteriol* **194:** 2594-2605

Smith PK, Krohn RI, Hermanson GT, Mallia AK, Gartner FH, Provenzano MD, Fujimoto EK, Goeke NM, Olson BJ, Klenk DC (1985) Measurement of protein using bicinchoninic acid. *Anal Biochem* **150:** 76-85

Soares EV (2011) Flocculation in *Saccharomyces cerevisiae*: a review. *J Appl Microbiol* **110:** 1-18

Sorgo AG, Heilmann CJ, Dekker HL, Brul S, de Koster CG, Klis FM (2010) Mass spectrometric analysis of the secretome of *Candida albicans*. *Yeast* **27:** 661-672

Staab JF, Ferrer CA, Sundstrom P (1996) Developmental expression of a tandemly repeated, proline-and glutamine-rich amino acid motif on hyphal surfaces on *Candida albicans*. *The Journal of biological chemistry* **271:** 6298-6305

Staab JF, Sundstrom P (1998) Genetic organization and sequence analysis of the hypha-specific cell wall protein gene *HWP1* of *Candida albicans*. *Yeast* **14:** 681-686

Steinberg G (2007) Hyphal growth: a tale of motors, lipids, and the Spitzenkorper. *Eukaryot Cell* **6:** 351-360

Sudbery P, Gow N, Berman J (2004) The distinct morphogenic states of *Candida albicans*. *Trends Microbiol* **12:** 317-324

Sudbery PE (2011) Growth of *Candida albicans* hyphae. *Nature reviews Microbiology* **9:** 737-748

Sutak R, Lesuisse E, Tachezy J, Richardson DR (2008) Crusade for iron: iron uptake in unicellular eukaryotes and its significance for virulence. *Trends Microbiol* **16:** 261-268

Tamarit J, Irazusta V, Moreno-Cermeno A, Ros J (2006) Colorimetric assay for the quantitation of iron in yeast. *Anal Biochem* **351:** 149-151

Thewes S, Kretschmar M, Park H, Schaller M, Filler SG, Hube B (2007) In vivo and ex vivo comparative transcriptional profiling of invasive and non-invasive *Candida albicans* isolates identifies genes associated with tissue invasion. *Mol Microbiol* **63:** 1606-1628

Thompson DS, Carlisle PL, Kadosh D (2011) Coevolution of morphology and virulence in *Candida* species. *Eukaryot Cell* **10:** 1173-1182

Torres AG, Perna NT, Burland V, Ruknudin A, Blattner FR, Kaper JB (2002) Characterization of Cah, a calcium-binding and heat-extractable autotransporter protein of enterohaemorrhagic *Escherichia coli*. *Mol Microbiol* **45:** 951-966

Uhl MA, Johnson AD (2001) Development of *Streptococcus thermophilus lacZ* as a reporter gene for *Candida albicans*. *Microbiology* **147:** 1189-1195

Urban C, Sohn K, Lottspeich F, Brunner H, Rupp S (2003) Identification of cell surface determinants in *Candida albicans* reveals Tsa1p, a protein differentially localized in the cell. *FEBS Lett* **544:** 228-235

Valentin E, Mormeneo S, Sentandreu R (2000) The cell surface of *Candida albicans* during morphogenesis. *Contrib Microbiol* **5:** 138-150

van Deventer AJ, van Vliet HJ, Hop WC, Goessens WH (1994) Diagnostic value of anti-*Candida* enolase antibodies. *J Clin Microbiol* **32:** 17-23

Vanden Bossche H, Koymans L, Moereels H (1995) P450 inhibitors of use in medical treatment: focus on mechanisms of action. *Pharmacology & therapeutics* **67:** 79-100

Verstrepen KJ, Klis FM (2006) Flocculation, adhesion and biofilm formation in yeasts. *Mol Microbiol* **60:** 5-15

Wakabayashi H, Abe S, Teraguchi S, Hayasawa H, Yamaguchi H (1998) Inhibition of hyphal growth of azole-resistant strains of *Candida albicans* by triazole antifungal agents in the presence of lactoferrin-related compounds. *Antimicrobial agents and chemotherapy* **42:** 1587-1591

Walker LA, Munro CA, de Bruijn I, Lenardon MD, McKinnon A, Gow NA (2008) Stimulation of chitin synthesis rescues *Candida albicans* from echinocandins. *PLoS Pathog* **4:** e1000040

Weig M, Jansch L, Gross U, De Koster CG, Klis FM, De Groot PW (2004) Systematic identification in silico of covalently bound cell wall proteins and analysis of protein-polysaccharide linkages of the human pathogen *Candida glabrata*. *Microbiology* **150:** 3129-3144

Weinberg ED (2009) Iron availability and infection. *Biochim Biophys Acta* **1790:** 600-605

Weinberg ED, Miklossy J (2008) Iron withholding: a defense against disease. *J Alzheimers Dis* **13:** 451-463

Weissman Z, Kornitzer D (2004) A family of *Candida* cell surface haem-binding proteins involved in haemin and haemoglobin-iron utilization. *Mol Microbiol* **53:** 1209-1220

Weissman Z, Shemer R, Conibear E, Kornitzer D (2008) An endocytic mechanism for haemoglobin-iron acquisition in Candida albicans. *Mol Microbiol* **69:** 201-217

Zhao X, Oh SH, Coleman DA, Hoyer LL (2011) ALS51, a newly discovered gene in the Candida albicans ALS family, created by intergenic recombination: analysis of the gene and protein, and implications for evolution of microbial gene families. *FEMS Immunol Med Microbiol* **61:** 245-257

Zhou LW, Haas H, Marzluf GA (1998) Isolation and characterization of a new gene, sre, which encodes a GATA-type regulatory protein that controls iron transport in Neurospora crassa. *Mol Gen Genet* **259:** 532-540

Ziegler L, Terzulli A, Gaur R, McCarthy R, Kosman DJ (2011) Functional characterization of the ferroxidase, permease high-affinity iron transport complex from Candida albicans. *Mol Microbiol* **81:** 473-485